Epileptic Disorders

Learn how to interpret and use intracranial EEG findings

B. Frauscher[1,2] | D. Mansilla[2,3] | C. Abdallah[2] | A. Astner-Rohracher[4] |
S. Beniczky[5,6] | M. Brazdil[7,8] | V. Gnatkovsky[9] | J. Jacobs[10,11] |
G. Kalamangalam[12,13] | P. Perucca[14,15,16,17,18] | P. Ryvlin[19] | S. Schuele[20] |
J. Tao[21] | Y. Wang[9,13] | M. Zijlmans[22,23] | A. McGonigal[24,25]

Correspondence
Birgit Frauscher, Duke Comprehensive Epilepsy Center, Department of Neurology, Duke University Medical Center, Hock Plaza, 2424 Erwin Street, Durham, NC, 27705, USA.
Email: birgit.frauscher@duke.edu

Abstract

Epilepsy surgery is the therapy of choice for many patients with drug-resistant focal epilepsy. Recognizing and describing ictal and interictal patterns with intracranial electroencephalography (EEG) recordings is important in order to most efficiently leverage advantages of this technique to accurately delineate the seizure-onset zone before undergoing surgery. In this seminar in epileptology, we address learning objective "1.4.11 Recognize and describe ictal and interictal patterns with intracranial recordings" of the International League against Epilepsy curriculum for epileptologists. We will review principal considerations of the implantation planning, summarize the literature for the most relevant ictal and interictal EEG patterns within and beyond the Berger frequency spectrum, review invasive stimulation for seizure and functional mapping, discuss caveats in the interpretation of intracranial EEG findings, provide an overview on special considerations in children and in subdural grids/strips, and review available quantitative/signal analysis approaches. To be as practically oriented as possible, we will provide a mini atlas of the most frequent EEG patterns, highlight pearls for its not infrequently challenging interpretation, and conclude with two illustrative case examples. This article shall serve as a useful learning resource for trainees in clinical neurophysiology/epileptology by providing a basic understanding on the concepts of invasive intracranial EEG.

KEYWORDS

atlas, interictal epileptiform discharges, intracranial electroencephalography, low-voltage fast activity, pathology, prognosis, seizure-onset pattern, stereo-electroencephalography

> **Learning objective of the International League against Epilepsy curriculum**
>
> To recognize and describe ictal and interictal patterns with intracranial recordings:
>
> - To learn basic principles of invasive intracranial EEG
> - To describe the most common ictal and interictal intracranial EEG patterns
> - To recognize basic considerations of invasive cortical stimulation
> - To be aware of pitfalls and potential limitations of intracranial EEG

> **Key points**
>
> - The purpose of intracranial EEG is to identify the seizure-onset zone, delineate the wider epileptic network and resection margins, and localize relevant eloquent cortex in relation to the epileptic network.
> - Given similar efficacy to identify the epileptogenic zone at significant lower complication rates, SEEG has become the method of choice for most intracranial EEG investigations.
> - Seizure-onset patterns containing fast activity are associated with a better postsurgical prognosis than seizure-onset patterns not including fast activity.
> - Seizure semiology is shaped by both spatial and temporal aspects of the ictal EEG change.
> - Interictal intracranial patterns are generally just partially mirroring underlying histopathological signatures.
> - Frequencies outside the Berger frequency spectrums such as high-frequency oscillations and direct current shifts have been shown to be useful to delineate the epileptogenic zone.
> - Seizure stimulation is integral part of every SEEG investigation given its usefulness to probe the epileptic network.
> - Even though subdural grids/strips may remain the preferred option for assessment of cortex in close vicinity to eloquent cortex, functional mapping is possible with SEEG.
> - Understanding consequences of the limited spatial sampling of intracranial EEG is important for a correct interpretation of the "apparent" seizure-onset zone.
> - Computerized approaches for the detection of the epileptogenic zone hold promise to assist the neurophysiologist/epileptologist in the interpretation of intracranial EEG studies.

1 | INTRODUCTION

Epilepsy surgery is the treatment of choice for many patients with drug-resistant focal epilepsy.[1] The standard investigations of phase 1 presurgical epilepsy work-up comprise video electroencephalography (EEG), neuroimaging, neuropsychological assessment, and auxiliary tests such as electromagnetic source imaging, positron emission tomography, single photon emission computed tomography, and functional magnetic resonance imaging.[2] Invasive intracranial EEG is the method of choice for patients who do not fulfill criteria for proceeding directly to surgery, but who are still deemed to be potentially good surgical candidates.[3] Two techniques are differentiated: subdural grids/strips recordings and stereo-electroencephalography (SEEG). Whereas this review will predominantly focus on SEEG given its recent increase in use around the world,[4,5] it will cover principles related to both techniques and have a section dedicated to special considerations in subdural grids/strips. Furthermore, whereas most principles of interpretation are transferable to the pediatric population, special considerations in children will be highlighted in a separate section.

This educational review paper addresses the following learning objective of the International League against Epilepsy curriculum: "1.4.11 Recognize and describe ictal and interictal patterns with intracranial recordings." Having a very good understanding of the current principles and pitfalls of this methodology is critical in order to most efficiently leverage advantages of this technique to accurately delineate the surgical targets in patients with drug-resistant focal epilepsy. One important difference to scalp EEG recording is the inherent sampling bias when using invasive intracranial EEG, which is independent of the technique used. This explains why one of the main questions to ask oneself when interpreting invasive intracranial EEG is always if the "true" initial seizure onset is

sampled, or whether what we see in the intracranial EEG corresponds to propagated activity as we are blind to the "true" seizure onset. Therefore, using the term "apparent seizure onset" may be more appropriate to reflect this important practical limitation.

In the following, we will review principal considerations of the implantation planning, summarize the literature for the most relevant ictal and interictal EEG patterns, review invasive stimulation for seizure and functional mapping, discuss caveats in the interpretation of intracranial EEG findings, provide an overview on

special considerations in children and in subdural grids/strips, and review available quantitative/signal analysis approaches and conclude with providing two illustrative case examples. After careful reading of this article, trainees in clinical neurophysiology/epileptology should have a basic understanding on the concepts of invasive intracranial EEG.

Importantly, different recording methods influence how the seizure "looks" different to the EEGer, which in fact led to different and somewhat contradictory conceptual models of how seizures arise in the brain.[6] Different uses of terminology and nomenclature also arose from these different models. The term "epileptogenic zone (EZ)" was first used by the French pioneers of SEEG, Jean Bancaud, and Jean Talairach, from the 1960s onward to indicate the "primary seizure organization",[7] reflecting the fact that seizure activity was typically observed near-simultaneously in a set of connected structures rather than a single structure. This term also reflects their view on the importance of early seizure propagation in seizure expression. A different definition of the EZ was later proposed by specialists of epilepsy surgery based on subdural grid use and especially by the school of Hans Luders, as the "area of cortex indispensable for the generation of epileptic seizures," the removal of which was necessary and sufficient for seizure freedom after surgery.[8] "Seizure-onset zone" (SOZ) according to this subdural grid-derived model was defined as the "region where the clinical seizures originate".[8] While the term SOZ does not capture the importance of initial seizure spatiotemporal dynamic architecture as evidenced by SEEG, in this article for simplicity, we have chosen to mainly use the term SOZ, recognizing its limitations and ambiguities.[9]

2 | PLANNING OF THE IMPLANTATION: FROM INDICATION TO IMPLANTATION

The past decade has seen the widespread adoption of SEEG for invasive exploration of the brain in patients with drug-resistant focal epilepsy.[4] A SEEG study aims to confirm or refute hypotheses of likely primary organization of seizures, in patients in whom non-invasive investigations alone suggest possible unifocal and operable epilepsy, but in whom alternative hypotheses need to be excluded to enable optimal surgical decision making. The goal of pre-implantation analyses of all non-invasive data of phase 1 work-up is to synthesize the findings into a most likely hypothesis as well as to identify secondary hypotheses to be excluded.[10] When there is complete concordance among the non-invasive data and there is no ambiguity in implicating a single brain region or well-defined network, an

invasive evaluation may be superfluous, unless for example relation to functional cortex requires to be investigated prior to surgical decision making. SEEG is primarily indicated when the non-invasive data are discordant or insufficient or point to multiple plausible brain regions, but only if a hypothesis of a single, spatially constrained, potentially operable region is supported by the non-invasive data. The end-goal of SEEG is resolution of these ambiguities by identifying the SOZ and early seizure organization in relation to any epileptogenic lesion (if present), to the zone involved by interictal spikes, and the functional specificities of the explored regions.[11] Apart from its primary indication, there are growing indications where SEEG is performed with the view to perform radiofrequency thermocoagulation or responsive neurostimulation, even though the SOZ is likely known or multifocal, such as, for example, in periventricular nodular heterotopia or bilateral mesiotemporal lobe epilepsy.[12–14]

SEEG is an invasive procedure that is not without risks. Complication rates in SEEG are in general estimated to be between 0.6% and 2.0% depending on the individual center's experience.[15–17] Up to 40% of patients undergoing SEEG are subsequently not offered surgery because the SOZ is less focal than expected, cannot be identified, or shows significant overlap between the SOZ and eloquent areas preventing a successful surgical intervention.[15–17] In order to reduce an unnecessary invasive diagnostic burden on patients where no focal SOZ can be identified, the 5-SENSE score was developed and validated to assist clinicians to predict patients where SEEG is unlikely to record a unifocal, spatially constrained SOZ (https://lab-frauscher.github.io/Sense_calc/).[18] Positive predictive variables of the score are the presence of a focal lesion on structural magnetic resonance imaging, the absence of bilateral independent spikes in scalp electroencephalography (with the exception of bitemporal spikes), a localizing neuropsychological deficit, a strongly localizing semiology, and a regional ictal scalp electroencephalography onset. Results of the score need to be interpreted in the clinical context. In the absence of overlap with functional areas, large and multilobar resections are sometimes possible and may allow to achieve good clinical outcomes.

A SEEG implantation has been originally designed around the concept of an epileptic "network": a set of connected anatomical structures that allow for an "anatomo-clinical-electrical correlation",[10] wherein electro-clinical correlations of successive features of seizure semiology are analyzed with respect to the sampled anatomical sites. The results obtained depend largely upon the accuracy of the SEEG implantation, which in turns depends on the prior hypotheses that have been formulated from the non-invasive phase. An early observation from SEEG studies was that the electrical disturbances arising from the presence of an epileptogenic cerebral lesion were often

non-contiguous with lesional anatomic boundaries. In addition, seizures could be observed to arise from structures distant from the lesion and even separate from the region of maximal interictal spiking.[19] In ~40% of cases, the SOZ corresponds to a relatively restricted area of the brain, in which seizure onset is limited to a unique dysfunctional area (focal organization), a situation corresponding to the classical notion of an "epileptogenic focus." In ~60% of cases, the seizure onset is characterized by discharges that simultaneously or very rapidly involve several distributed brain regions (network organization).[20] Signal analysis studies applied to SEEG data have allowed quantification of epileptogenicity (see section "Overview on quantitative / signal analysis approaches"), with the seizure onset being distinguishable from propagation and non-involved zones.

In general, involvement of specific brain networks is suspected on the basis of seizure semiology and ictal surface EEG (as well as supporting data from neuroimaging): for instance, a rising abdominal feeling followed by oro-alimentary automatisms is classically associated with a mesial temporal lobe seizure origin.[21] Another example is a unilateral somatosensory aura progressing to hemi-clonic movements associated with a contralateral per-irolandic process. Thus, one speaks of a limbic network (involving one or more of the hippocampi, amygdala, temporal neocortex, cingulate, orbitofrontal, insular, and medial parietal areas) or a central network (vertical extent of the pre- and post-rolandic areas, the cingulate motor area, and mid-insular region). Other examples of networks are medial frontal (the mesial premotor frontal cortex, cingulum, postcentral parietal lobe, dorsolateral frontal cortex, and the contralateral mesial frontal cortex), frontopolar/orbitofrontal (basal frontal lobe, anterior cingulate region, temporal pole, anterior opercular–insular region), or posterior cortex (medial and lateral occipital lobe, posterior temporal region, posterior parietal lobe, and precuneus) networks.[10]

While seizure organization may be non-contiguous with a certain lesion, the presence of lesion and especially type of pathology contributes heavily to implantation strategy. For large single lesions (e.g., lobar pachygyria, polymicrogyria, and schizencephaly) or multiple lesions (periventricular nodular heterotopia, tuberous sclerosis), in which surgical decision making will be heavily influenced by lesional boundaries, SEEG network interrogation may comprise sampling as much of the lesional area as possible, with additional electrodes placed to assess relevant adjacent cortical function and to decide whether initial ictal involvement suggests that a lesional target for resection is likely to produce seizure freedom.

SEEG evaluation aims above all to inform surgical decision making by confirming and refuting hypotheses of epilepsy organization. It fulfills the following sub-goals: (i) to identify the SOZ, or alternatively the core regions of the epileptogenic network when onsets are simultaneous over more than one structure; (ii) to delineate the early propagation epileptic network; (iii) to localize relevant functional cortex in relation to the epileptic network; and (iv) to refute alternative hypotheses. Figures 1 and 2 show these principles in practice in two patients. The subgoals of SEEG need to be achieved with a fixed maximum number of electrodes and recording contacts, constraints that demand specific details of the implantation strategy with reference to each electrode, such as the number of contacts on that electrode and its optimum trajectory of passage. In addition, the implantation should achieve an equipoise between using the available contacts to sample widely – to cover the structures connected within the primary hypothesized network and refute alternative hypotheses – and to sample closely and densely – for example to map sensorimotor function in the central region. Figure 1 illustrates the first situation and Figure 2 the second. Though traditionally orthogonal trajectories (i.e., parallel to the gridlines defining the Talairach coordinate system) are used, oblique trajectories possible with modern stereotaxic systems are increasingly used to maximize the sampling yield. Orthogonal trajectories carry clear advantages, for example, in the temporal lobe where both lateral and mesial structures are systematically sampled or in the frontal lobe where a single electrode can target both the supplementary motor area, the frontal eye field, and the hand motor area. Finally, and due to the fundamentally visual nature of SEEG interpretation, clear diagrammatic depictions of the implantation map at the planning stage (Figures 1B, 2B) and accurate in situ views of the electrodes in the patient's native MRI space after implantation (Figures 1C, 2D) are essential.

SEEG is a highly interdisciplinary clinical enterprise, involving at minimum personnel from neurology, clinical neurophysiology, neurosurgery, and neurodiagnostic technology. The procedural aspects of SEEG are complex and prone to human error. Communication among key personnel remains paramount: between neurology and neurosurgery in formulating an overall management and implantation strategy, between neurodiagnostics and operating room staff to ratify the actual electrodes used with their unique identifiers, and between neurology and neurodiagnostics for checking physical connections during EEG hookup. Although a 200/256 Hz sampling frequency may be sufficient for conventional routine visual review of SEEG,[11] for more complex analyses, it is recommended to sample at much higher frequency rates (512, 1024, 2048, or higher) for research or advanced clinical applications (e.g., high-frequency oscillation (HFO) analysis). In addition, the high-pass filter should be chosen as close to
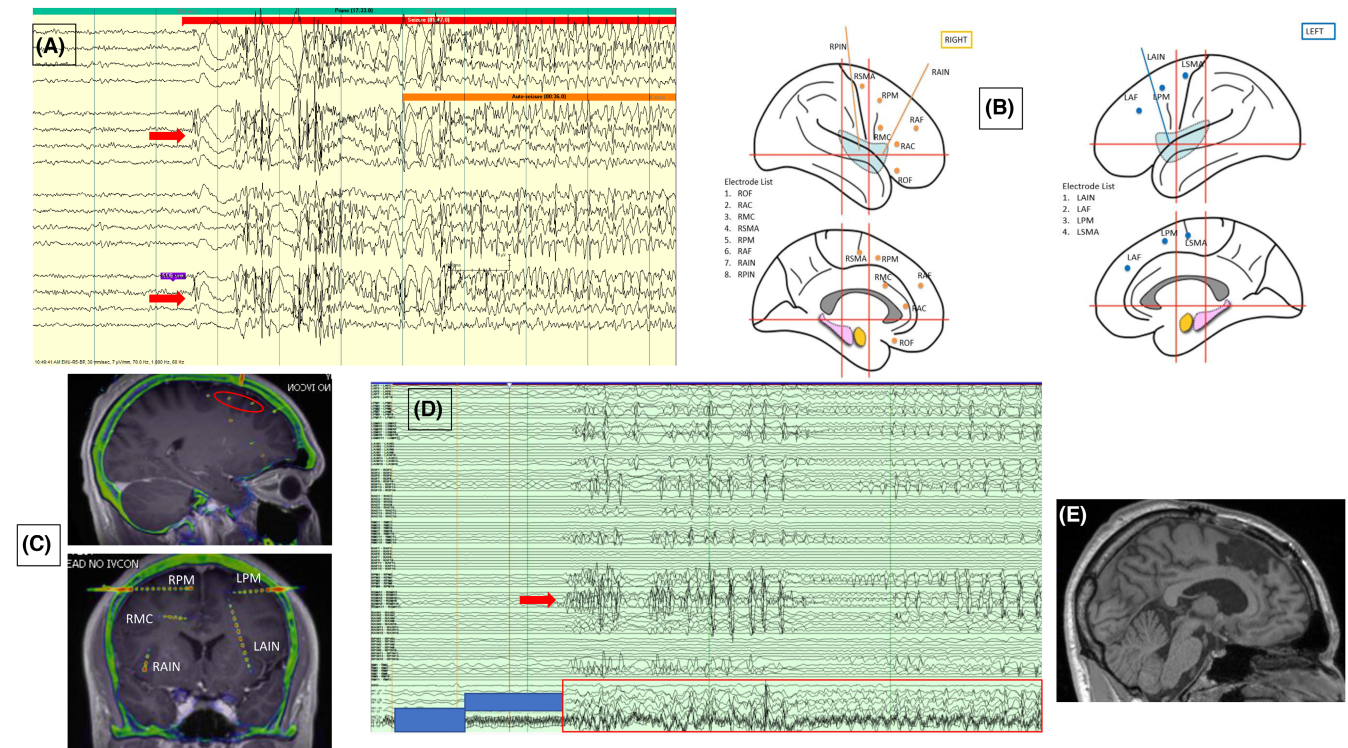
FIGURE 1 Implantation strategy to SEEG to resection on a 23-year-old right-handed man with drug-resistant sleep-related bilateral tonic–clonic seizures. Neurological examination, 3T structural MRI, and PET were normal. Interictal EEG showed right paracentral rhythmic slowing and generalized but maximum right hemispheric spikes/polyspikes. Ictal EEG showed a rapidly generalizing pattern preceded by a right hemispheric maximal polyspike discharge (A; arrows). Seizure semiology comprised asymmetric tonic posturing followed by generalized tonic and clonic movements incorporating a "sign of 4" with left arm extension suggesting right hemispheric lateralization. Spike sources localized by MEG were in the right inferior and middle frontal gyri (extending to the superior frontal sulcus) and anterior insula. Neuropsychological evaluation identified frontal executive deficits. The implantation strategy (B) is driven by the hypothesis of a right anterior frontal lobe epilepsy with secondary bilateral synchrony. The lack of an imaging lesion mandated broad premotor coverage that included MEG sources. Both hemispheres were sampled with a right-sided emphasis covering the precentral region and the insula, with medial contacts of RSMA and LSMA intended to sample supplementary motor area and the other orthogonal electrodes targeting the medial frontal cortex more anteriorly along the superior frontal and cingulate gyri. Two oblique trajectories sampled the anterior and posterior insular cortex. However, all non-insular electrodes were verified on reconstruction to lie anterior to the SMA. Electrodes were visualized by co-registration (C; bone-windowed and green-yellow colored). The coronal slice shows the relative positions of all seven non-insular electrodes along the midline of the right frontal lobe. The red ellipse encircles the RSMA and RPM electrodes. The coronal view is in the plane of the RPM/LPM electrodes. Interictal SEEG showed profuse multifocal and bilateral spike/polyspike trains and bursts, with the RSMA electrode consistently leading or simultaneously with RPM (not shown). The ictal recording (D; 4s window shown for clarity, double-distance bipolar montage, 1–128 Hz passband) showed a polyspike activity occurring near-simultaneously across widespread bilateral regions, led by the middle and lateral contacts of RSMA (arrow). Concurrent scalp recordings recapitulated the Phase I findings with rapid bilateral involvement (boxed). Electrical stimulation confirmed the absence of eloquent function in any of the right frontal electrodes, with marked hyperexcitability of multiple contacts of RSMA and RPM. The patient underwent a resection of the mid-portion of the right superior frontal gyrus delimited approximately by the trajectories of the RSMA and RPM electrodes (E). He was deficit free post-operatively, and at 2-year follow-up, he was seizure-free on medications.

direct current (DC) as possible to be able to benefit from the very low-frequency components of the signal (see section "Beyond the Berger frequency band: high-frequency oscillations and DC shifts"). It is important to remember that high frequencies can be aliased into lower frequencies on conventional computer screens and a 10s page display.[22] Redisplay on a higher resolution computer screen and/or an expanded timescale (5s or less per page) will clarify the presence of aliased power. Alternatively, the

low-pass filter can be adjusted downward on the display software or the digitized signal down sampled prior to review. We recommend that preliminary montages are made in advance of the patient returning from the operating room after their implantation; upon connection, it is straightforward to check signal fidelity and exclude noisy and flat channels and often also channels localized in white matter to create more compact final montages. It is important to have precise co-registration of the electrodes
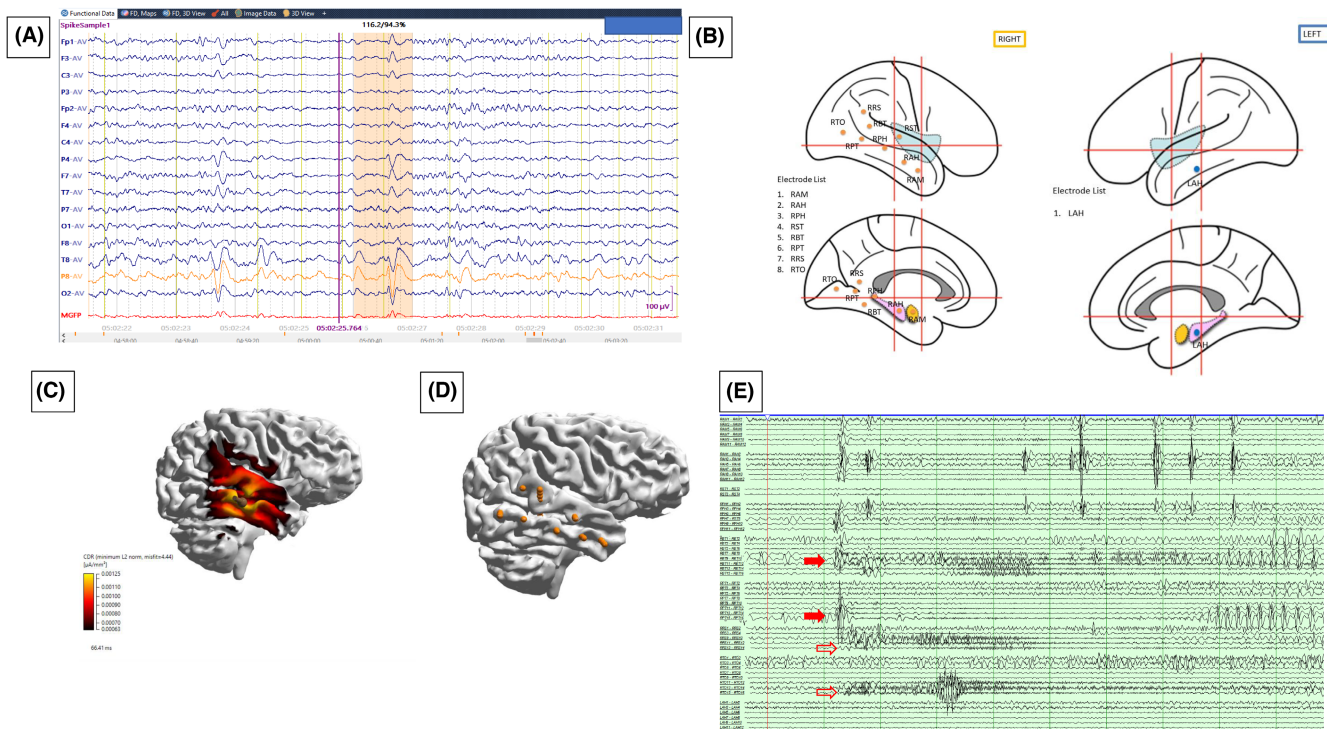
FIGURE 2 Non-invasive data (A, C) to implantation strategy (B) electrode visualization (D) and ictal SEEG (E) in a 29-year-old right-handed man with a family history of left handedness. Epilepsy onset was in his teens with sleep-related bilateral tonic–clonic seizures persisting despite multiple antiseizure medications as frequent episodes of nausea and confusion. MRI brain was normal. Interictal EEG showed frequent right mid- and posterior temporal spikes and runs of rhythmic delta, with rarer left anterior temporal spikes. Seizures were recorded as episodes of cognitive slowing with hesitant speech and incorrect answers to simple questions that were recollected in retrospect as a "funny" internal feeling. Ictal EEG showed a diffuse maximum right temporal pattern. FDG-PET showed right temporal hypometabolism. Neuropsychology indicated better nonverbal than verbal performance with some difficulty with verbally mediated tasks. Intracarotid methohexital (Wada test) confirmed bilateral-dependent language representation and impaired free recall memory in the right hemisphere. Scalp interictal EEG spikes (A) were source-localized to the mid and posterior temporal regions (B; minimum L2 norm estimate of current source density heat map with brown ball-stick indicating location of the corresponding dipole). The implantation strategy (C) queried a right neocortical temporal hypothesis in the right co-dominant hemisphere. A single sentinel electrode was placed in the opposite hippocampus. This was due to the combination of his ambidexterity as well as the interictal and ictal EEG not completely excluding a significant left temporal lobe contribution to his seizure syndrome. Paralimbic structures often implanted in suspected mesial temporal lobe syndromes (orbitofrontal cortex, insular cortex) were not sampled due to the strongly neocortical nature of the presentation. Electrodes were visualized by image co-registration between a pre-implantation T1-weighted volumetric MRI and the post-implantation volumetric CT to show the lateral surface electrode entry points (D) as well as the deeper trajectories. Ictal onset on SEEG (E) was confirmed over the lateral mid- and posterior temporal region with later hippocampal involvement. The single page shown (10s, 5–100 Hz bandpass, bipolar montage with selected isoelectric channels removed for clarity) demonstrates a herald spike over multiple right hemispheric contacts with paroxysmal fast activity evolving to rhythmic spikes in the lateral contact of the RPH and RPT electrodes (solid arrows). The spiking right hippocampus was recruited later in the seizure; the left hippocampal electrode remained quiet. Fast activity was also seen within 500 ms at the RRS and RPT lateral contacts (hollow arrows) that evolved less robustly. Stimulation mapping for language did not definitely confirm functional impairment at any site. The patient underwent a conventional right anterior temporal lobectomy with the posterior margin defined by the posterior-most neocortical electrode contact active at ictal onset. Word-finding difficulties were noted in the immediate post-operative period that gradually resolved over several months. He remained seizure free for a year though seizures recurred when he self-discontinued antiseizure medications. He has since restarted medications and remains seizure-free under regular follow-up.

on the patient-specific MRI to exactly delineate where each recording lead is located. To do so, there are several freely and commercially available software platforms.[23] To create final montages is important and will allow proper visualization of the selected SEEG channels; having all SEEG channels displayed at the same sensitivity will not allow proper inspection of the SEEG signals as certain pathologies such as periventricular nodular heterotopias and certain anatomical structures such as the amygdala have a significant lower amplitude than other pathologies such as hippocampal sclerosis or certain anatomical structures such as the hippocampus.

As for scalp EEG, choice of the reference and ground electrode is important in SEEG. The various centers follow

different strategies and most centers select a "flat" white matter contact as reference. Alternatively, an epidural electrode fixed in the bone far from the epileptic field (e.g., over the parietal lobe opposite to the epileptic focus) can be used. Traditionally, SEEG tracings are viewed in a bipolar montage between adjacent contacts of one electrode (e.g., 1–2, 2–3, 3–4, 4–5, 5–6, 6–7, 7–8, 8–9, 9–10, with 1 being the deepest contact and 10 being the most superficial contact), whereas activity of interest picked up on this montage can then be also analyzed in a referential montage. Commonly used SEEG electrodes have cylindrical 5–18 contacts usually with a 2 mm length, 0.8 mm diameter, and 1.5-mm inter-contact spacing (Figure 3). Differently from scalp EEG, sensitivity/amplitude is adjusted channel specifically to allow for optimal visualization. To facilitate the review of SEEG tracings involving often more than 150 contacts, some authors suggest a "screening" (or "double-distance") bipolar montage (where an electrode with contacts 1–10 would be connected in the five derivations 1–2,

3–4, 5–6, 7–8, and 9–10). No electrode contact is repeated in the scheme and data display on the screen is minimized, allowing for rapid "bird's-eye" review of long segments.

2.1 | Interictal patterns

The most important interictal SEEG pattern is determined by the epileptogenicity of the investigated brain site (i.e., by the presence of interictal spikes ± pathologic high-frequency oscillations, HFOs). Nonetheless, an understanding of normal and abnormal non-epileptiform interictal activity is useful.

2.1.1 | Physiological EEG patterns

Physiological SEEG activities vary from one region to another, and for example, faster beta activities
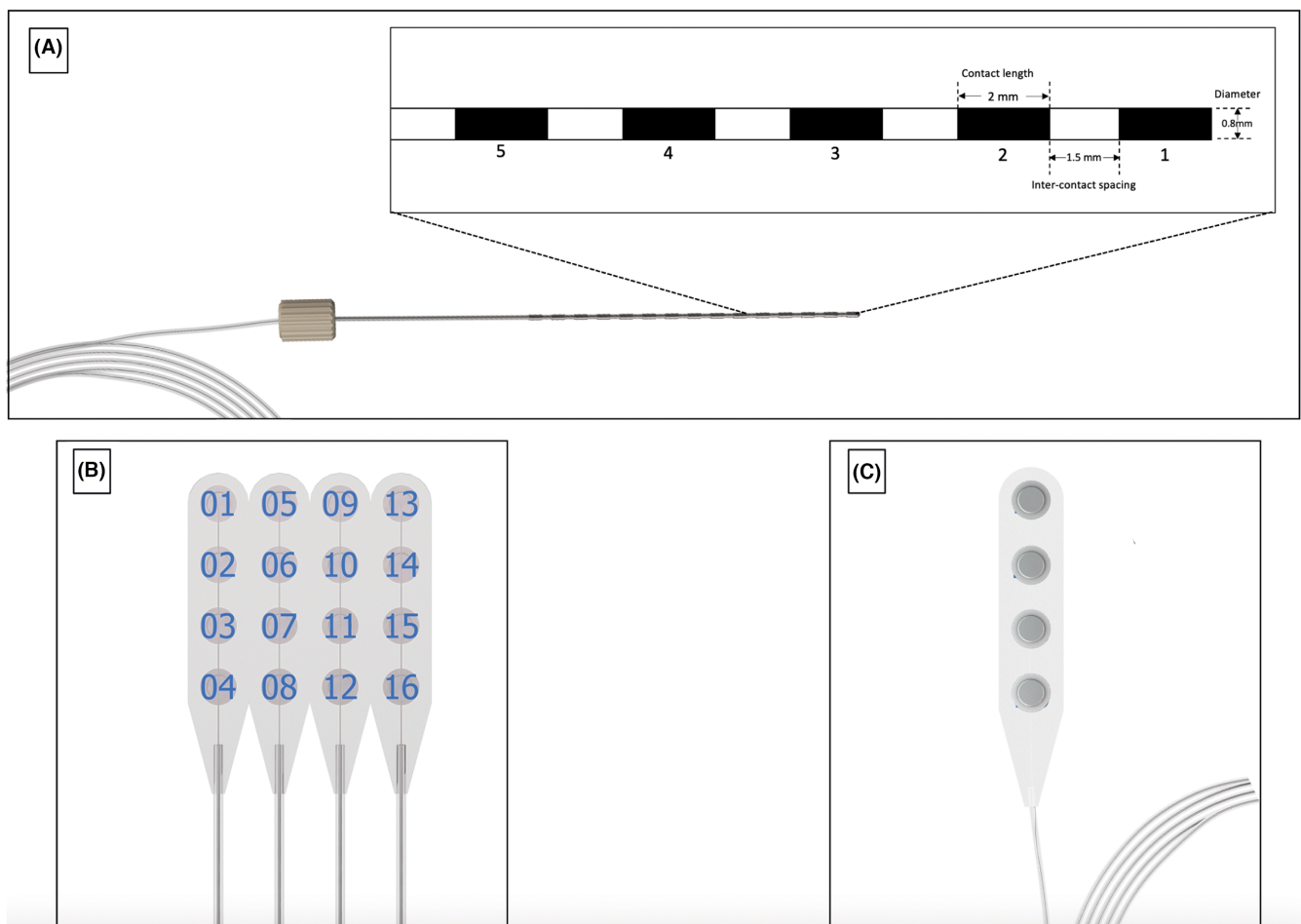

FIGURE 3 Different types of electrodes used in invasive EEG studies. (A) 15-contact SEEG depth electrode. Contact length, inter-contact spacing, and electrode diameter are displayed in the inset. Contacts are numbered starting from the tip of the electrode. (B) 16-contact subdural grid, arranged in four rows of four contacts each. Contact diameter is 4.0 mm, with a 10-mm contact spacing. Larger grid sizes (i.e., 32 contacts) are also commercially available (C) 4-contact subdural strip. Contact diameter and spacing are the same as in grids. All electrode images are used with authorization of DIXI medical.

(20–24 Hz) are particularly prominent in the frontal lobes,[24] while theta and alpha frequencies are prevalent in the temporo-parieto-occipital recordings.[25,26] Within the temporal lobes, delta activity can be found as well (0.75–2.25 Hz), with a maximum over the hippocampal regions.[26] The mu and alpha rhythms are easily seen in central (mu is abolished by hand movement) and occipital regions.[25] Well-sustained beta frequencies of about 25 Hz were described in the precentral and postcentral gyri with lower frequencies present in the postcentral region (Figure 4).[27] In the brain atlas of normal SEEG recordings based on data of 106 subjects from three tertiary epilepsy centers, alpha activity was seen in a lower frequency in the temporal lobe (7.75–8.25 Hz) when compared to the occipital regions.[26] But still, in clinical practice, it is complicated to reliably identify brain regions just from their SEEG patterns. Physiologic high-frequency oscillations (HFOs) mostly occurring in the

ripple range (80–250 Hz) are predominantly seen in the pre- and postcentral gyri, the mesiotemporal region and the occipital lobe (Figure 5).

2.1.2 | Specifics on interictal epileptiform discharges in SEEG

The definition of interictal epileptiform discharges (IEDs) follows the same criteria as the ones used in the visual analysis of scalp EEG. The International Federation of Clinical Neurophysiology defines an IED as a waveform that fulfills at least 4 out of 6 of the following: (1) di- or tri-phasic wave with sharp or spiky morphology (i.e., pointed peak); (2) different wave durations than the ongoing background activity; (3) asymmetry of the waveform, with a sharply rising ascending phase and a more slowly decaying descending phase, or
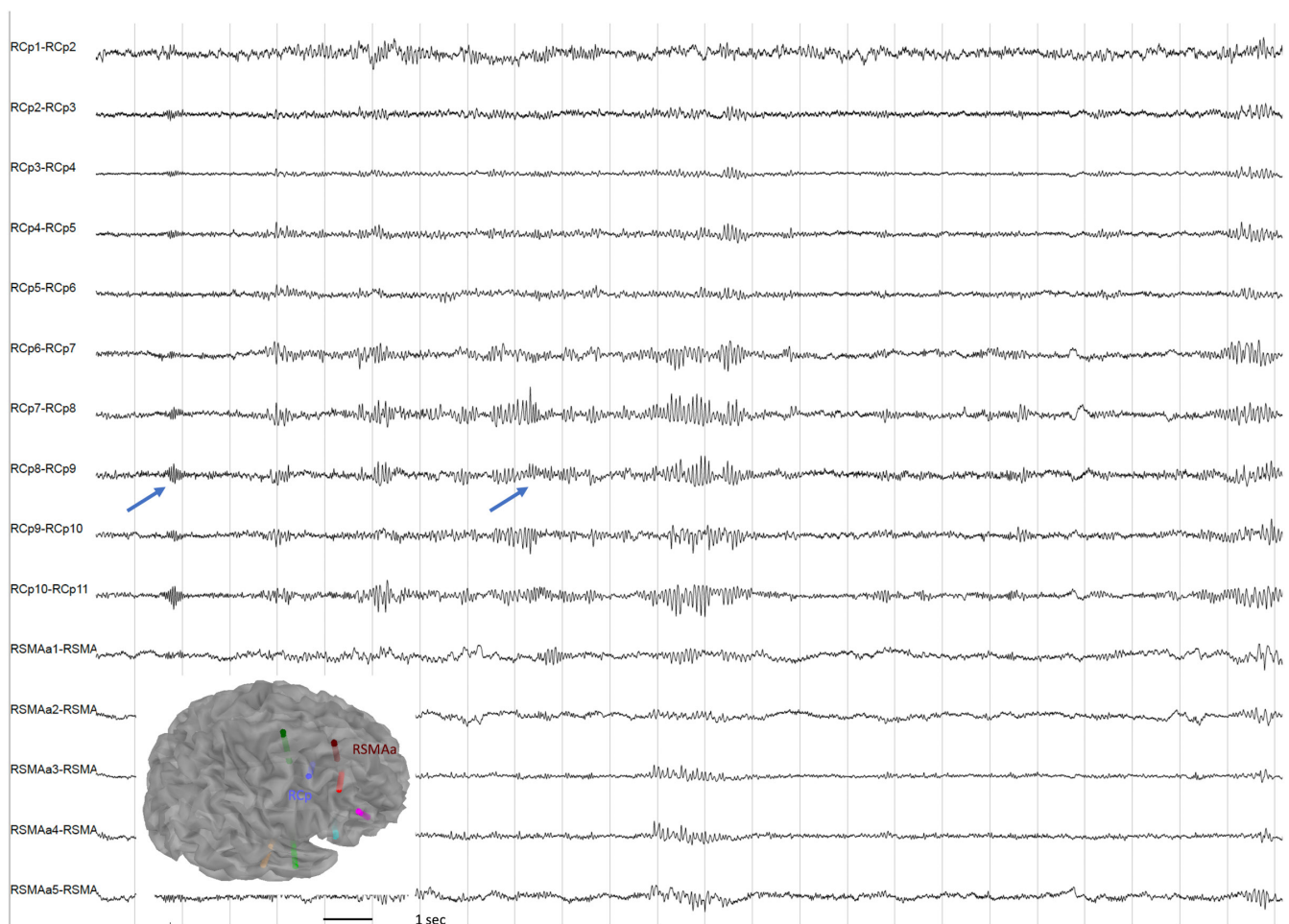
FIGURE 4 Physiological beta activity. SEEG recording during wakefulness from a 42-year-old man with a right orbitofrontal DRE. Bursts of beta activity (blue arrows) are typically present over the motor and premotor areas. RCp was targeting the right mid-cingulate, and RSMAa was targeting the right pre-supplementary motor area. *Display parameters*: *Bipolar montage – a selection of electrodes is showed for educational purposes – BP: [0.5–100 Hz].* DRE, Drug-resistant epilepsy; SEEG, Stereo-electroencephalography.
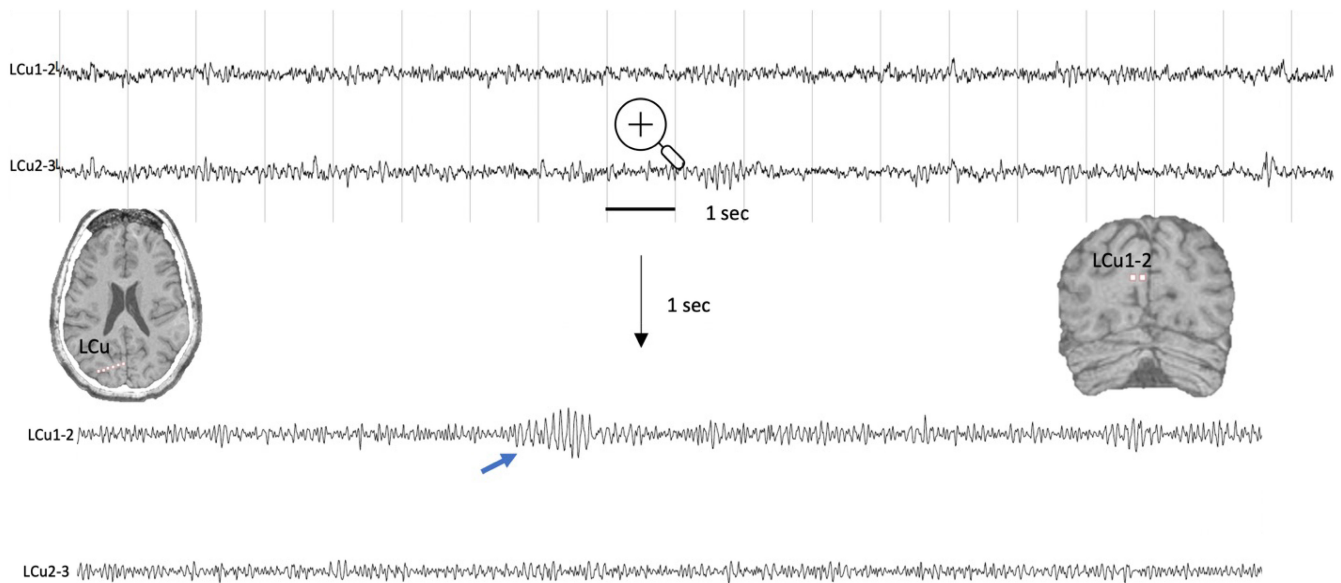
FIGURE 5 Physiological high-frequency oscillations (HFO). SEEG recording during wakefulness from a 26-year-old woman with a left temporal DRE. LCu was targeting the left cuneus. *Display parameters*: *Bipolar montage – a selection of electrodes is showed for educational purposes – BP: [0.5–100 Hz]* before the zoom. After applying a high-pass filter of 150 Hz, a physiological HFO with more than four oscillations (blue arrow) is visible over the contacts targeting the cuneus. DRE, Drug-resistant epilepsy; SEEG, Stereo-electroencephalography.

vice versa; (4) the transient is followed by an associated slow after-wave; (5) the background activity surrounding IEDs is disrupted by the presence of the IEDs; (6) distribution of the negative and positive potentials on the scalp suggests a source of the signal in the brain, corresponding to a radial, oblique, or tangential orientation of the source.[28] Special clarification needs to be mentioned regarding the 6th criterion, considering that (a) artifact signals are far less frequently seen in intracerebral contacts in comparison with the scalp, (b) the non-uniform distribution of the sensor space in SEEG does not allow for a quick access to voltage maps, and (c) in intracerebral recordings, it is not unusual for IEDs to have positive and/or negative polarities (in referential montage), and more than one positive and/or negative phase reversal (in bipolar montage). This is explained by the orientation in which the electrode contacts face the dipole layer.[29] Signals are also significantly sharper contoured and of higher amplitude than what is seen on the scalp given lack of attenuation by the skull, and also due to the solid angle in which the contacts see the dipole layer.[29] Most of the time the visual analysis by a trained neurophysiologist is enough to establish that the source of the suspected IED is in the brain. In the case of very focal IEDs, analysis of polarity reversal along the set of contacts could be used to locate the generator. In this situation, analyzing the SEEG tracings in a referential montage could be useful.

2.1.3 | Pathology-specific patterns

Historically, interictal non-epileptiform activity, in particular persistent focal slowing, has been used to define the lesional zone by SEEG.[7] However, the correspondence with the SOZ is limited (Figure 6). Unfortunately, no specific pattern for the temporal lobe epilepsy interictal activity has been described in the literature yet – see comprehensive review of Paredes-Aragon et al..[30] Recordings from hippocampal sclerosis are characterized with a mixture of slow activities and high-amplitude spikes or spike slow waves (Figures 7 and 8). But analogous findings can be seen in the gliotic or histologically normal hippocampus.

In contrast however, several interictal SEEG patterns have been described in focal cortical dysplasia (FCD): (i) continuous or subcontinuous epileptiform discharges (Figures 9 and 10): rhythmic epileptiform discharges occurring for at least 10 s in frequency of >1 Hz,[31] (ii) repetitive bursting spikes: burst of rhythmic polyspikes lasting 2–10 s,[31,32] (iii) slow wave/gamma burst: slow wave or spike-and-slow wave complex (0.5–1 Hz) superimposed by low-voltage gamma oscillations (40–55 Hz).[20,33,34] The existence of a peculiar interictal pattern characterized by the presence of repetitive and rhythmic spike and polyspike and wave, frequently associated with short bursts of fusiform micro polyspikes (Figure 11), has been revealed in FCD type IIb by the group at the Niguarda Hospital, Milan, Italy.[35] Later, the same group characterized lesion-specific
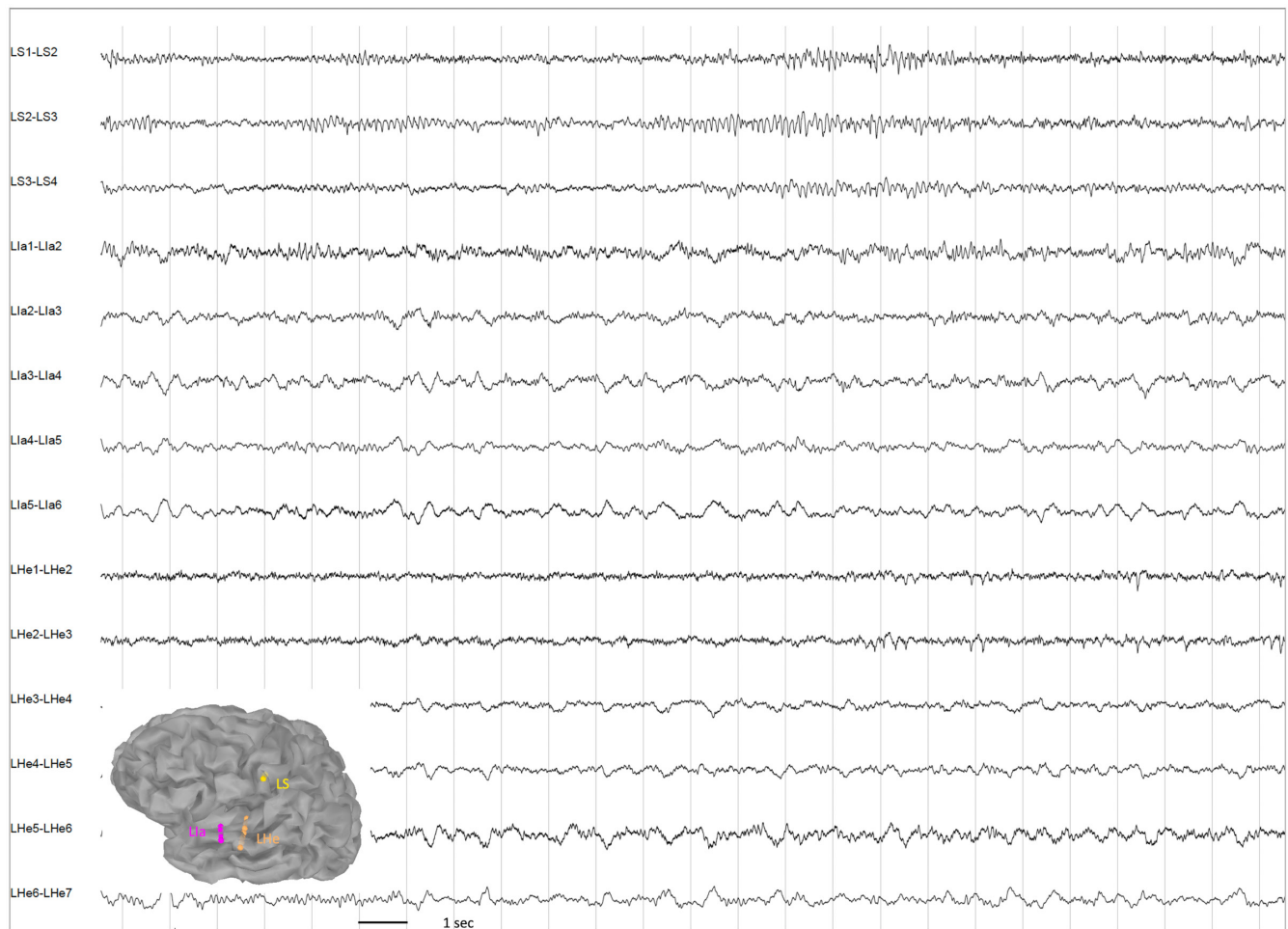
FIGURE 6 Pathological slow wave activity. SEEG recording during wakefulness from a 36-year-old woman with a left insular DRE. While normal awake background was seen over LS, pathological slow wave activity in the delta range was visible over the contacts targeting the left anterior insula–anterior temporal gyrus (LIa1-6) as well as the contacts targeting the left Heschl's gyrus (LHe3-7). LS was targeting the left postcentral gyrus, LIa was targeting the left anterior insula, and LHe was targeting the posterior insula-Heschl's gyrus. *Display parameters*: *Bipolar montage – a selection of electrodes is showed for educational purposes – BP: [0.5–100 Hz].* DRE, Drug-resistant epilepsy; SEEG, Stereo-electroencephalography.

interictal activity in FCD type II by total absence of background activity and pseudoperiodical occurrence of "brushes" – repetitive, high amplitude, and fast spikes.[36]

A lesion-specific interictal SEEG activity was shown in periventricular nodular heterotopia: intranodular background rhythms consisted of flattening periods mixed with low-voltage low-frequency activities, with frequent angled high-voltage spikes, asynchronous among different nodules and synchronous with the overlying cortex in the majority of cases (Figure 12).[36] Interictal lesion-specific findings have been described for tubers, presenting as continuous or near-continuous trains of rhythmic

focal spike-and-wave discharges on an attenuated background.[37,38] In the case of polymicrogyria, an interictal pattern characterized by low-voltage background associated with fast activities has also been described.[36]

To conclude, interictal SEEG patterns are generally just partially and weakly mirroring the underlying epileptogenic lesion. In selected cases, detailed analyses of interictal SEEG signals, including HFO rates, spikes, and their characteristics, together with functional connectivity measures seem to be able to uncover a lesion-specific "fingerprint," and using a predictive model to identify the quintessence of the epileptogenic lesion.[39]
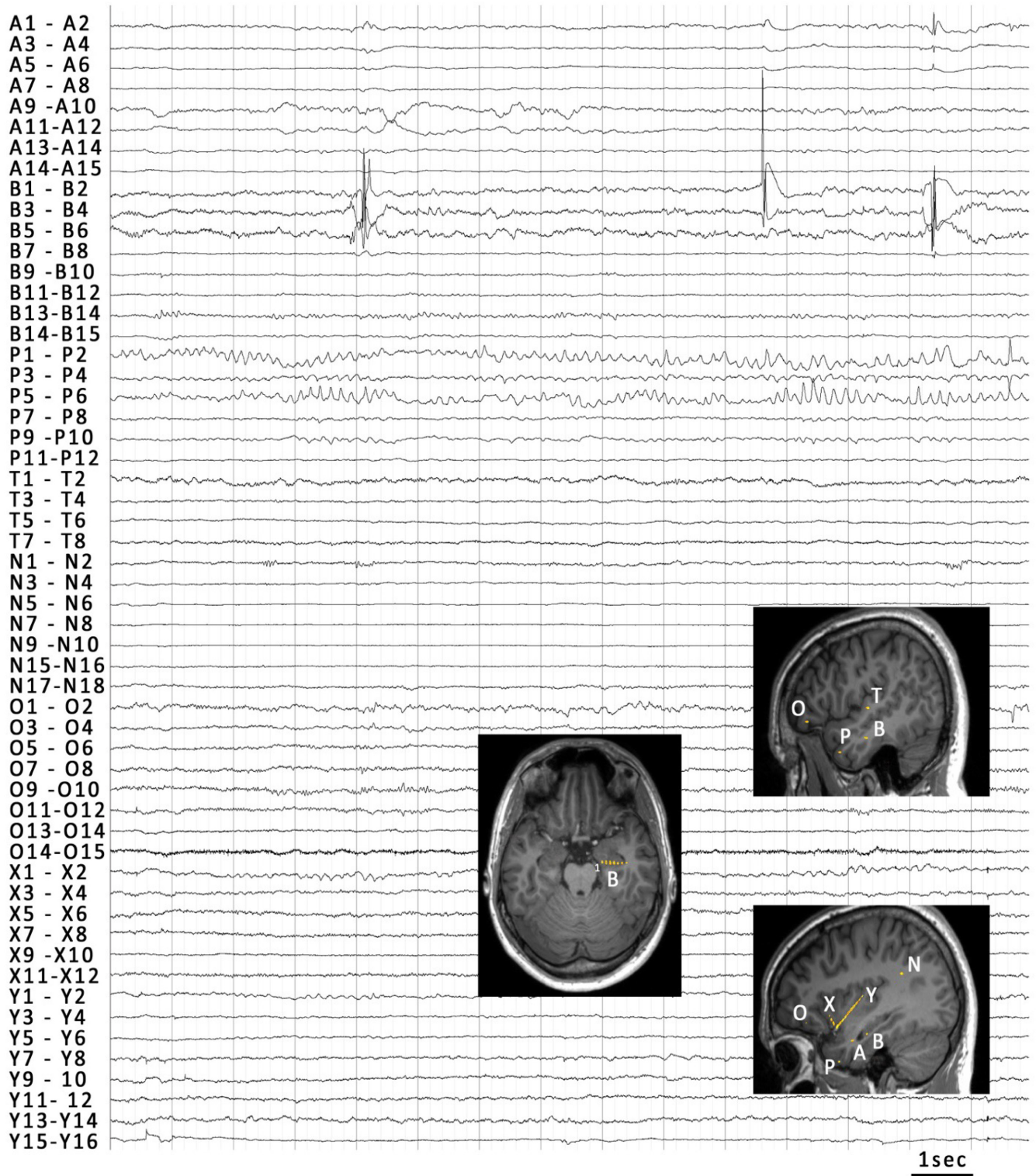
FIGURE 7 High-amplitude spikes and spike-slow waves within the sclerotic hippocampus (contacts B 1–5) propagating to the ipsilateral amygdala (contacts A 1–4).
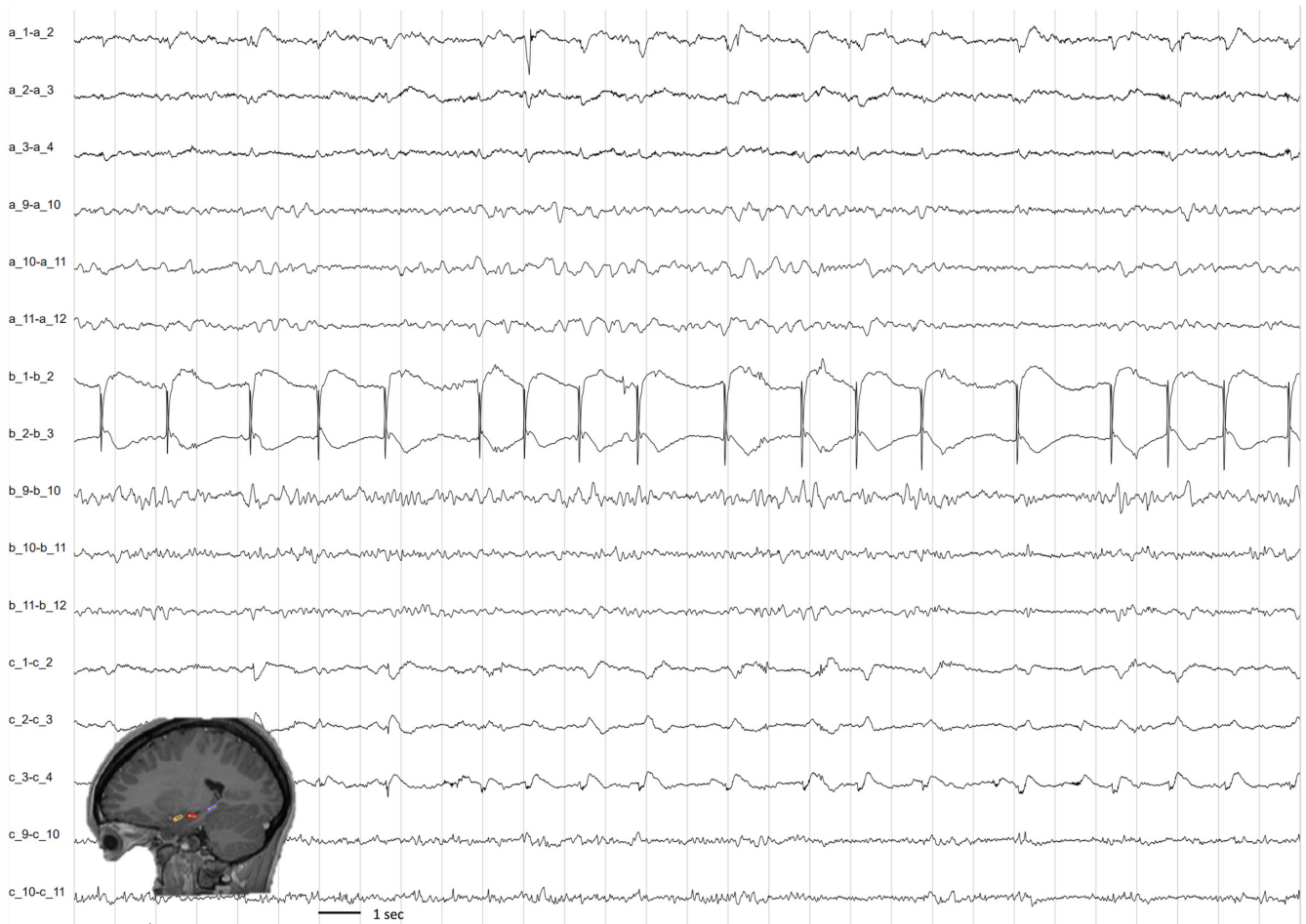
FIGURE 8 Typical interictal pattern of hippocampal sclerosis. SEEG recording from a 22-year-old woman with a left mesiotemporal DRE. The interictal activity from wakefulness is characterized by abundant low-frequency high-amplitude pseudo-periodic spikes involving mainly the anterior hippocampus (b_1–3) with a diffusion to the left amygdala (a_1–4), and posterior hippocampus (c_1–4). An increase of the sensitivity is needed for the visualization of the activity in the amygdala. Electrode a_ was targeting the left amygdala, b_ was targeting the left anterior hippocampus, and c_ was targeting the left posterior hippocampus. This patient underwent a standard left anterior temporal lobectomy. Pathology confirmed hippocampal sclerosis. She is Engel Ia with a follow-up of 4 years. *Display parameters*: *Bipolar montage – a selection of electrodes is showed for educational purposes – BP: [0.5–100 Hz]*. Figure showed with the courtesy of Dr Philippe Kahane from the University Hospital of Grenoble (France). DRE, Drug-resistant epilepsy; SEEG, Stereo-electroencephalography.

FIGURE 9 Continuous epileptiform discharges in FCD IIa (contacts F1–3) (A) Bipolar montage, (B) Unipolar montage.
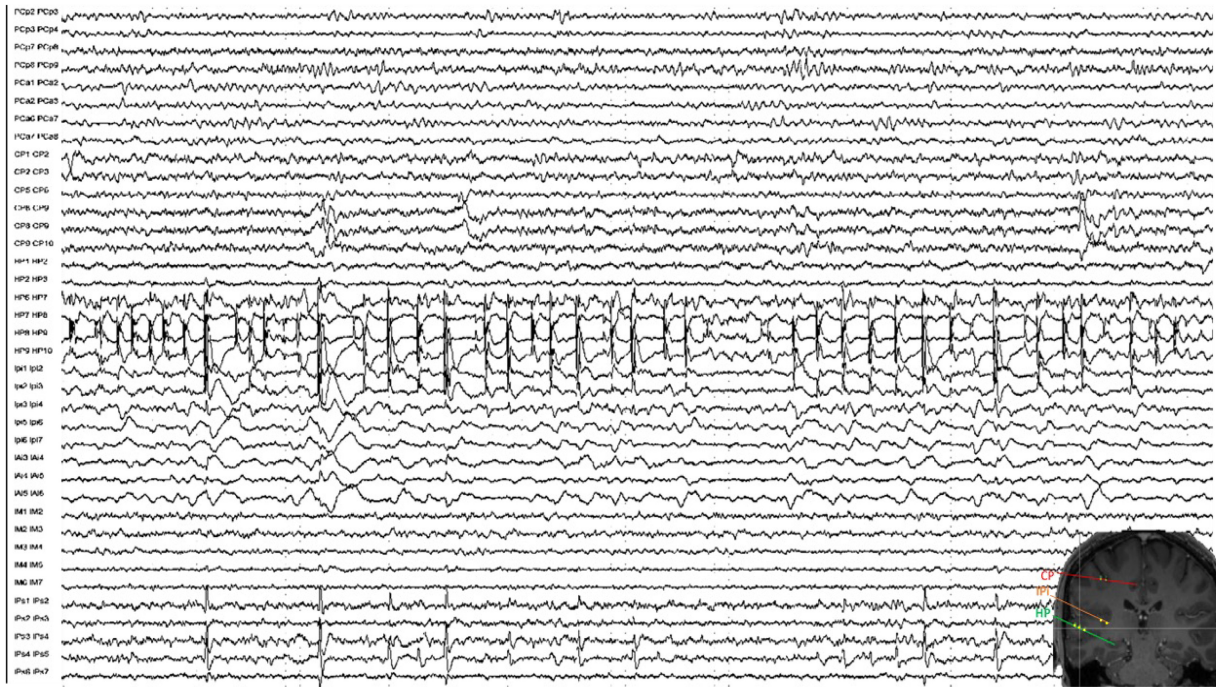
FIGURE 10 Typical interictal pattern of a FCD type II. Interictal SEEG recording of a 23-year-old woman with a right temporo-insular DRE. The interictal SEEG pattern is characterized by high-frequency low-amplitude repetitive spiking in the lateral contacts of electrode HP (HP 7–8, HP 8–9, HP 9–10) as well as the mesial contacts of electrode IPi (IPi 1–2, IPi 2–3, IPi 3–4, IPi 4–5) and to a lesser extent IPs (IPs 1–2, IPs2-3, IPs 3–4). Electrode HP was targeting the posterior part of the hippocampus with the most active contacts (HP 7–8, HP 8–10) located in the superior temporal gyrus, close to the Heschl's convolutions, concordant with the semiology of unilateral acoustic sensations as the initial symptom of the patient's seizures. Electrode IPi and IPs targeted the posterior part of the insula inferior and superior. The patient underwent laser ablation of the right superior temporal gyrus and posterior part of the insula with a seizure outcome of Engel 1B.

FIGURE 11 Rhythmic spikes and polyspike and waves in FCD IIb in a referential montage (contacts T'1–T'2). Analyzing the SEEG tracings in a referential montage can be useful for locating the generator and should be used in addition to the analysis in a bipolar montage.
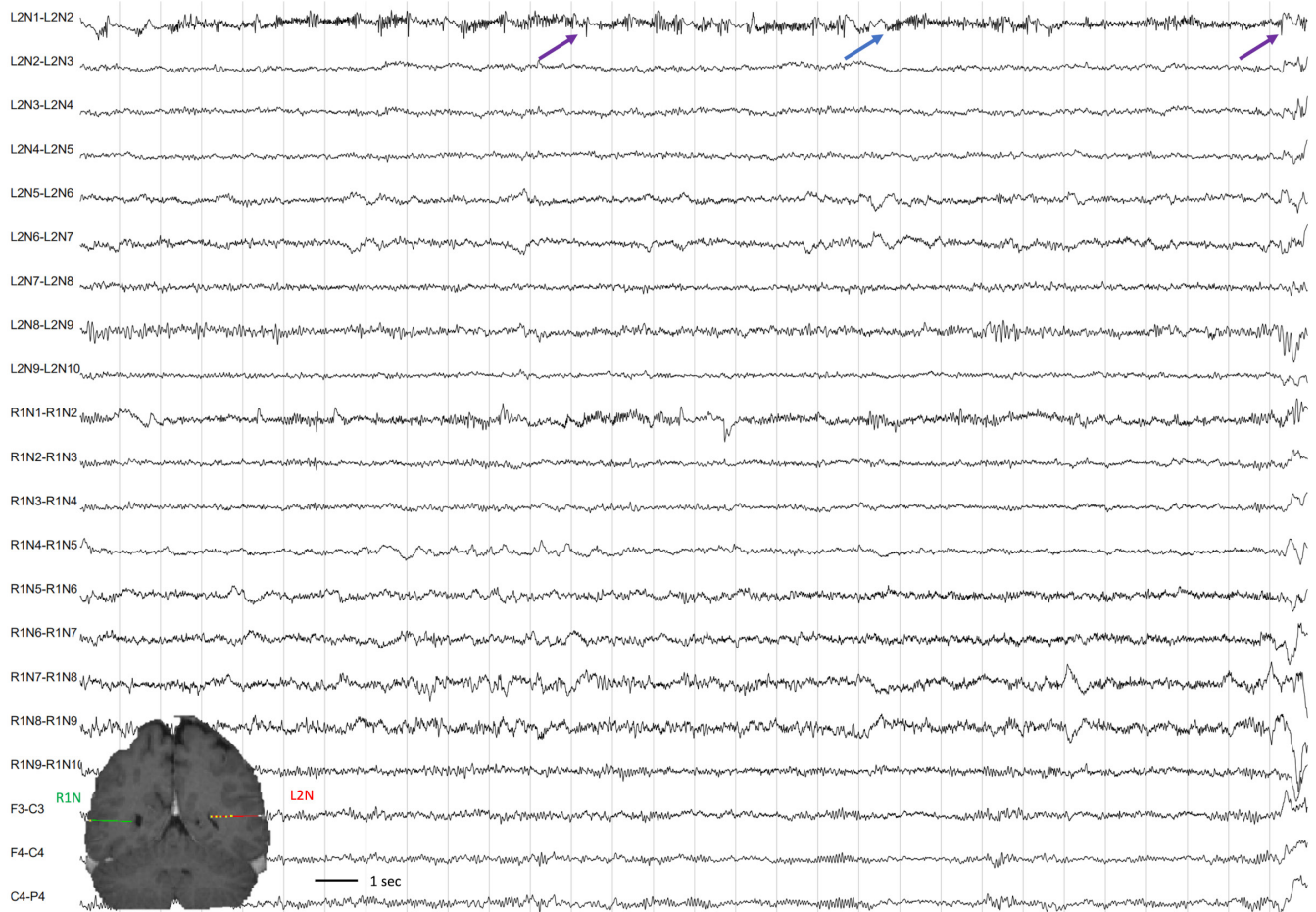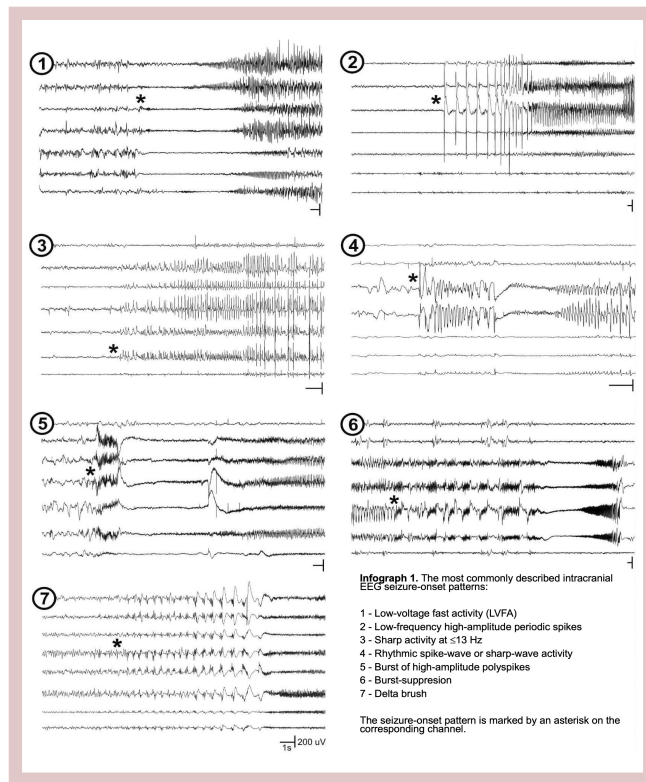
FIGURE 12 Typical interictal pattern of periventricular nodular heterotopia. SEEG recording from a 29-year-old woman with a left posterior quadrant DRE. The interictal activity from NREM 2 sleep is characterized by abundant bursts of LVFA (blue arrow) and low-amplitude spikes (purple arrows), sometimes associated with spikes with a triangular morphology, involving mainly L2N 1–2. For visualization, an increase of the sensitivity is needed to correctly evaluate the activity within the nodular heterotopia. L2N was targeting one of the left posterior nodules, R1N was targeting one of the posterior nodules. *Display parameters*: *Bipolar montage – a selection of electrodes is shown for educational purposes – BP: [0.5-100 Hz]*. DRE, Drug-resistant epilepsy; LVFA, Low-voltage fast activity; NREM, Non-rapid eye movement; SEEG, Stereo-electroencephalography.

2.2 | ICTAL PATTERNS

Given that a seizure is a dynamic process, it is important to carefully analyze the dynamics and pay attention to the following four points: (i) The first clinical signs should be observed after or at least concomitantly with the SEEG onset (otherwise the "true" SOZ has been missed); (ii) it is important how the onset emerges from the trace with respect to the interictal activity (in FCD, one often sees an acceleration of interictal spikes followed by a polyspike discharge prior to LVFA); (iii) it should be analyzed how the discharge evolves (some channels may exhibit a convincing fast activity at onset, but the evolution shows that they stop seizing); and (iv) a careful analysis of the offset is important as well and it should be assessed which channels are flat at seizure termination.

2.3 | Description of intracranial EEG seizure-onset patterns

Infograph 1. The most commonly described intracranial EEG seizure-onset patterns:

1 - Low-voltage fast activity (LVFA)
2 - Low-frequency high-amplitude periodic spikes
3 - Sharp activity at ≤13 Hz
4 - Rhythmic spike-wave or sharp-wave activity
5 - Burst of high-amplitude polyspikes
6 - Burst-suppression
7 - Delta brush

The seizure-onset pattern is marked by an asterisk on the corresponding channel.

Intracranial EEG signals at seizure-onset can be classified[40] according to different parameters, including frequency, spatial distribution, and morphology.[41] Here, we focus on morphological patterns based on visual inspection. Numerous descriptions of intracranial EEG seizure-onset patterns exist in the literature, and consensus on which terminology should be used is still lacking.[33] Also, some of the terms used in SEEG deviate from standard EEG terminology,[42] another aspect that may benefit from standardization. Generally speaking, we can differentiate between seizure-onset patterns with and without low-voltage fast activity (LVFA). Rather than listing all published descriptions, we refer to the first comprehensive classification describing intracranial EEG seizure-onset patterns,[43] which include the following:

1. *LVFA* characterized by a clearly visible >13 Hz activity, typically <10 μV in initial amplitude, which may be accompanied by a slow wave or DC shift[20,36,41,43–46] (Figure 13). LVFA is the most common and most important intracranial EEG seizure-onset pattern, found in approximately 60% of patients undergoing SEEG investigations[20,33,36,43] or intracranial recordings with subdural strips/grids.[41] LVFA can be extremely focal, but also widely extended (focal versus network organization).
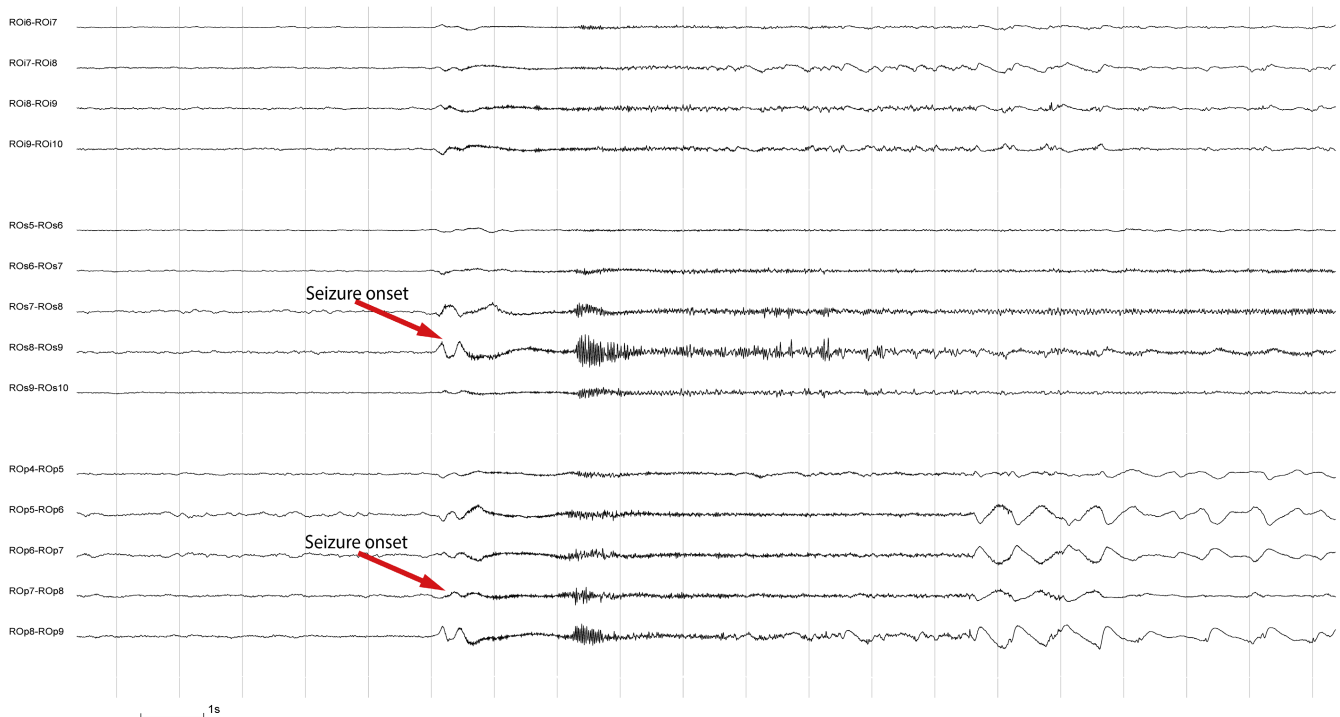
FIGURE 13 Type 1 seizure-onset pattern characterized by a 20–25 μV LVFA and baseline shift in electrode contacts ROp 5–9 and ROs 6–10. *Display parameters: Bipolar montage – a selection of electrodes is shown for educational purposes – BP: [0.5–100 Hz].* LVFA, Low-voltage fast activity; RLi, Right lingual gyrus; ROi, Right occipital inferior; ROp, Right occipital pole; ROs, Right occipital superior.

2. *Low-frequency high-amplitude periodic spikes*, consisting of high-voltage spiking at 0.5–2.0 Hz, which lasts >5 s[20,43,47,48] (Figure 14). The prevalence of this patterns in series of patients undergoing intracranial EEG recordings varies widely (0%–20%), according to the type of patients studied and is most frequently found in mesiotemporal lobe epilepsy with hippocampus sclerosis.[20,33,46]

3. *Sharp activity at ≤13 Hz* is defined by low- to medium-voltage (higher than LVFA) sharply contoured or sinusoidal rhythmic activity, typically in the alpha–theta range that shows a clear evolution in time[20,36,41,43–45,49] (Figure 15). This pattern has been found in 10%–20% of patients undergoing intracranial EEG investigations.[36,43]

4. *Rhythmic spike-wave or sharp-wave activity* is characterized by medium- to high-voltage spike-wave or sharp-wave complexes, generally occurring at a greater frequency than low-frequency high-amplitude periodic spikes (i.e., ≥2.0 Hz)[43,44,46,49] (Figure 16). This pattern has been reported in 5%–15% of implanted patients.[33,43,46]

5. *Burst of high-amplitude polyspikes* consist of a single brief (<5 s) burst of high-voltage, high-frequency (typically >12 Hz) polyspikes, followed by LVFA[20,41,43,44] (Figure 17). This definition shows some deviation from

EEG standard terminology, in that burst should not be used as synonym of paroxysm, and in its stricter sense, the designation of paroxysm of high-amplitude polyspikes might be better aligned with the current standard EEG terminology.

6. *Burst suppression, or better termed repetitive spike bursts*, is defined by brief bursts of medium- to high-voltage spikes alternating with brief periods of voltage attenuation, followed by sustained fast activity[20,43] (Figure 18).

7. *Delta brush* consists of rhythmic delta waves occurring at 1.0–2.0 Hz, with brief bursts of low-amplitude fast (20–30 Hz) activity superimposed on each delta wave. Similar to other patterns, delta brush is typically followed by LVFA[43] (Figure 19). In standard EEG terminology however, delta brush is a designation used to describe a normal neonatal graphoelement that consists of a combination of delta wave with superimposed fast activity >8 Hz.[42]

The most commonly described intracranial EEG seizure-onset patterns are shown in Infograph 1. Burst of high-amplitude polyspikes, burst suppression, and delta brush are less common than other patterns, having been described in <10% of patients undergoing intracranial EEG investigations.[20,43,44]
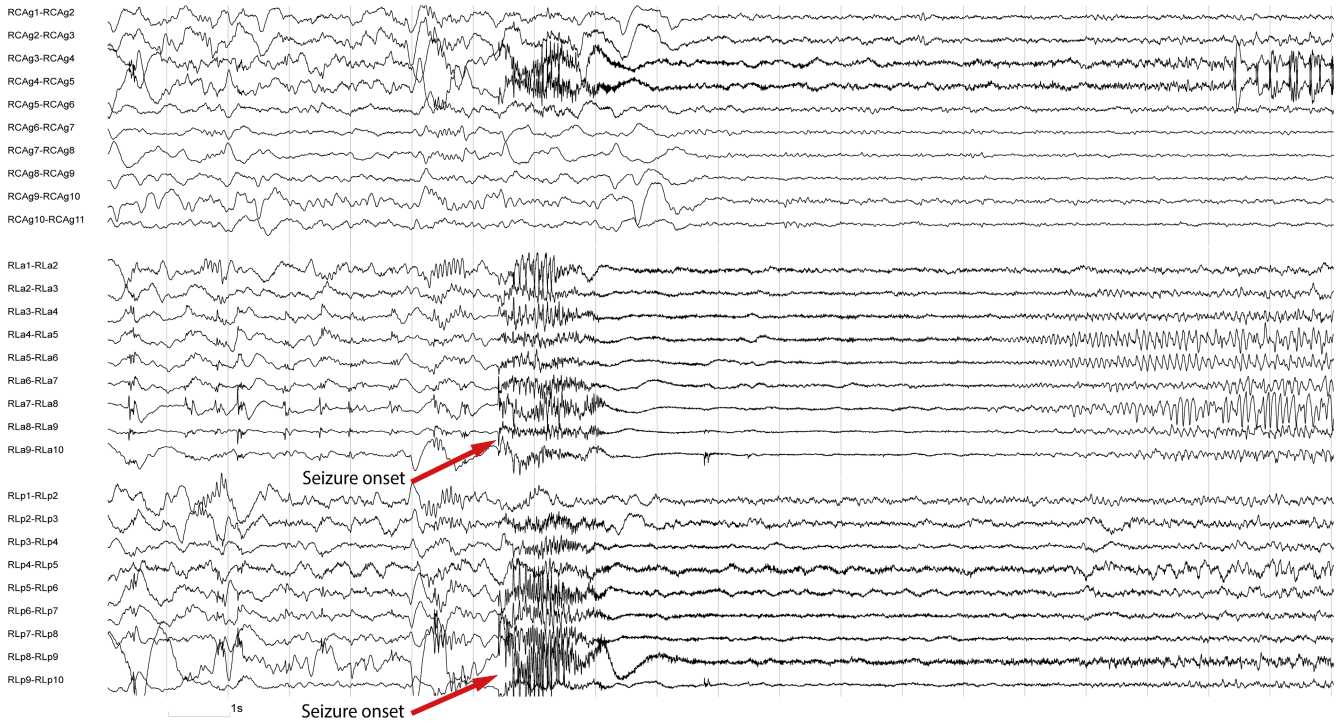

FIGURE 14 Type 2 seizure-onset pattern characterized by low-frequency and high-amplitude periodic spikes seen in RH 1–3. *Display parameters: Bipolar montage – a selection of electrodes is shown for educational purposes – BP: [1.0–100 Hz].* RA, Right amygdala; RH, Right anterior hippocampus; RHp, Right posterior hippocampus.
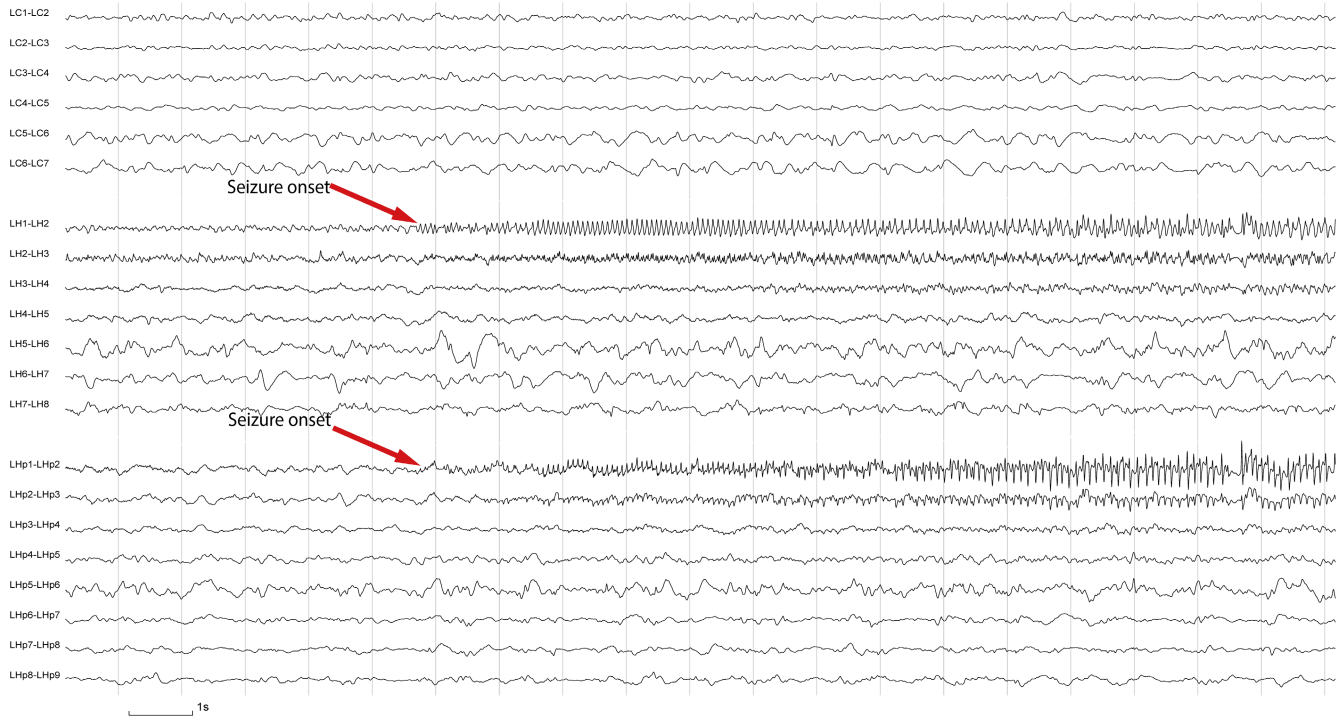
FIGURE 15 Type 3 seizure-onset pattern characterized by ≤13 Hz sharp activity seen in LH 1–3 and LHp 1–2. *Display parameters: Bipolar montage – a selection of electrodes is shown for educational purposes – BP: [1.0–100 Hz].* LC, Left cingulate; LH, Left anterior hippocampus; LHp, Left posterior hippocampus.
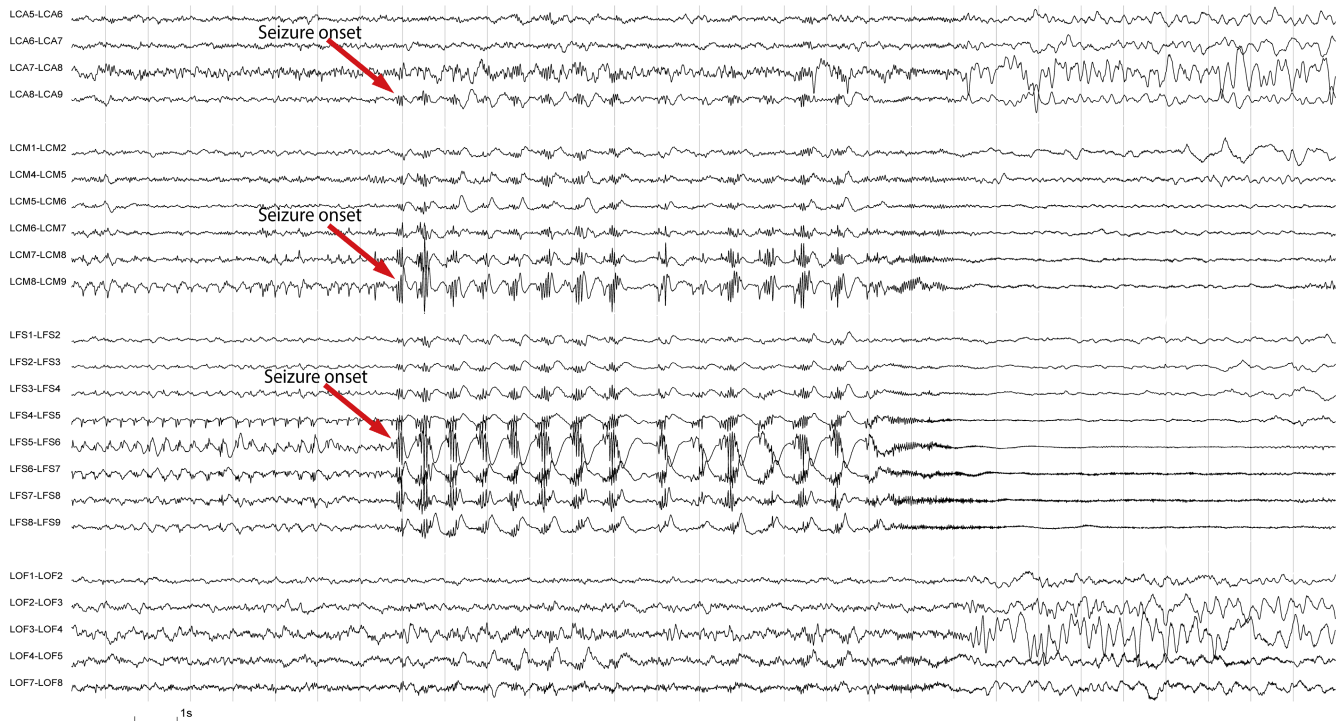

FIGURE 16 Type 4 seizure-onset pattern characterized by spike-and-wave activity seen in ROF 7–10. *Display parameters: Bipolar montage – a selection of electrodes is shown for educational purposes – BP: [1.0–100 Hz].* RA, Right amygdala; ROF, Right orbitofrontal.

FIGURE 17 Type 5 seizure-onset pattern characterized by a burst of high-amplitude polyspikes involving multiple contacts in electrodes RLp, RLa, and RCag. *Display parameters: Bipolar montage – a selection of electrodes is shown for educational purposes – BP: [1.0–100 Hz]*. RCag, Right anterior cingulate gyrus; RLa, Right hemisphere anterior to lesion; RLp, Right hemisphere posterior to lesion.
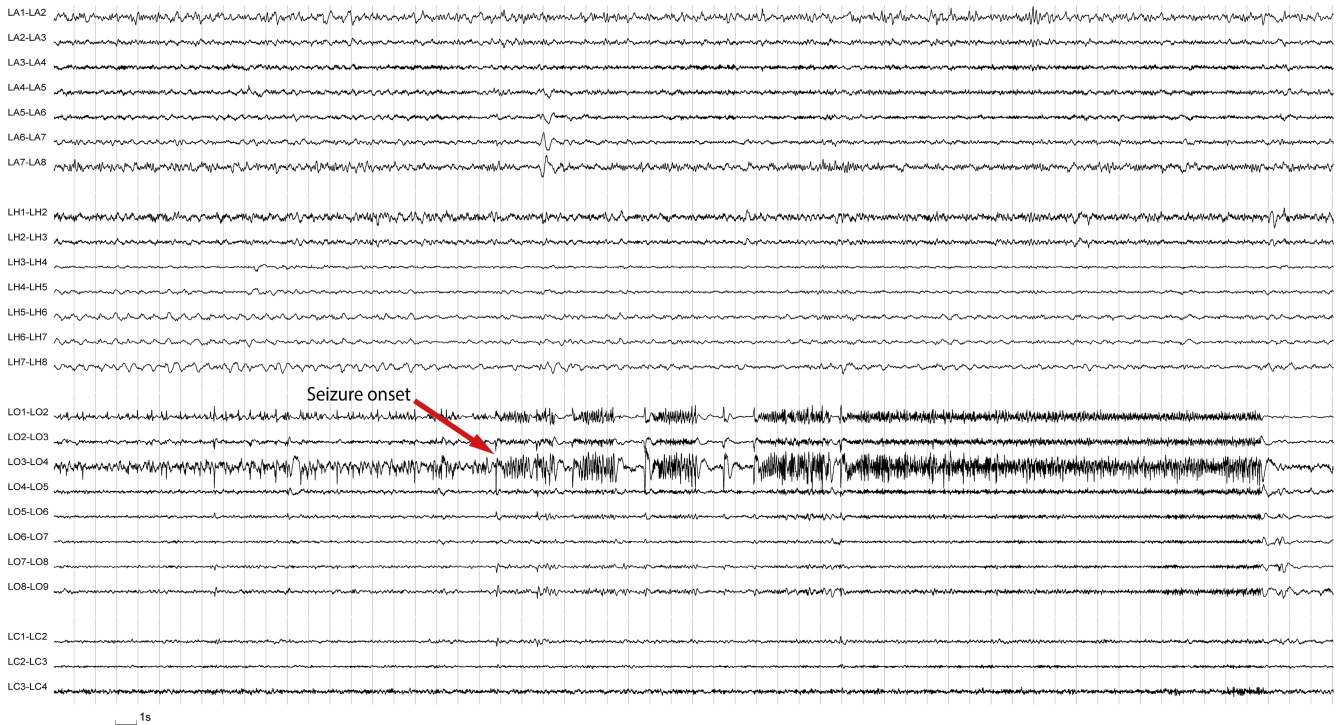
FIGURE 18 Type 6 seizure-onset pattern characterized by 2.0–2.5 s bursts of polyspikes alternating with 1.0–1.5 s voltage attenuation periods involving contacts LO 1–4. This pattern has been described in previous publications as a "burst suppression-like" pattern. *Display parameters: Bipolar montage – a selection of electrodes is shown for educational purposes – BP: [1.0–100 Hz]*. RLa, Right hemisphere anterior to lesion; RLp, Right hemisphere posterior to lesion; RSMA, Right supplementary motor area.

FIGURE 19 Type 7 seizure-onset pattern characterized by rhythmic delta activity with superimposed fast activity (delta brush-like activity), involving multiple contacts in electrodes LFS, LCM, and LCA. *Display parameters: Bipolar montage – a selection of electrodes is shown for educational purposes – BP: [0.5–100 Hz].* LCA, Left anterior cingulate; LCM, Left mid-cingulate; LFS, Left superior frontal; LOF, Left orbitofrontal.

2.4 | Spectral analysis of seizure-onset patterns

Spectrograms can be useful for the assessment of the different seizure-onset patterns. Some of the ictal patterns described above, as well as their interictal-to-ictal transition, show distinctive visual features that can be easily identified, depending on the characteristics of the time-frequency plot obtained. LVFA seizure-onset patterns are accompanied by a decrease or suppression of power in lower frequency bands (i.e., delta–theta), and more distinctively, they are associated with an abrupt increase in power in one or more narrow high-frequency bands (gamma or higher) that show a progressively descending slope, also known as down-chirping (Figure 20).[50] These patterns can be immediately preceded by a single spike or a burst of rhythmic pre-ictal spikes, which are characterized by short and repetitive broadband increases in power, mainly in the slow (delta to theta) and high (gamma or higher)-frequency power bands (Figure 20). Special methodologies of signal processing can be further applied to visually emphasize these specific seizure-onset changes (also known as "fingerprint"), which will be described later in this article (see Figure 44).

2.5 | Significance of seizure-onset patterns

Research of the past decade revealed that accounting for the different seizure-onset patterns is important for postsurgical prognosis.[20] On a group level, it was shown that patterns including LVFA are associated with a better postsurgical seizure outcome than slow seizure-onset patterns not including LVFA. In general, patterns with rhythmic alpha, theta, and delta activity should raise suspicion of a propagating instead of a true "ictal onset" pattern (Figure 21). This suspicion, however, should be based on more arguments than the seizure-onset pattern alone, as some patients with slow seizure-onset patterns do indeed become seizure free after epilepsy surgery.[20] Finally, it is also important to consider that the simple presence of LVFA does not necessarily imply that implanted electrodes sample the "true" SOZ but may also be seen in propagation areas including subcortical structures such as the thalamus (Figure 22).

It is known that similar lesions can generate distinct seizure-onset patterns, and conversely, that a seizure-onset pattern can be generated by distinct lesions.[20,33,43,51] Nevertheless, some seizure-onset patterns are more frequently encountered in certain pathologies.
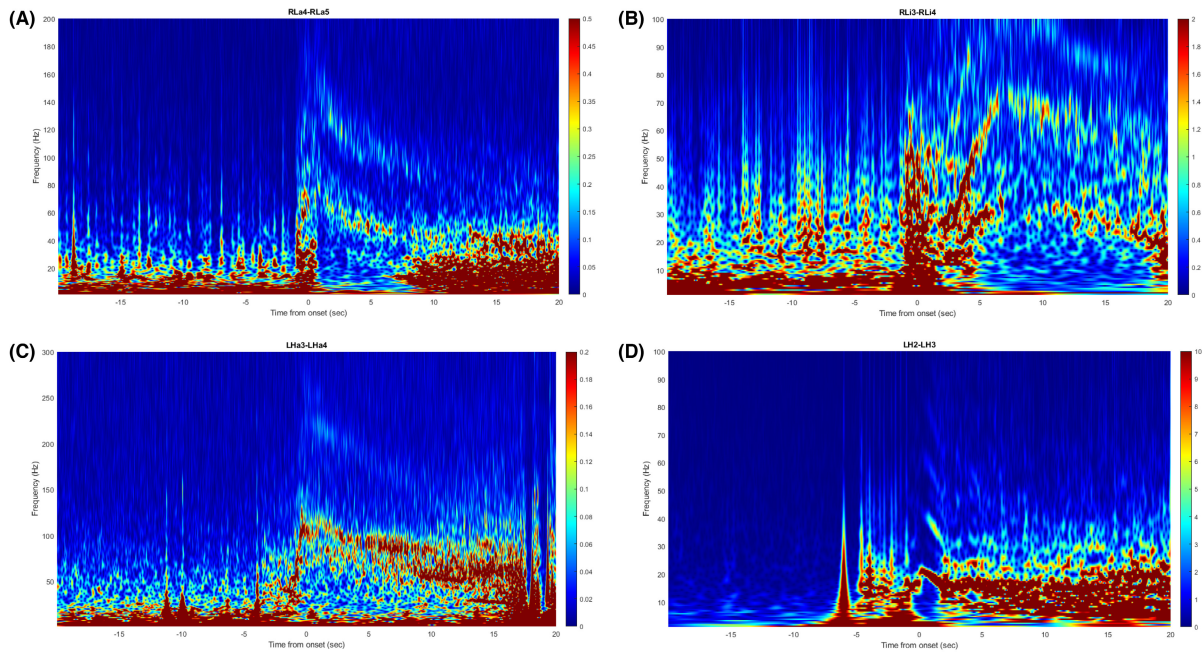
FIGURE 20 Spectrograms in different anatomical structures and pathologies. Time-frequency plots obtained from SEEG contacts located inside the SOZ of four patients with focal DRE showcasing pre-ictal spikes, fast activity, and suppression of low frequencies. Time 0 represents the ictal SEEG onset. Right after the onset, down-chirps (preceded or not by brief up-chirps) can be seen as a narrow band in the fast activity fundamental frequency, accompanied by one or more additional narrow bands in supraharmonic frequencies. (A) contacts RLa 4–5 are located in the anterior margin of a lesion (FCD 2B) in the right superior parietal lobule. (B) contacts RLi 3–4 are located in the inferior margin of a lesion (FCD 2A) in the right frontal convexity. (C) contacts LHa 3–4 are located inside a periventricular nodular heterotopia in the vicinity of the left anterior hippocampus. (D) contacts LH 2–3 are located in the left anterior hippocampus in a patient with anterior temporal FCD 3A and hippocampal sclerosis. Time-frequency plots were computed in MATLAB using the method described by Grinenko et al.,[50] without applying a baseline normalization. DRE, Drug-resistant epilepsy; FCD, Focal cortical dysplasia; LH, Left hippocampus; LHa, Left anterior hippocampus; RLa, Right lesion anterior; RLi, Right lingual gyrus; SOZ, Seizure-onset zone.
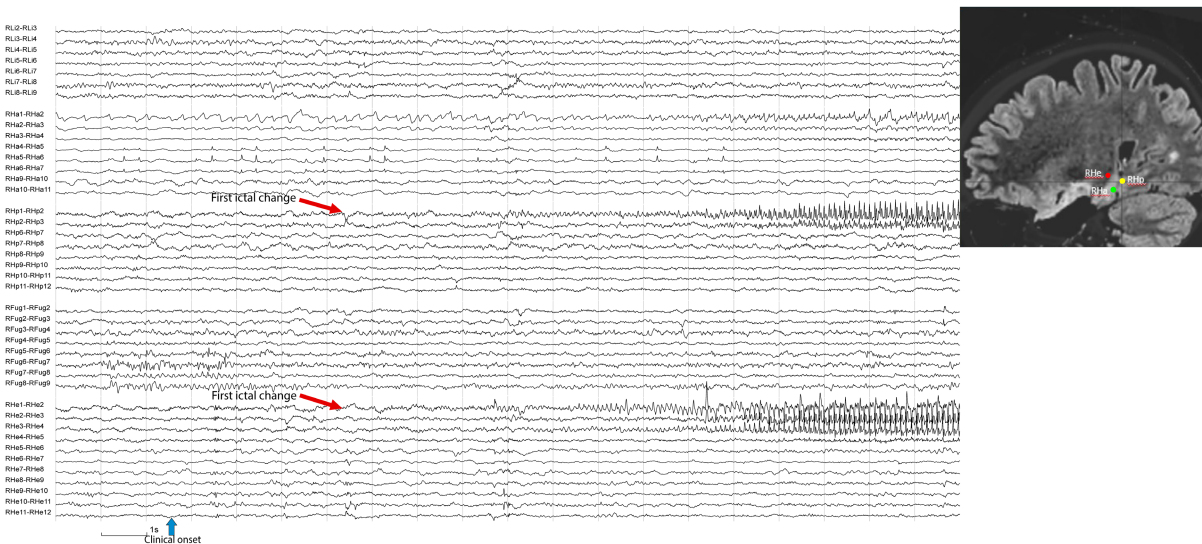

FIGURE 21 Missed real seizure onset. SEEG performed in a 36-year-old woman with right temporal drug-resistant epilepsy and history of two previous anterior temporal lobe resections. (A) First ictal changes (red arrow) were seen 4.5 s after the patient recognized the first clinical symptoms (blue arrow) in the posterior hippocampus. (B) Sagittal T2 FLAIR displaying the distal contacts of electrodes RHa, RHp, and RHe, located inside or in the vicinity of the posterior hippocampus. Notice the previous resection cavity and increased signal of the anterior mesiotemporal remnant. Lack of electrodes in that region was due to technical constraints during the implantation procedure. *Display parameters: Bipolar montage – a selection of electrodes is shown for educational purposes – BP: [0.5–100 Hz].* RFug, Right fusiform gyrus; RHa, Right anterior hippocampus; RHp, Right posterior hippocampus; RLi, Right temporal lobe (inferior to lesion). Only selected electrodes are seen for display purposes.

Low-frequency high-amplitude periodic spikes are a typical feature of seizures arising from the mesiotemporal lobe, especially in the presence of hippocampal sclerosis.[20,43,47,48] Low-frequency high-amplitude periodic spikes were shown to be associated with a good surgical outcome in mesiotemporal lobe epilepsy.[52] In contrast, bursts of polyspikes prior to LVFA and delta brush-like patterns are typically seen in focal cortical dysplasia (FCD) provided that they are preceded by an acceleration of the "interictal" subcontinuous spiking activity.[33,43] This latter finding is also of particular clinical interest in patients with MRI-negative epilepsy, because in this case, the observation of these patterns suggests the presence of an underlying pathology of FCD type II that is classically associated with a better postsurgical seizure outcome.

Apart from region and pathology, age may also play a role in the expression of the seizure-onset pattern. It was shown that children who had LVFA as their predominant seizure-onset pattern type were older than patients who did not have LVFA.[53] Finally, in a patient with unifocal epilepsy, more than one single seizure-onset pattern may be observed (Figure 23).[54] It was shown that the presence of multiple seizure-onset patterns emerging from the same SOZ compared to the presence of a single seizure-onset pattern was associated with a less favorable postsurgical outcome.[53]
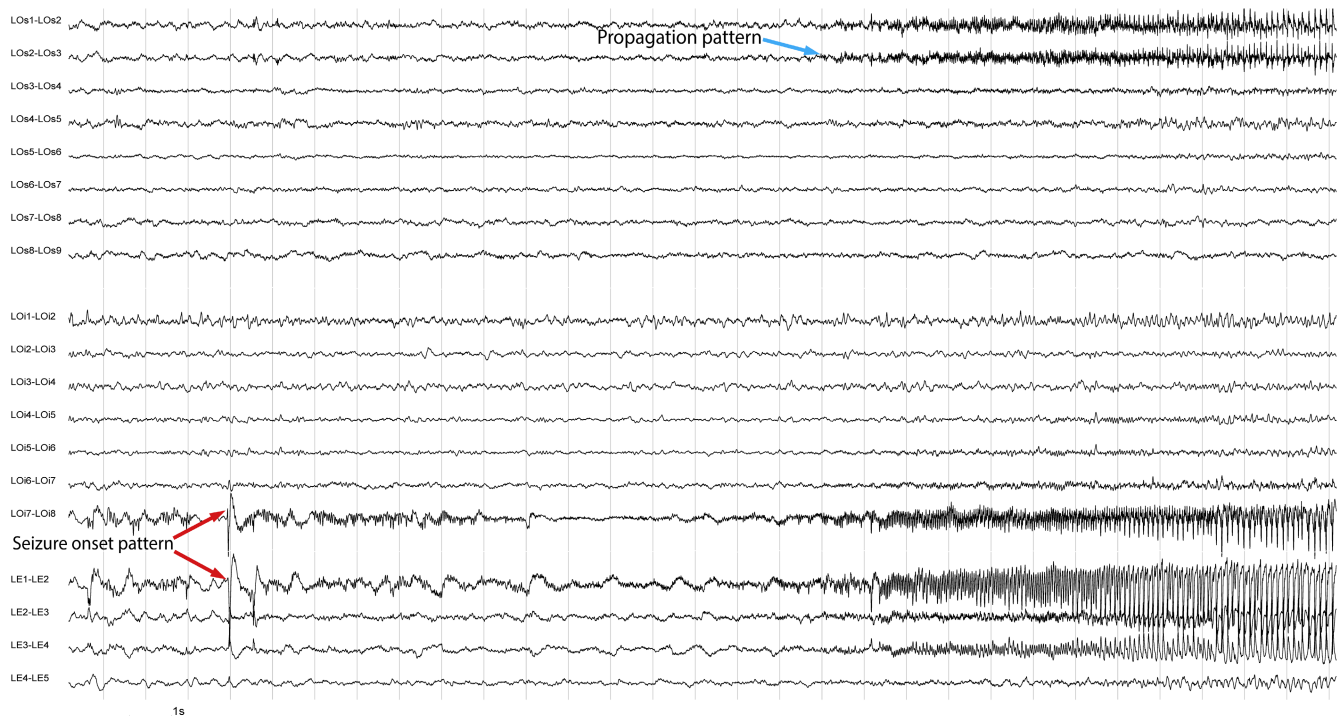
FIGURE 22 LVFA as an ictal propagation pattern. SEEG performed in a patient with left occipital drug-resistant epilepsy. First ictal changes were characterized by a 25–30 µV LVFA in infracalcarine contacts (red arrows in LOi 7–8 > LE 1–2; this was preceded by an increase in rhythmicity of the habitual interictal continuous spike/polyspike and wave pattern), before spreading to supracalcarine contacts (blue arrow), in which a LVFA pattern is also seen. If undersampled, the assumption of a seizure-onset zone in the supracalcarine cortex could have been made in this case. However, key here is that this LVFA was not preceded by the typical spike evolution as seen in the SOZ. This example illustrates how important it is to carefully analyze not only the seizure itself but the interictal-ictal transition to be able to differentiate the true SOZ from propagated activity. *Display parameters: Bipolar montage – a selection of electrodes is showed for educational purposes – BP: [0.5–100 Hz].* LE, Lesion; LO, Left occipital pole; LOi, Left infracalcarine cortex; LOs, Left supracalcarine cortex; LPC, Left precuneus; LVFA, Low-voltage fast activity.

FIGURE 23 Different SOPs arising from the same region. Right temporal DRE in a patient with HS. (A) typical mesial temporal lobe onset pattern (red arrow) is seen in LH 1–2, characterized by 1.0 Hz periodic spiking followed seconds later by rhythmic spikes at 4.0–5.0 Hz. (B) SOP is seen in LH 1–2 (red arrow), characterized by a 18–22 µV LVFA that later evolves into a rhythmic 10–11 Hz activity. (C) SOP characterized by 9–10 Hz repetitive spikes in LH 1–2 (red arrow), and also in LA 1–3, and LHp 1–3. *Display parameters: Bipolar montage – a selection of electrodes is showed for educational purposes – BP: [0.5–100 Hz].* DRE, Drug-resistant epilepsy; HS, Hippocampal sclerosis; LA, Left amygdala; LFP, Left frontal pole; LH, Left anterior hippocampus; LHp, Left posterior hippocampus; LOF, Left orbitofrontal cortex; LVFA, Low-voltage fast activity; SOP, Seizure-onset pattern.

(A) Preictal spiking
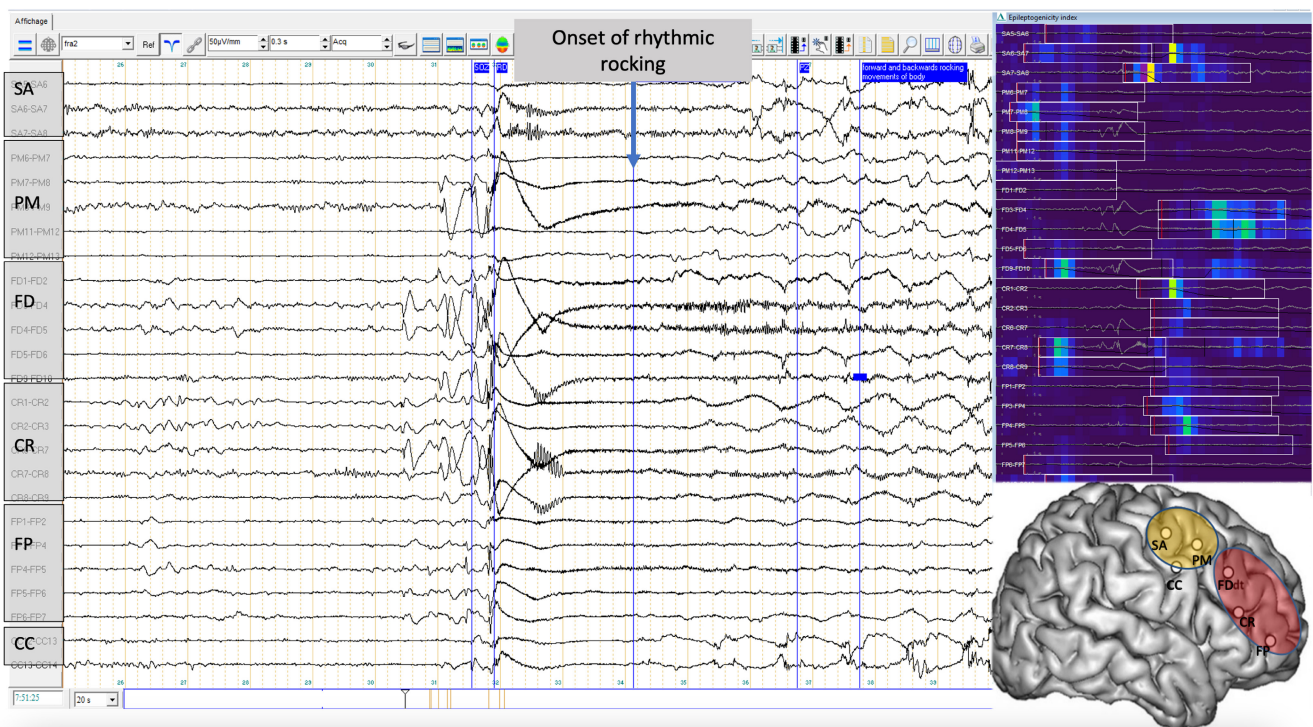
(B) Seizure onset
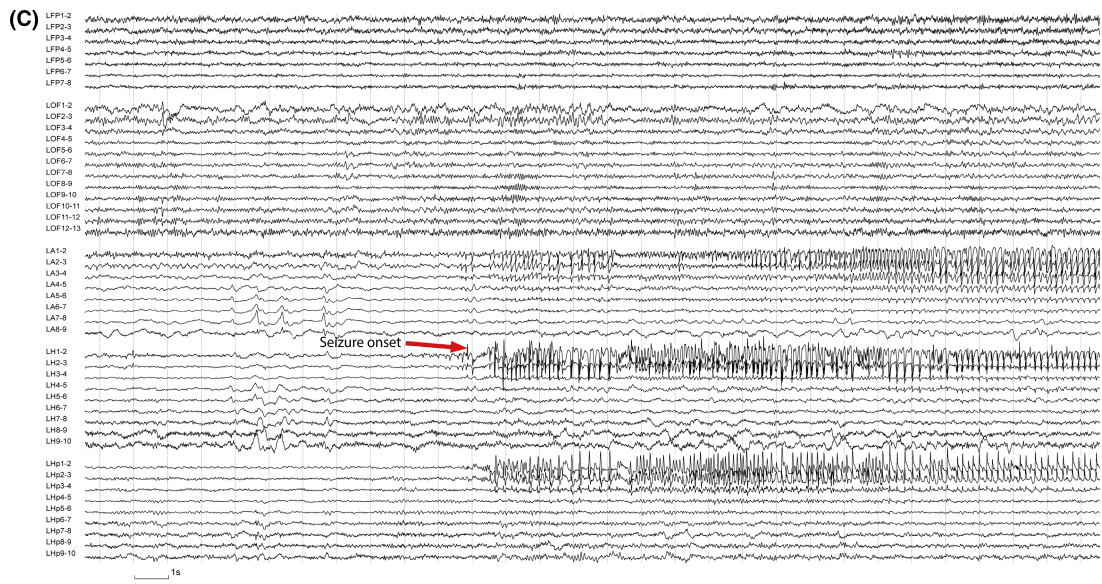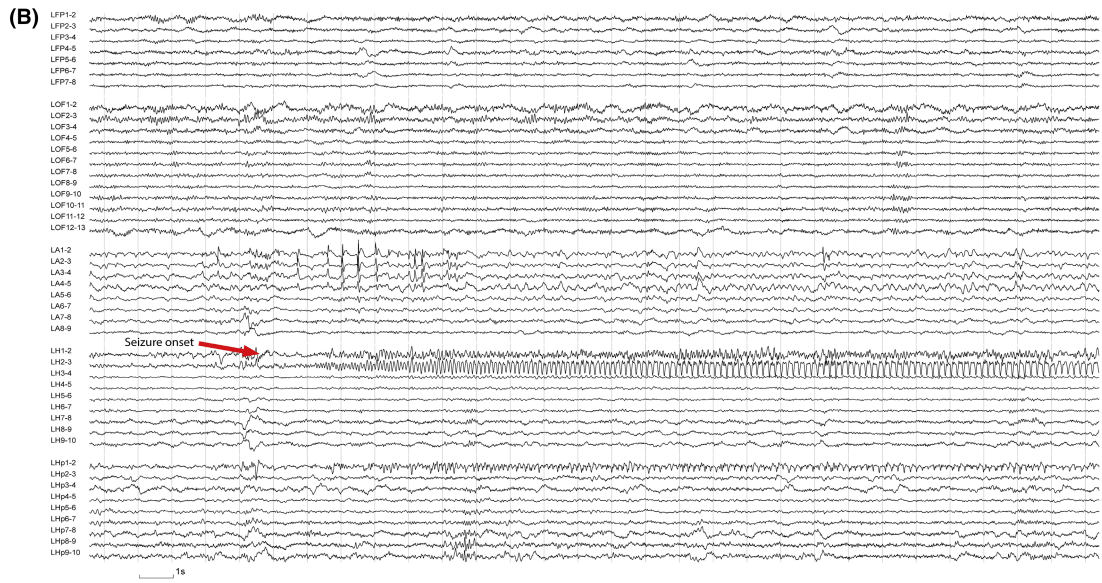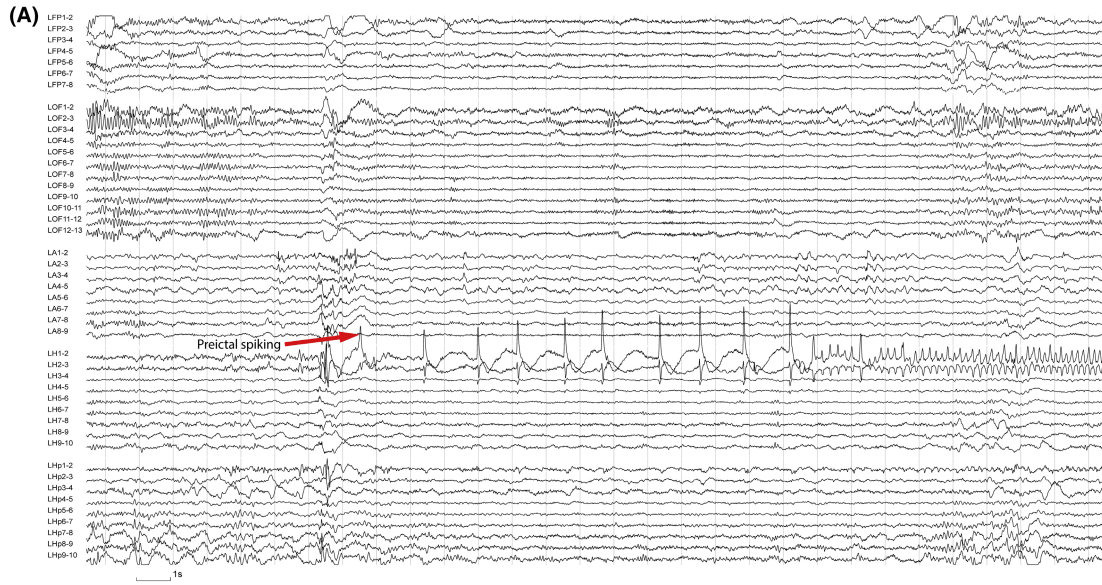
(C) Seizure onset

2.6 | Ictal patterns and correlation with clinical semiology

Analyzing clinical expression of seizures in conjunction with electrical onset pattern is a fundamental process in epileptology. Since Henri Gastaut's first proposals for classification of seizures and of epilepsies, electro-clinical patterns have formed the basis of seizure categorization.[55] The electrical and clinical aspects of a seizure can be considered as two different expressions of the same underlying network dynamic.[56] However, deciphering the relation between these is not always very straightforward or intuitive. This is further complicated by the fact that SEEG for the most part ignores participation of subcortical regions for ictal semiology and has a limited spatial sampling (see also section 3 "Caveats in the interpretation of intracranial EEG findings").

Electro-clinical correlations vary markedly according to anatomical location of the seizure onset, for example, in terms of whether unimodal or heteromodal cortex is involved and whether the seizure organization is very focal or widespread.[57] Unimodal cortex seizure onset will usually be clearly indicated by clinical seizure expression involving the physiological function of that cortex (e.g., clonic jerks in primary motor cortex; auditory hallucinations in auditory cortex). On the other hand, heteromodal cortex (cortical regions including the prefrontal cortex and parieto-occipital cortex, which receive input from multiple sensory or multimodal areas) is involved functionally in more complex or integrated activities, and thus, seizures in these regions tend to give rise to more complex and diverse semiological patterns that have complex relation to electrical activity[6] (see Figure 24, prefrontal seizure).

Seizure semiology is most often expressed during the propagation phase of the seizure, that is, with a certain time delay (which may be more or less short) between electrical seizure onset and clinical onset. This usually coincides with changes in electrical seizure organization that may involve a wider set of anatomical structures than the electrical onset alone (see Figure 25, example of a mesial temporal lobe seizure). It may also coincide with changes in discharge characteristics, for example, emergence of slower frequencies than those occurring at


FIGURE 24 SEEG trace of a habitual seizure characterized by abrupt onset of rhythmic antero-posterior body rocking in a 32-year old lady with pharmacoresistant frontal lobe epilepsy (MRI-negative). Semiological onset occurred 2 s after onset of low-voltage fast activity (blue arrow). Lower right inset shows schematic representation of SEEG electrodes in the right hemisphere. Six orthogonal electrodes explored the right frontal lobe, reaching mesial structures. There is also one contralateral electrode FD', symmetric with FD (not shown in figure). The red oval represents the zone maximally involved by seizure onset (electrodes FP, CR, and FD), and the yellow oval represents the zone of seizure propagation (electrodes SA, PM, and CC). The top right inset shows a map of the Epileptogenicity Index[149] (see text for explanation) for this seizure, which shows maximal values at seizure onset in the external contacts of FD and CR (right dorsolateral prefrontal cortex). Reproduced with permission (Elsevier) from Zalta A, Hou JC, Thonnat M, Bartolomei F, Morillon B, McGonigal A. Neural correlates of rhythmic rocking in prefrontal seizures. Neurophysiologie Clinique. 2020 Oct 1;50(5):331–8.[60]

seizure onset. Assessment of these is dependent on SEEG sampling as well as the role of anatomical (spatial) spread. Some work from SEEG studies has shown a correlation between the appearance of specific semiological patterns or features and specific changes in the time patterns of the discharge,[6] for example, desynchronization between orbitofrontal cortex and amygdala seizure activity in seizures with acute alteration in emotional behavior,[58] and synchronization in theta band activity between temporal lobe and opercular cortex structures during ictal chewing automatisms.[59] Even when the semiological expression is complex, not clearly localizable to individual cortical regions and likely dependent on cortico-subcortical interactions, a cortical time-signature may be detectable by studying quantified SEEG signal, for example, in prefrontal seizures characterized by rhythmic body rocking[60] (see Figure 24).

Main differences can be seen between mesial temporal lobe seizures and neocortical seizures involving associative cortex. Mesial temporal seizures tend to evolve slowly and with propagation phases that involve lower discharge frequencies, reflected in a fairly slow evolution and long duration of clinical signs that remain within a limited repertoire across patients (hence, readily recognizable to clinicians) (see Figure 25). In contrast, neocortical seizures, especially of extra-temporal origin, are typically characterized by high-frequency discharges with faster and more widespread and variable propagation patterns; seizure semiology may emerge in a rapid and explosive way in the context of a widespread fast discharge involving multiple connected regions (Figure 24). This helps to explain the diverse semiological manifestations of frontal lobe seizures for example. The underlying etiology plays another important factor for seizure dynamics.
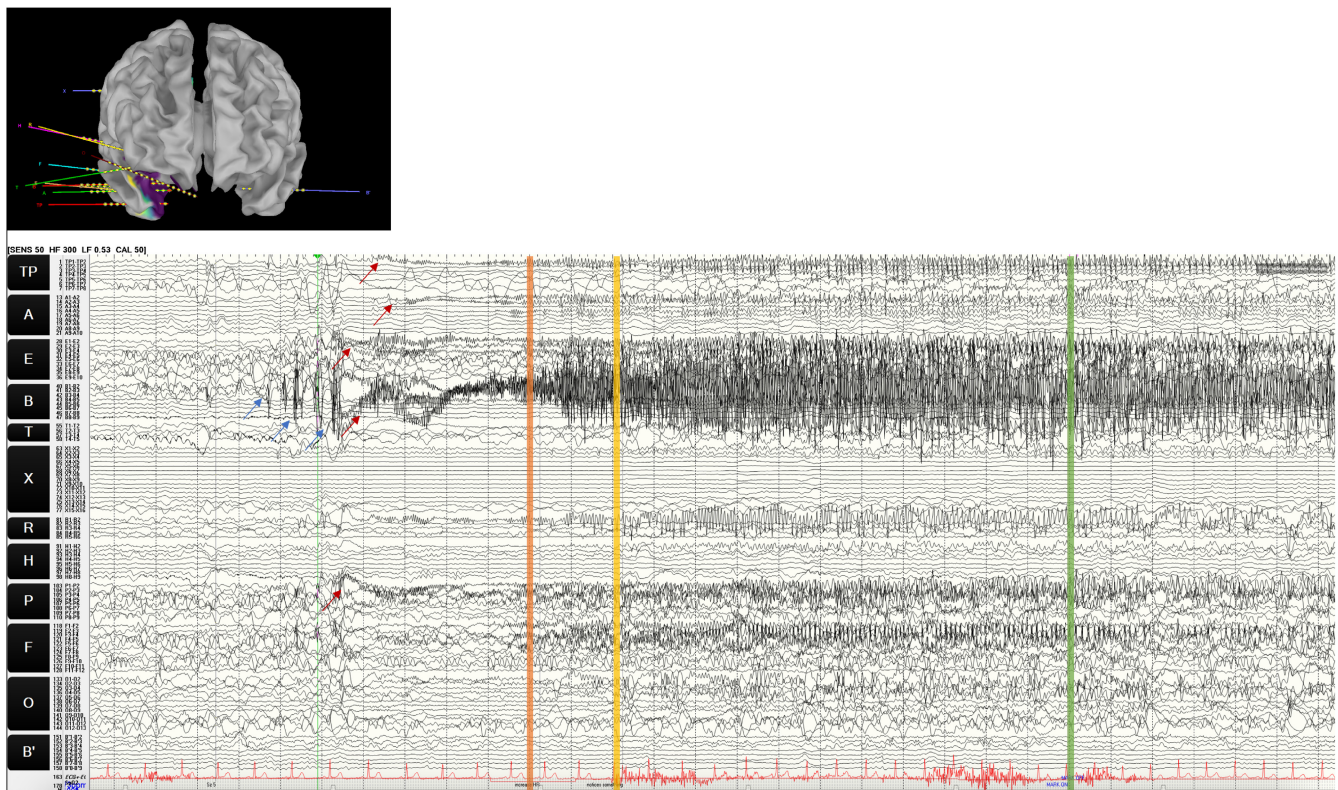

FIGURE 25 Example of a habitual right mesial temporal seizure in a 60-year-old man undergoing SEEG for MRI-negative, PET-negative drug-resistant cryptogenic temporal lobe epilepsy. Thirty seconds of trace are shown on this page; sensitivity 50 microvolts/mm, high-frequency filter 300 Hz, low-frequency filter 0.53 Hz. Pre-ictal spikes (blue arrows) are seen in the mesial contacts of electrode B exploring the right hippocampus, followed by a baseline shift and low-voltage fast activity (red arrows), which also recruits the mesial contacts of electrode E (right entorhinal cortex), P (right parahippocampal cortex), and, to a lesser and slightly later degree, A (right amygdala) and TP (right temporal pole). The orange vertical line marks an increase on heart rate on ECG. The yellow line marks the first objective clinical sign, which is a change in facial expression as if the patient feels something. This occurs around 7 s after electrical onset, at which time the discharge has propagated more widely to mesial temporal structures with a slower frequency than seizure onset, the green line is the moment when the patient presses the button to signal the seizure. When the nurse enters, he can converse normally and describes a feeling of déjà vu, his habitual seizure onset. There is some bilateral upper limb and lower limb piloerection but no other objective signs. Inset: model of electrode placement using Brainstorm software. A measure of Epileptogenicity Mapping based on energy ratio of signal over the seizure has been calculated and shows maximal values (purple color) in the right mesial temporal region.

2.6.1 | Beyond the Berger frequency band: HFOs and DC shifts

The invasive EEG contains information in frequencies that were not reviewed and even filtered away for a long time. This concerns on the high end of the spectrum, above the gamma frequency, HFOs (conventionally separated into ripples from 80 to 250 Hz, fast ripples from 250 to 500 Hz, and very fast ripples above 500 Hz) and on the low end infra slow activity (ISA), also described as DC shifts or ictal baseline shifts (IBS). HFOs and ISA have been related to the SOZ.

HFOs have been found in invasive SEEG, electrocorticography, intraoperative electrocorticography, surface EEG, and magnetoencephalography.[61-65] HFOs are thought to represent out-of-phase firing of groups of hypersynchronous firing neurons in epileptogenic cortex.[66] HFOs exist as interictal and ictal events and about 50% of the interictal HFOs co-occur with spikes.[67] Fast ripples seem more specific for epileptogenic tissue than ripples, and very fast ripples above 500 Hz seem even more specific.[68] Fast ripples that co-occur with ripples or spikes and ripples that co-occur with spikes seem more specific than single events.[67,69] The normal brain does not produce these high frequencies except for some areas, which are typically the hippocampus, sensorimotor cortex, visual cortex, and language areas.[70-75] Physiological HFOs have slightly different morphology, with longer duration, lower amplitude, and a more waxing and waning appearance, compared to epileptic HFOs (Figure 26).[76]
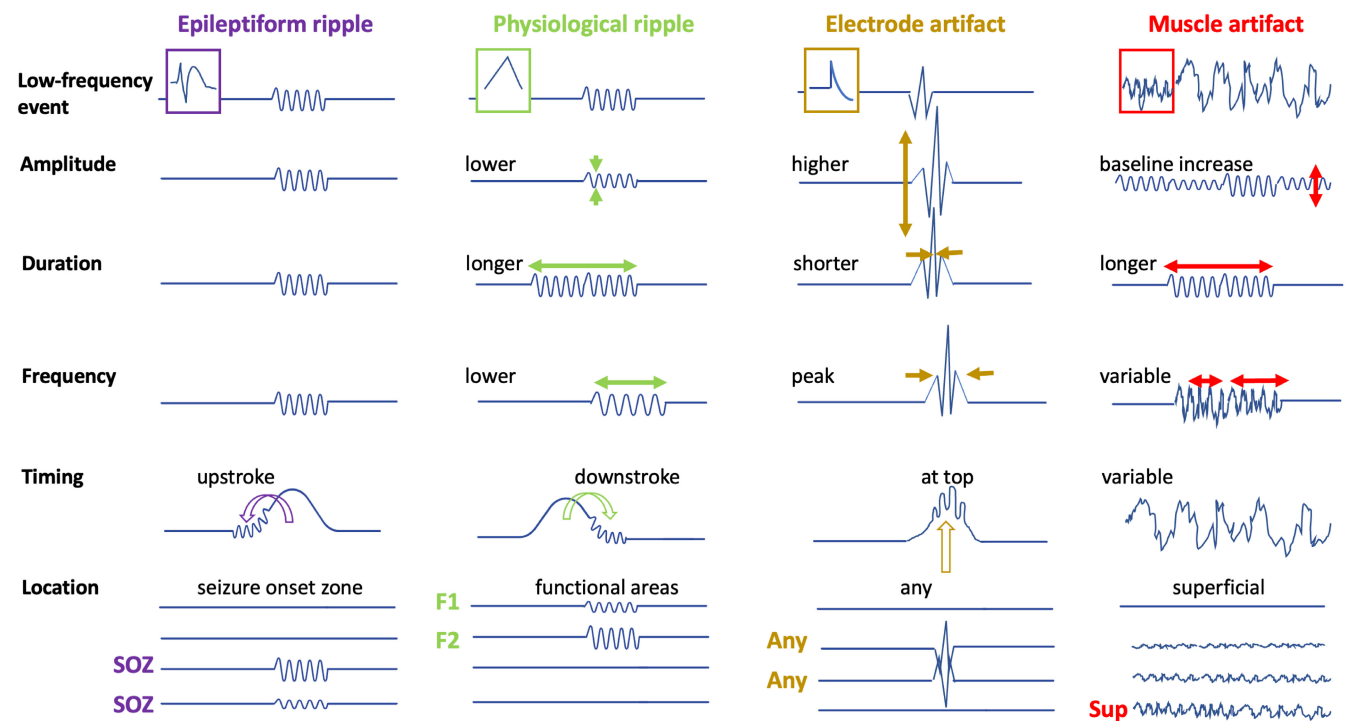
FIGURE 26 Some clues on how to distinguish physiological ripples, electrode artifacts, and muscle artifacts from epileptiform ripples. Clues can be found in the co-occurring low-frequency events, ripple amplitude, ripple duration, ripple frequency, timing compared to lower frequencies events, and location within the brain. F1, functional area 1; F2, functional area 2; SOZ, seizure-onset zone; Sup, superficial intracranial EEG channel.

FIGURE 27 High-frequency oscillations (HFOs) and common visual analysis differentials. Examples of SEEG signals with different LPF and spectrograms of spike-ripple, fast ripple, physiological ripple, artifact ripple, and spike-filtering effect are shown. Visual analysis of the HFOs was performed using finite impulse response (FIR) high-pass filter, with a cutoff frequency set accordingly to the band to be analyzed (displayed in every example). Time zero in each spectrogram matches the (*) seen in EEG signals. (A) Spike associated with a ripple. Spectrogram shows a blob with a maximum power between 150 and 200 Hz. LCp, Left posterior cingulate (B) Fast ripple seen independently from spikes. RDa, Electrode implanted close to lesion. (C) Physiological ripple registered in visual cortex contacts. RCu, Right cuneus. (D) Myogenic artifact seen in the more superficial intercerebral contacts. Scalp EEG channel F4-C4 added for comparison, showing a rhythmic myogenic masticatory artifact that is synchronous to the ripple-band activity captured in SEEG contacts RLA9-10. Time-frequency plots were obtained using MATLAB *wt* function, after computing the filter banks using 40 db Voices Per Octave and the frequency limits shown in each example. RLa, Right lingual gyrus. (E) Spiker-filtering effect seen after applying a LPF of 80 Hz. ROF, Right orbitofrontal. *Display parameters: Bipolar montage – a selection of electrodes is shown for educational purposes. LPF = Low-pass filter.*
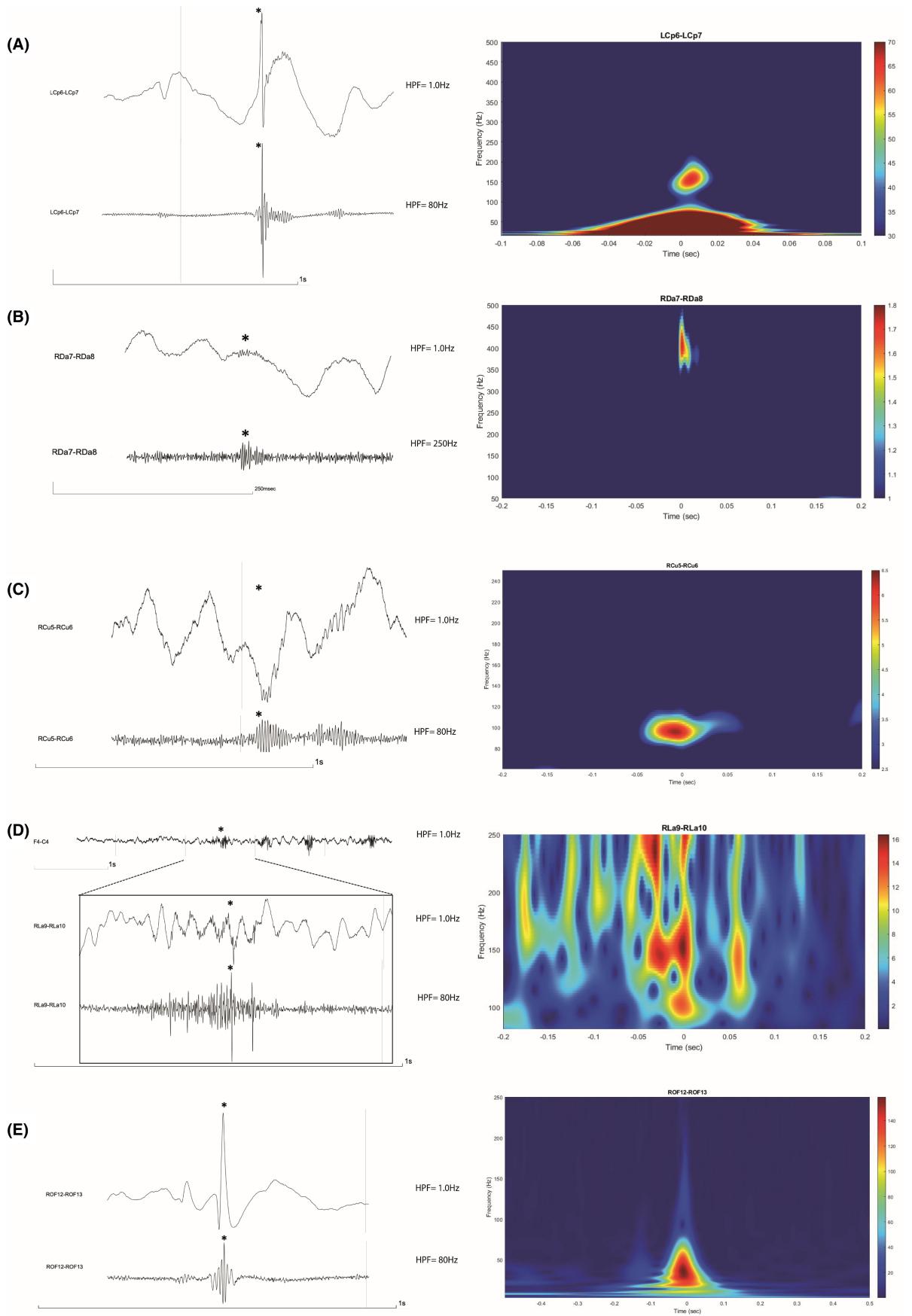
The literature on the clinical value of recording HFOs is contradictory. A recent randomized controlled trial using electrocorticography tested the non-inferiority of HFO-guided tailoring of epilepsy surgery to spike-guided tailoring on seizure freedom at 1 year. The primary endpoint of non-inferiority of HFOs versus spikes was not reached. Only secondary and post hoc analyses controlling for pathology associated with poor prognosis showed non-inferiority for extra-temporal but not temporal lobe epilepsy.[77] The low clinical value for recording HFOs in temporal lobe epilepsy where the question is often whether the hippocampus needs to be removed may result from the physiological high-frequency activity produced by the hippocampus.[71]

For the recording of HFOs, a sampling rate of ≥2000 Hz is recommended. Software containing a high-order finite impulse response high-pass filter of 80 and 250 Hz is needed to visualize HFOs. For visual inspection, a time resolution of 1 s is usually selected. Multiple automated detection algorithms exist. Caution is warranted to misinterpret high-frequency filtered artifacts from broken electrodes, spike-filtering effects, muscle activity, or movements as epileptic HFOs (Figures 26 and 27). Innovative recording methods like high-density electrocorticography may yield improved gain from recording HFOs.[78,79]

Another only more recently introduced marker is spike-gamma[80,81]: gamma activity in the 30–100 Hz frequency range that precedes a spike.[80] In a large group of 83 patients, it was shown to be the best of 135 spike features for predicting surgical outcome. More specifically, the rate of spikes with preceding gamma activity in wakefulness performed better for surgical outcome classification than the SOZ and the ripple rate. This was true across all patients and across various pathologies with FCD showing the best discrimination. Channels with a spike-gamma rate exceeding 1.9/min had an 80% probability of being in the SOZ.[80] Spike-gamma seems therefore to be promising
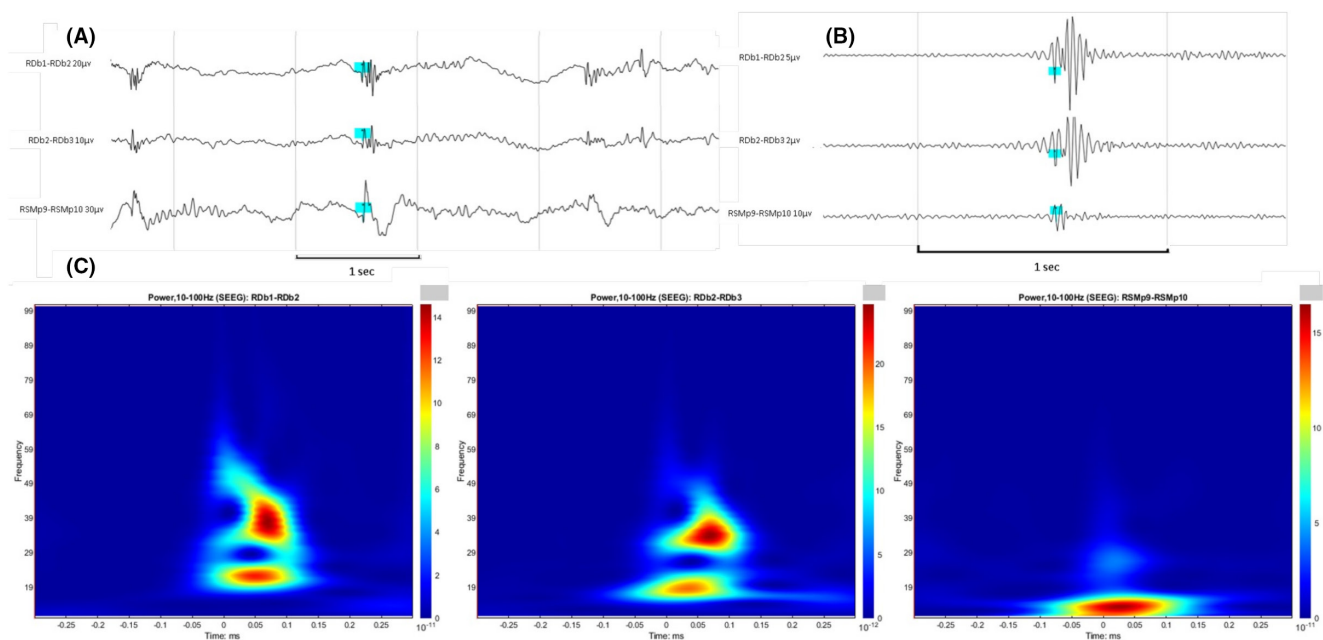
FIGURE 28   Spike-gamma activity during wakefulness was recorded from a 25-year-old woman with a right precuneal–cingulate DRE (Appendix A). In Panel A, the onset (blue*) of typical interictal activity (a burst of polyspikes) from FCD type II is shown. Panel B demonstrates the spike-gamma activity after applying a finite impulse response (FIR) filter with a high-pass cutoff of 30 Hz. It should be noted that the gamma activity preceded the onset of the polyspikes over the contacts RDb1-RDb2 and RDb2-RDb3. No gamma activity was observed before the spike over the contact RSMp9-RSMp10. To properly evaluate the spike-gamma activity, it is necessary to increase the sensitivity and expand the time scale for visualization. Panel C displays the time-frequency plots corresponding to each marked activity over RDb1–RDb2, RDb2–RDb3, and RSMp9–RSMp10. The isolated blobs confirm that a gamma activity (30–100 Hz) started before the onset (time zero) of the burst of polyspikes over RDb1-RDb2 and RDb2-RDb3, while no gamma activity was observed over RSMp9-RSMp10. These results suggest that RDb1-RDb2 and RDb2-RDb3 are involved in the presumed epileptogenic zone, contrary to RSMp8-RSMp 9, which constitutes a propagated zone. This patient underwent a tailored precuneal–cingulate resection without removing any contact of the electrode RSMp. The pathology confirmed FCD IIa. She is Engel Ia with a follow-up of 4 years. Time-frequency plots were computed using Brainstorm (Morlet wavelets). *Display parameters*: *Bipolar montage – a selection of electrodes is shown for educational purposes – Panel A BP: [0.5-100 Hz], Panel B FIR BIP: [30–100 Hz]*. RDb was targeting the FCD visible in the structural MRI and RSMp was targeting the mid-cingulate gyrus. DRE, Drug-resistant epilepsy; FCD, Focal cortical dysplasia.

marker, in particular as it is also easily accessible to visual analysis. Examples are provided in Figure 28.

DC shifts are EEG changes over a time constant of >2 s. DC shifts were described as ictal phenomena in animal models.[82] Recording these low-frequency shifts is a challenge for DC amplifiers. Modern alternating current (AC) amplifiers allow filter settings to record near DC shifts: a time constant of 10 s corresponds to the cutoff frequency of a high-pass filter above 0.016 Hz. They can be recorded with electrocorticography and with scalp EEG.[83] They appear restricted to a few channels on electrocorticography within the borders of the presumed epileptogenic area and have been suggested to help define the SOZ.[84] They have been related to potassium shifts and glial activity.[85] DC shifts either precede (active DC shift as seen in habitual seizures in chronic epilepsy where the DC shift usually precedes the ictal HFOs) or follow the seizure onset (passive DC shift as seen in acute symptomatic seizures).[86]

Ictal DC shifts can occur on the same electrocorticography channels as ictal HFOs, in which case the DC shifts tend to precede the HFOs.[87] A direct comparison showed higher occurrence rate of ictal DC shifts compared to ictal HFOs, while complete resection of both areas predicted favorable outcome.[84] HFOs and DC shifts co-occur also in the interictal periods.[86]

2.6.2 | Modulation of interictal and ictal activity across the sleep–wake cycle

As known from scalp EEG, sleep is a significant modulator of both interictal and ictal activities[88]: non-rapid eye movement (NREM) sleep is known to increase rates and the field of IEDs and HFOs, whereas rapid eye movement (REM) sleep decreases rates and the field of IEDs and HFOs.[89–93] This behavior undergoes further specific spatiotemporal dynamics, with earlier sleep having higher rates as compared to late sleep, and mesiotemporal regions being differently modulated than neocortical regions.[89,90,94] Finally, morphology of interictal activities was shown to be affected as well as seen particular well in FCD and mesiotemporal lobe structures (Figures 29 and 30). Seizures are reported to occur more often during NREM sleep as compared to wakefulness with lowest rates occurring in REM sleep.[95] Interestingly, a recent work showed that the dynamics of seizures occurring during wake and NREM sleep did not deviate from the variability between one of the two states. This suggests that once the brain surpasses the seizure threshold, it will follow the underlying epileptic network irrespective of the vigilance state.[96] It is further interesting that even minor electro-clinical seizures or pure EEG discharges
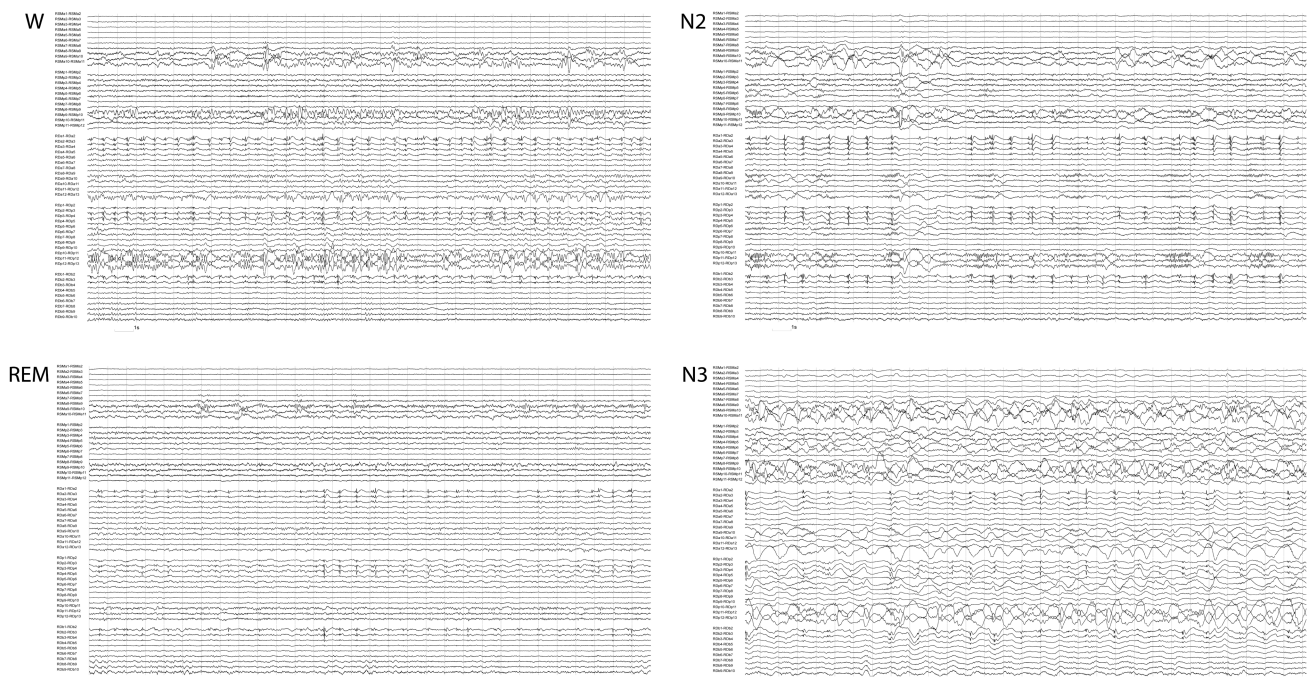
FIGURE 29 Modulation of IEDs during sleep–wake cycle in a patient with a right frontal FCD. 30-s SEEG epochs during wakefulness (W), NREM 2 (N2), NREM 3 (N3) and REM stages. Notice the variation in frequency and field extension of spikes in deep contacts of RDa, RDp, and RDb, with a decrease in both features during N3 and notably during REM sleep. Physiological graphoelements of NREM sleep can be seen in superficial contacts of some electrodes, such as RDp. *Display parameters: Bipolar montage – a selection of electrodes is showed for educational purposes – BP: [0.5–100 Hz].* FCD, Focal cortical dysplasia; IEDs, Interictal epileptiform discharges; NREM, Non-rapid eye movement sleep; RDa, Right frontal anterior to dysplasia; RDb, Right frontal inferior to dysplasia; RDp, Right frontal posterior to dysplasia; REM, Rapid eye movement sleep; RSMAa, Right supplementary motor area anterior; RSMp, Right supplementary motor area posterior.
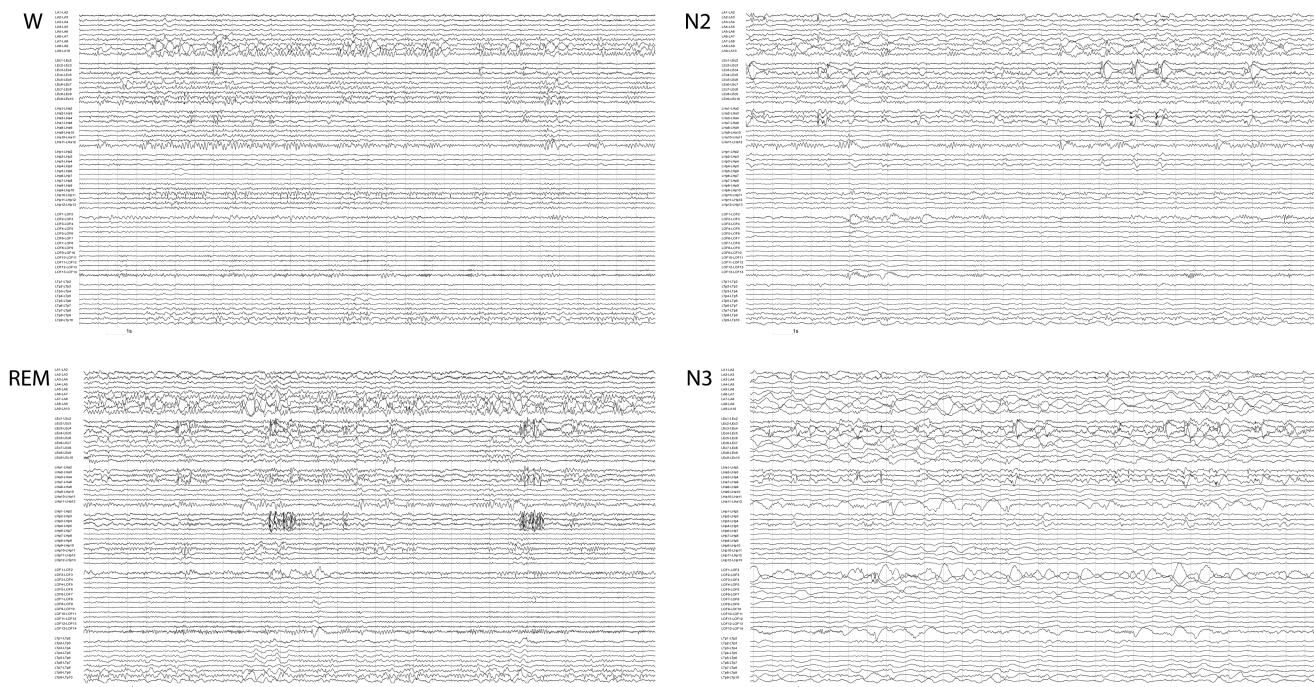
FIGURE 30 Modulation of IEDs during the sleep–wake cycle in a patient with left mesiotemporal epilepsy. 30-s SEEG epochs during wakefulness (W), NREM 2 (N2), NREM 3 (N3), and REM stages. Notice the increase in frequency of spikes seen in deep contacts of LHa, LHp, LA, and LEc during N2, and also REM sleep. *Display parameters: Bipolar montage – a selection of electrodes is showed for educational purposes – BP: [0.5–100 Hz].* IEDs, Interictal epileptiform discharges; LA, Left amygdala; LEc, Left entorhinal cortex; LHa, Left anterior hippocampus; LHp, Left posterior hippocampus; LOF, Left orbitofrontal; LTp, Left temporal pole, NREM, Non-rapid eye movement sleep; REM, Rapid eye movement sleep.

can result in awakenings and hence sleep fragmentation,[97] something that cannot be well appreciated in scalp EEG recordings.

2.6.3 | Stimulation

*Stimulation parameters and patterns*

Electrical stimulation is considered an essential part of every SEEG investigation. It is used during presurgical phase 2 epilepsy evaluation for both mapping of the seizure network and functional mapping.[10] Seizure stimulation dates back to the pioneering work of Jasper and Penfield, who used stimulation to reproduce the habitual auras in patients with epilepsy in the operating theater.[98] Later, Bancaud and Talairach applied this method in the operating theater to help confirm organization of the EZ, when stimulation of specific structures could trigger seizures that reproduced all or part of the habitual electro-clinical pattern. They found seizure stimulation particularly useful given time restraints preventing to record spontaneous seizures in the acute setup (since video-telemetry was not yet available in the earliest days of SEEG) and to disentangle the primary epileptogenic area from areas of propagation.[7]

In clinical practice, electrical stimulation is most frequently done as either high-frequency or train stimulation at 50 or 60 Hz, or low-frequency or pulse (shock) stimulation at 1.0 Hz. High-frequency stimulation in SEEG is usually performed with increasing intensities using biphasic pulses at 0.5–1.0 ms and a total train duration of 3–8 s, whereas low-frequency stimulation is done for durations of 20–60 s at a single output current (many centers use 3.0 mA) and a pulse width of 0.5–3.0 ms.[11] The output current is dependent on the duration of the pulse width and electrode size and can be calculated based on the following equation:

$$D\left(\frac{\mu C}{cm^2}\right) = I\,(mA) \times t\,\frac{ms}{A}\,(cm^2),$$

where D is the charge density in $\mu C/cm^2$, I the intensity in mA, t the time in ms, and A the geometric surface area in cm^2.

Important is to keep in mind that the charge density per phase should not exceed 57 $\mu C/cm^2$.[99] The contact surface for a typical SEEG contact is around 0.05 cm^2, whereas the contact surface for a typical subdural contact is 0.08 cm^2. Intensities are therefore usually significant lower in SEEG as compared to subdural grids/strips (see review of Prime
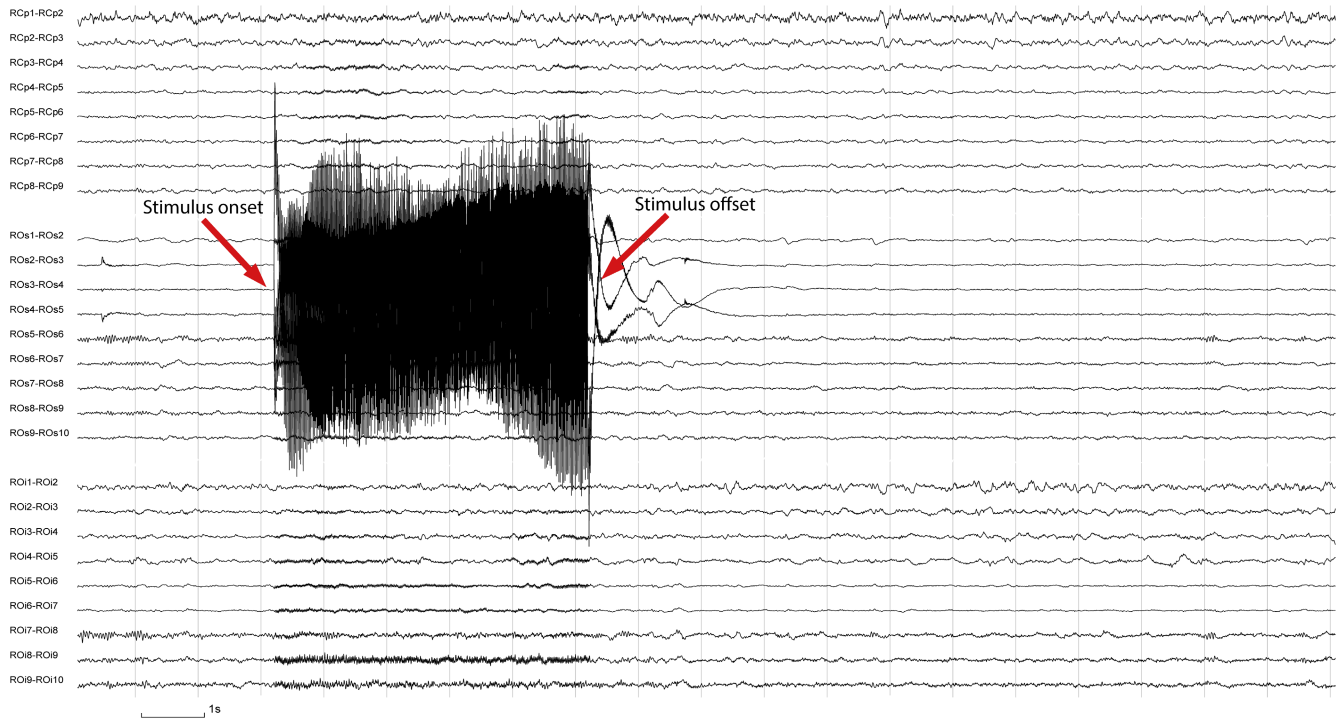
FIGURE 31   High-frequency stimulation artifact. Bipolar stimulation was performed on electrode contacts ROs 3–4 using the following parameters: 50 Hz frequency, 2.0 mA intensity, 0.5 ms biphasic pulse, 5 s of duration. A high-frequency artifact can be seen during the 5 s of stimulation involving stimulated contacts (higher amplitude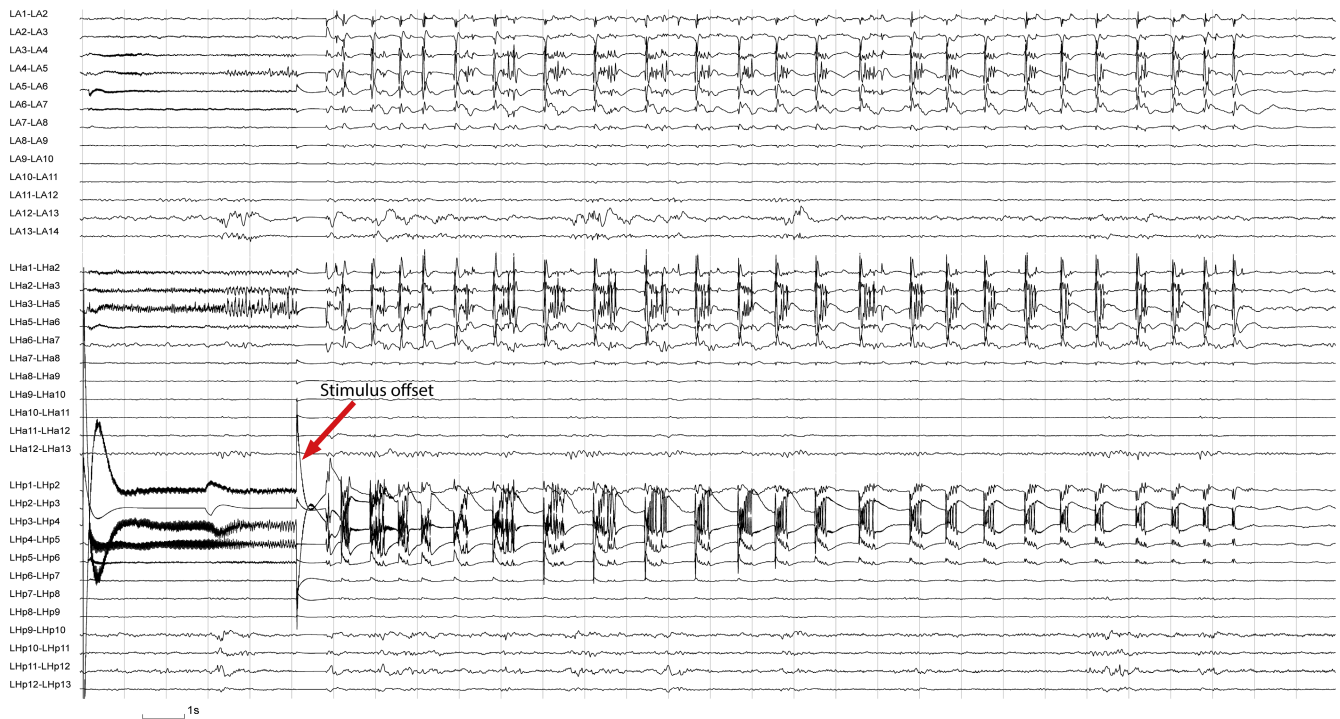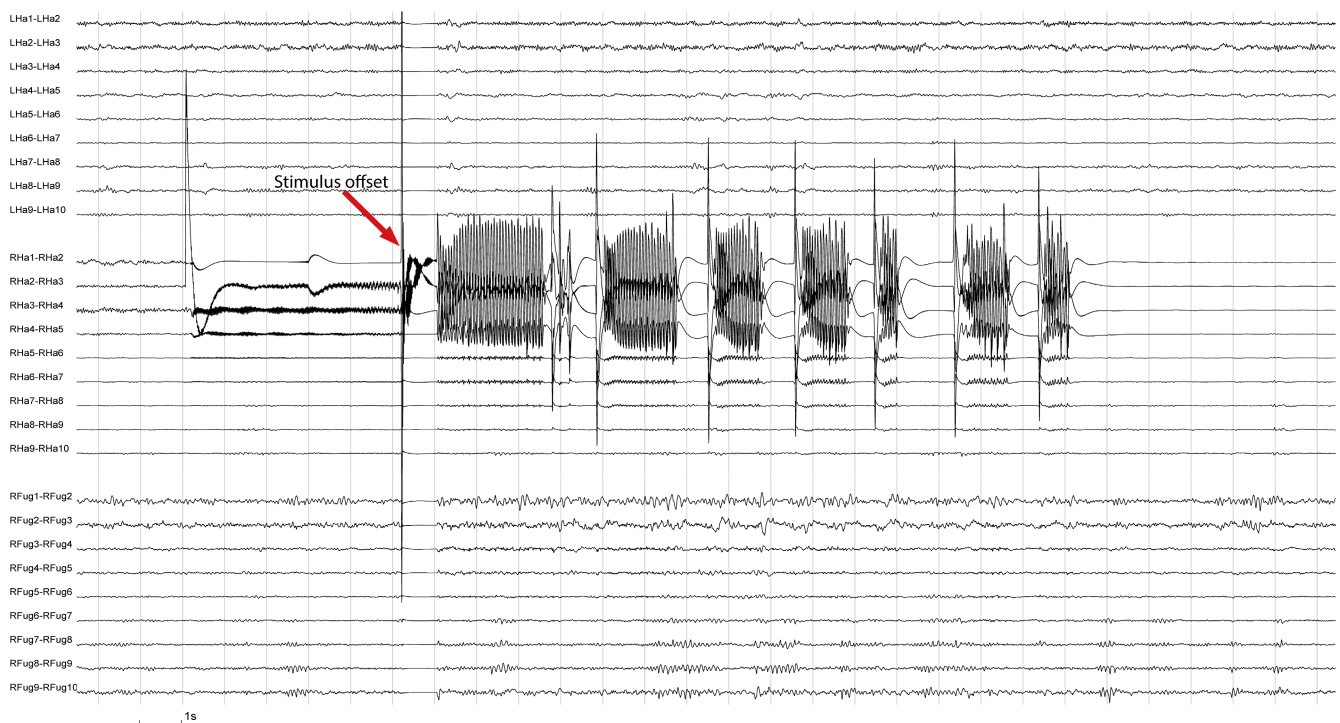), as well as nearby or functionally connected contacts and electrodes (lower amplitude). *Display parameters: Bipolar montage – a selection of electrodes is shown for educational purposes – BP: [1.0–100 Hz].* RCp, Right posterior cingulate gyrus; ROs, Right superior occipital (supracalcarine cortex); ROi, Right inferior occipital (infracalcarine cortex).
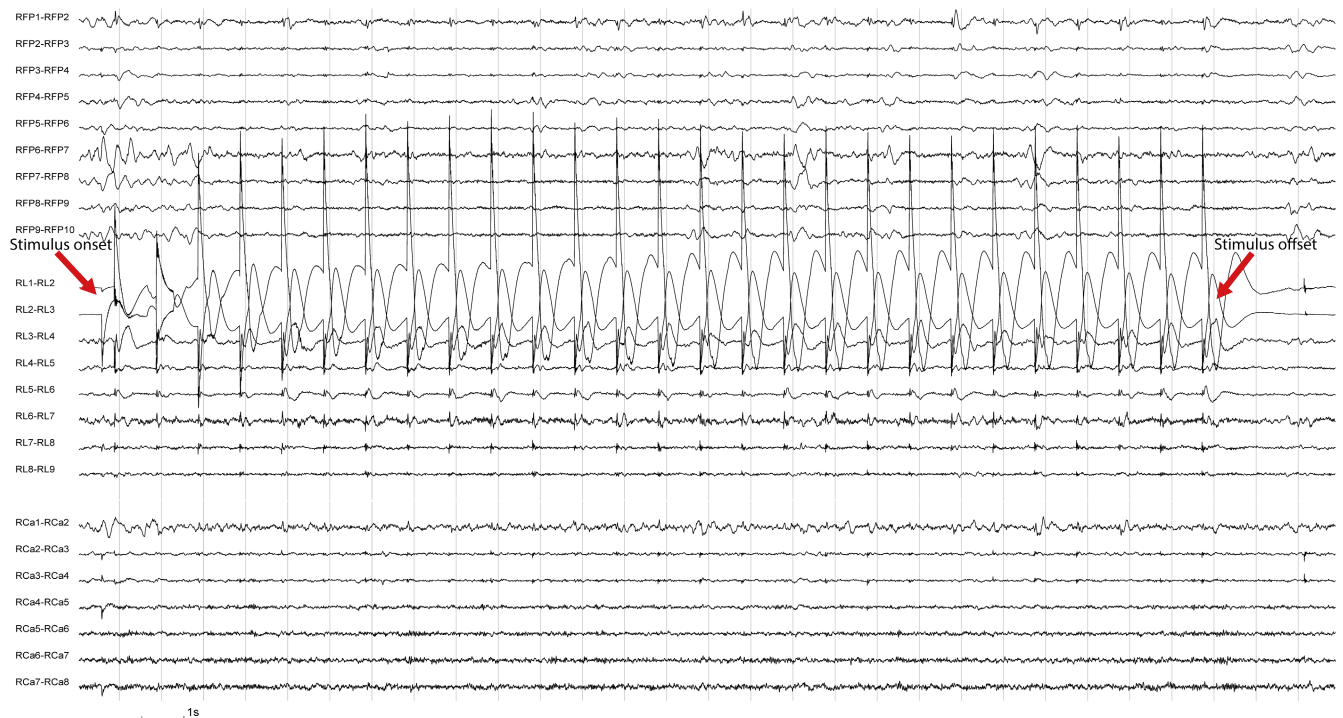
FIGURE 32   Low-frequency stimulation artifact. Bipolar stimulation was performed on electrode contacts RL 1–2 using the following parameters: 1.0 Hz frequency, 2.0 mA intensity, 1.5 ms biphasic pulse, 25 s duration. A low-frequency monomorphic artifact can be seen during the 25-s stimulation involving stimulated contacts (higher amplitude), as well as nearby and functionally connected contacts and electrodes (lower amplitude). *Display parameters: Bipolar montage – a selection of electrodes is shown for educational purposes – BP: [1.0–100 Hz].* RCa, Right anterior cingulate gyrus; RFP, Right frontal pole; RL, Right lesion (targeting the vicinity of the epileptogenic lesion).

FIGURE 33 Polyspike bursts pattern. Thirty-second epoch showing a high-frequency bipolar stimulation on contacts LHp 2–3 at 1.5 mA. Elicited discharges were characterized by polyspike bursts lasting 22 s involving mesiotemporal contacts (LHp 1–5, LHa 1–6, and LA 1–7). No clinical response was observed. *Display parameters: Bipolar montage – a selection of electrodes is shown for educational purposes – BP: [1.0–100 Hz].* LA, Left amygdala; LHp, Left posterior hippocampus; LHa, Left anterior hippocampus.

FIGURE 34 Sequential spikes pattern. Thirty-second epoch showing a 50 Hz bipolar stimulation on contacts RHa 1–2 at 2.0 mA. Elicited discharges were characterized by sequential spikes interspersed with 1.0- to 1.5-s attenuation periods ("pauses"), involving contacts RHa 1–6. No clinical response was observed. *Display parameters: Bipolar montage – a selection of electrodes is shown for educational purposes – BP: [1.0–100 Hz].* LHa, Left anterior hippocampus; RHa, Right anterior hippocampus; RFug, Right fusiform gyrus.

(A)

(B)
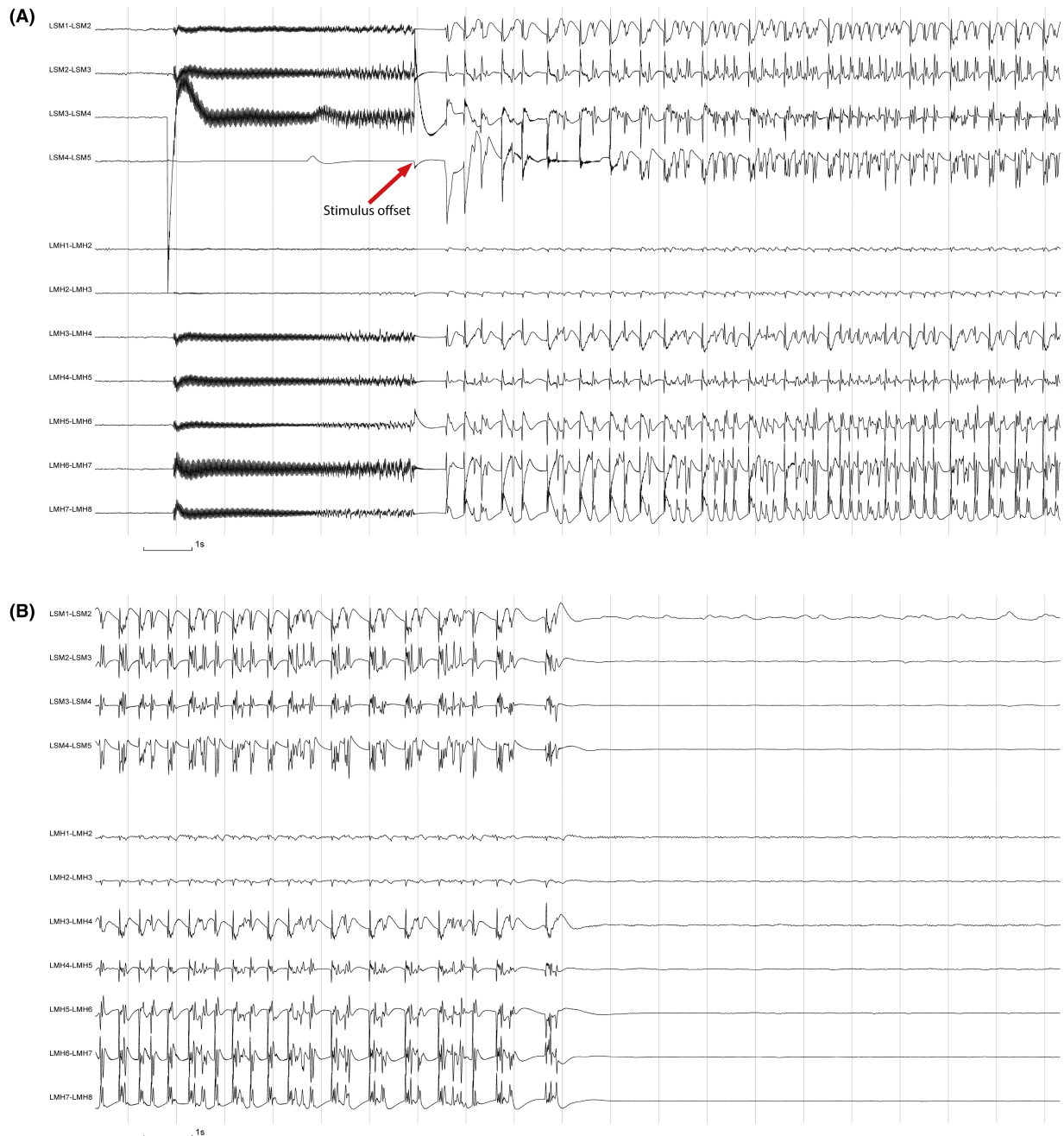
FIGURE 35 Spike-wave pattern. 50 Hz bipolar stimulation on contacts LSM 4–5 at 1.0 mA. Elicited discharges were characterized by spike and waves involving contacts LSM 1–5 and LMH 3–8. There was no spatial evolution, and no clinical response was observed. *Display parameters: Bipolar montage – a selection of electrodes is shown for educational purposes – BP: [1.0–100 Hz].* LSM, Left primary sensory cortex; LMH, Left primary motor cortex.

et al.[100]). According to the above formula, a SEEG stimulation at 3 mA with a 1 ms pulse duration results in a charge density of 60 μC/cm^2, thus slightly above the upper recommended safety limit. We are aware of centers performing low-frequency stimulations with a pulse duration of 3 ms or stimulation intensities of up to 8 mA, and thus recommend avoiding pulse durations >1 ms or >3 mA at a 1 ms pulse duration. Figures 31 and 32 show two representative examples of the artifacts seen with both stimulation types.

Note is made that for high-frequency stimulation most of the after-discharges or evoked discharges are seen only after the train stimulation artifact.

Most centers do stimulations after at least one spontaneous seizure has been recorded, but it can also be done without prior seizure recording. Moreover, seizure stimulation is usually performed first with 1.0 Hz and then 50 Hz stimulation and comprises multiple short recording sessions of 1–2 h. Even though no systematic data are
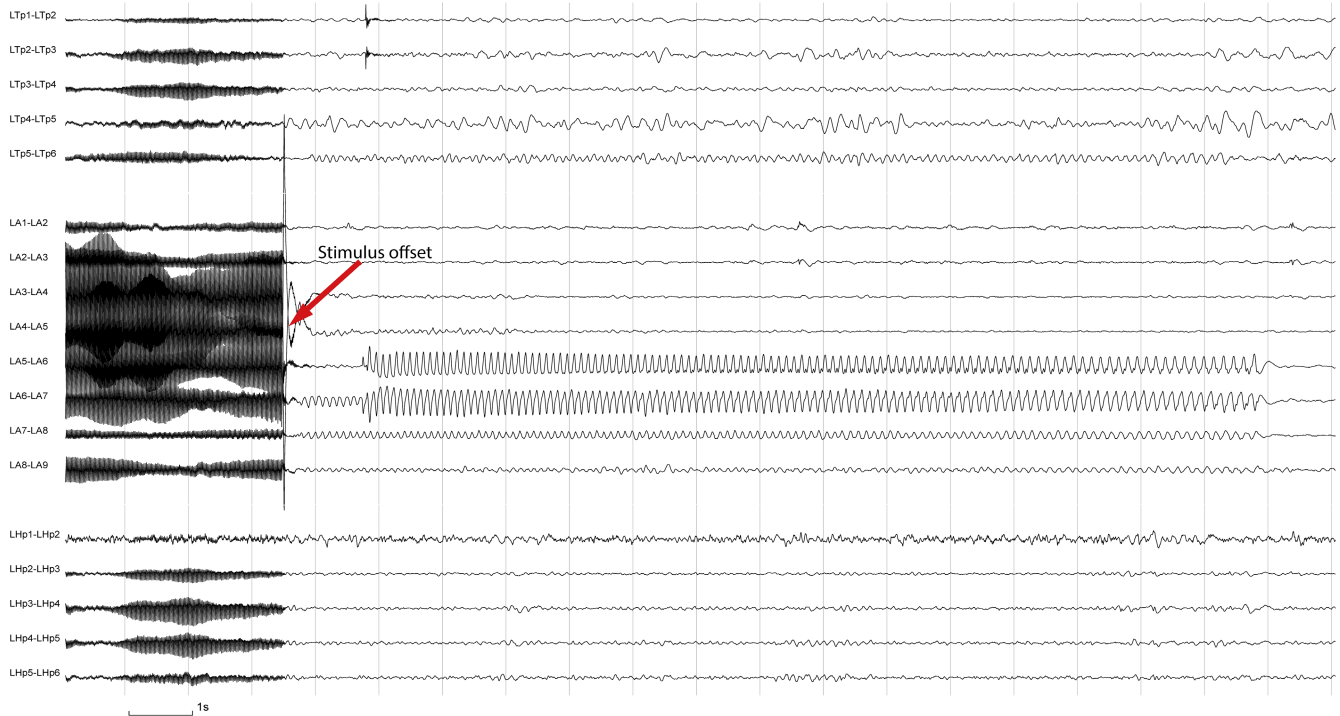
FIGURE 36 Sequential waves of approximately constant period. This 20-s epoch shows a 50 Hz bipolar stimulation on contacts LA 4–5 at 1.6 mA. Elicited discharges were characterized by rhythmic 9–10 Hz activity involving contacts LA 5–9 and LTp 5–6. No clinical response was observed. *Display parameters: Bipolar montage – a selection of electrodes is shown for educational purposes – BP: [1.0–100 Hz].* LA, Left amygdala; LTp, Left temporal pole. A selection of electrodes is shown for educational purposes.
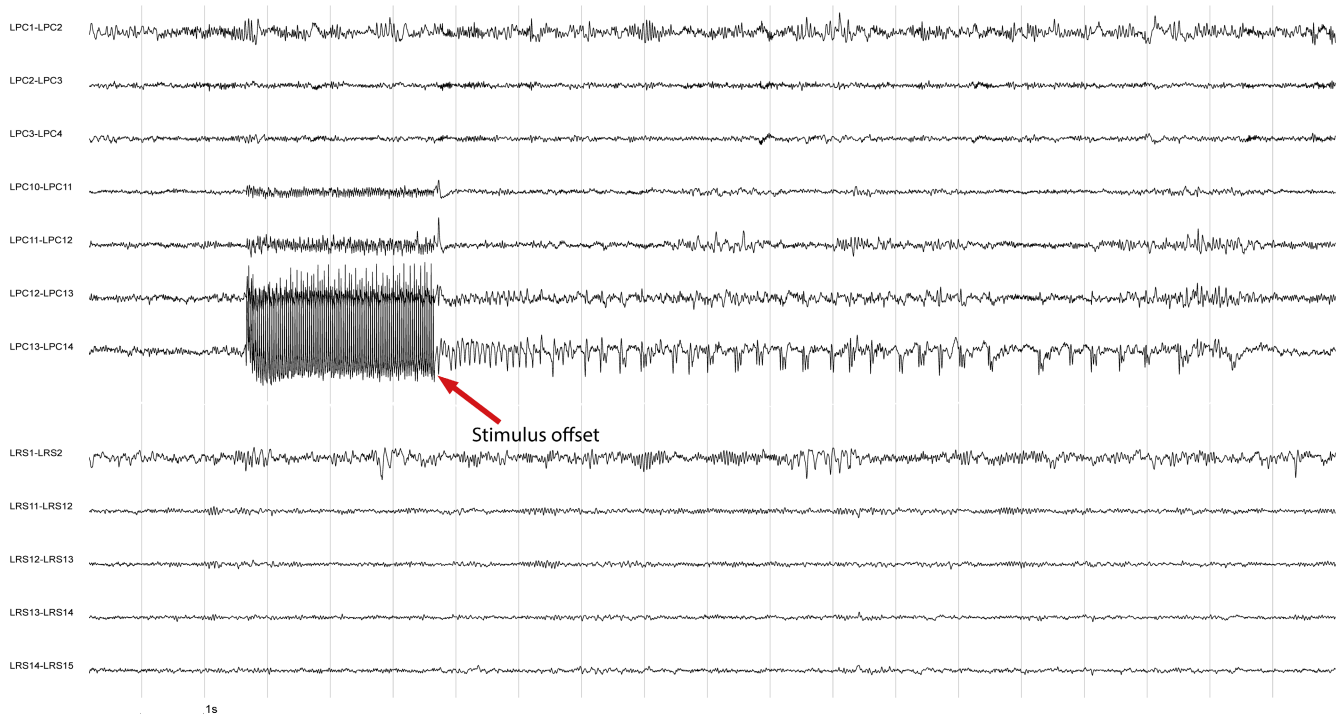
FIGURE 37 Sequential waves evolving into spike and waves. This 20-s epoch shows a 50 Hz bipolar stimulation artifact on contacts LPC 14–15 (not displayed). Elicited discharges were characterized by rhythmic 11–12 Hz activity transitioning into rhythmic spike and wave involving contacts LPC 13–14. No clinical response was observed. *Display parameters: Bipolar montage – a selection of electrodes is shown for educational purposes – BP: [1.0–100 Hz].* LPC, Left precuneus; LRS, Left.
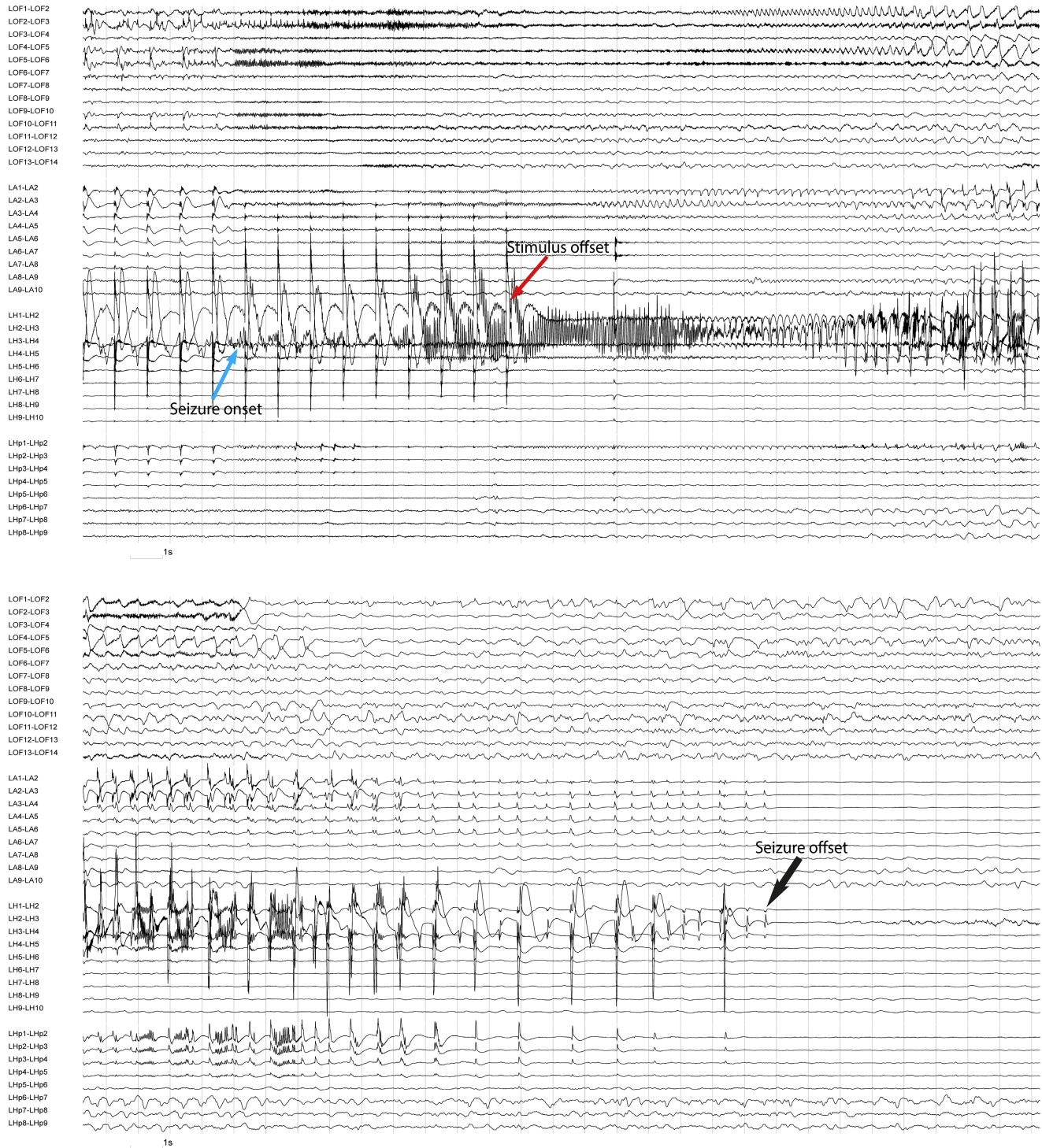
FIGURE 38 Seizure induced by low-frequency stimulation at 1.0 Hz and 2.0 mA. A seizure onset characterized by fast activity can be seen on electrode contacts LH 1–3 while stimulation is still ongoing (red arrow). There is simultaneous involvement of other mesiotemporal and orbitofrontal structures, which can be seen as LVFA in contacts LHp 1–3, LA 1–5, and LOF 1–5 (i). Seizure duration was 48 s (ii, offset marked by blue arrow). *Display parameters: Bipolar montage – a selection of electrodes is shown for educational purposes – BP: [1.0–100 Hz].* LA, Left amygdala; LH, Left anterior hippocampus; LHp, Left posterior hippocampus; LOF, Left orbitofrontal cortex; LVFA, Low-voltage fast activity.
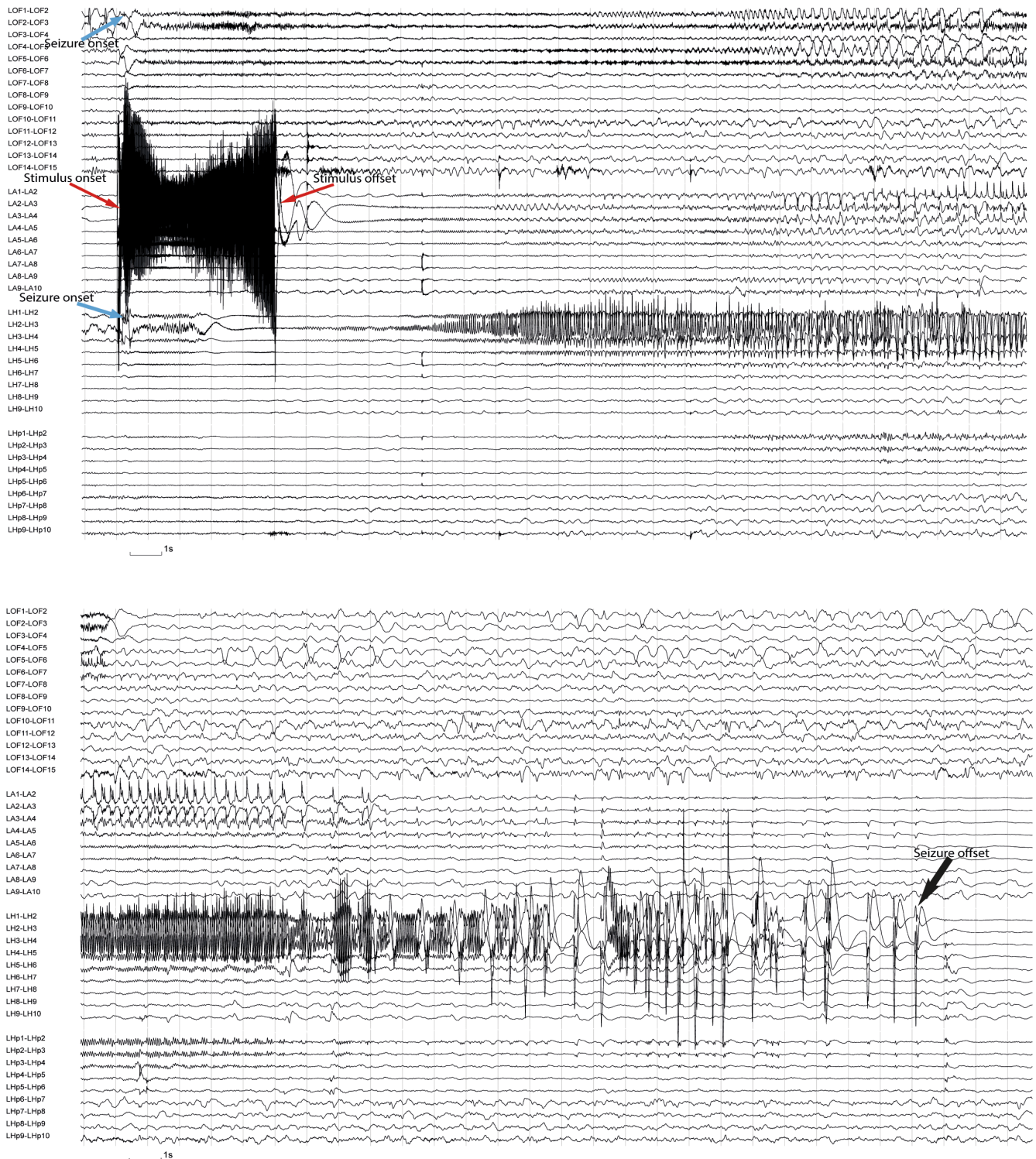
FIGURE 39 Seizure induced by high-frequency stimulation at 50 Hz and 1.0 mA. 300 ms after the beginning of stimulation on electrode contacts LA 2–3, an ictal onset pattern characterized by a sharp wave followed by fast activity can be seen in contacts LH 1–5 and LOF 1–7. Two seconds later, reacceleration of the ictal pattern in the form of 18–20 μV LVFA can be seen in LH 1–4, with rapid involvement of LHp 1–4. LA 1–5 shows an ictal pattern right after the stimulus artifact offset is seen, meaning that an earlier involvement of those contacts cannot be ruled out. Seizure duration was 55 seconds (ictal offset marked by black arrow). *Display parameters: Bipolar montage – a selection of electrodes is shown for educational purposes – BP: [1.0–100 Hz].* LA, Left amygdala; LH, Left anterior hippocampus; LOF, Left orbitofrontal cortex; LHp, Left posterior hippocampus; LVFA, Low-voltage fast activity.

available, most centers do electrical stimulation while on full medication or only slightly reduced medication, given the suspected higher risk of generalization or non-habitual seizures when completely off medication.

Here, we describe the most common EEG patterns observed during electrical stimulation with SEEG and comment on their clinical significance. After-discharges are rhythmic, usually repetitive, sharply contoured discharges that are mostly triggered at the stimulated channel and potentially further connected channels.[101] The most frequently observed pattern consists of polyspike bursts (Figure 33). Other patterns comprise in descending frequency: sequential spikes with and without pause, spike waves at 1.0–3.0 Hz, rhythmic waves, and rhythmic waves evolving into spike waves (see Figures 34–37). It is important to be aware that the hippocampus, the superior temporal neocortex, the motor cortex, the visual cortex, and certain pathologies such as FCD type II require usually a much lower stimulation intensity to induce elicited discharges than other anatomical structures and other pathologies. Moreover, it can be recommended to always start with low-frequency stimulation in the hippocampus and the motor cortex, and avoid high-frequency stimulation in those regions if low-frequency stimulations have been positive.[102,103] After discharge thresholds and occurrences vary from trial to trial, as can the distribution of electrodes showing elicited discharges. Systematic investigations show that there is no consistent relationship between the site of stimulus eliciting discharges and that of spontaneous seizures.[101,104,105] On the contrary, pure occurrence of elicited discharges and lack of evoking a habitual electro-clinical seizure are suggestive that the given anatomical site is not part of the SOZ. Finally, elicited discharges are frequently observed when higher output currents are used in high-frequency stimulation.

For seizure stimulation, subthreshold stimulation should be avoided. Contrary to functional mapping, evoking elicited discharges is actually the intended goal to differentiate non-epileptogenic from epileptogenic areas. In two large case series, the frequency of evoked electro-clinical seizures ranged between 57% and 75%, with high-frequency stimulation having a higher probability to induce seizures than low-frequency stimulation.[106,107] In contrast to elicited discharges, habitual electro-clinical seizures were shown to provide similar information to spontaneous seizures and to predict surgical outcome. Evoking habitual electro-clinical seizures during stimulation was shown to be associated with good surgical outcome, and removal of channels eliciting habitual electro-clinical seizures as well as removal of the SOZ of evoked seizures was associated with a more favorable outcome than incomplete removal of these sites.[106] Furthermore, it was shown that the risk of recurring seizures after surgery was lower when a seizure could be triggered with low-frequency stimulation.[107] Lack of stimulating a habitual electro-clinical seizure might indeed point to a more widespread SOZ or missed SOZ, but could also be explained by differences in underlying pathologies. Importantly, the absence of stimulating a seizure should not prevent a patient to undergo surgery if all other findings are in favor of having identified the SOZ. Electrographically, seizures most often arise from sequential spiking.[105] Figures 38 and 39 provide SEEG examples of evoked electro-clinical seizures during both 1.0 Hz and 50 Hz stimulation. Videos 1–3. provide examples of evoked habitual electro-clinical seizures. It is important to clarify the resemblance of the recorded seizures compared to the ones observed habitually at home with the patient or family. A recent work suggests that the semiological evolution pattern might be more rapid than the one observed in spontaneous seizures.[108] Seizure subjective symptoms without EEG changes are indicative of the symptomatogenic zone depending on the anatomical localization or could alternatively indicate possibly suboptimal sampling. Finally, the risk of evoking non-habitual seizures with SEEG is low, being around 8% for high-frequency stimulation and 1.5% for low-frequency stimulation.[106]

In summary, we recommend seizure stimulation as an integral part of every SEEG investigation to provide a controlled observation of seizures. Given complementary information, we suggest performing both low-frequency and high-frequency stimulation, whenever possible. Habitual electro-clinical seizures were shown to have a good correlation with spontaneous electro-clinical seizures, and removal of the SOZ and eliciting channels of these evoked seizures was associated with a better surgical outcome. Finally, eliciting seizures by cortical stimulation is a marker of favorable surgical outcome.

Stimulation for functional evaluation

Many aspects of the mechanisms underlying electro-clinical observations in patients undergoing direct electrical stimulation studies in SEEG remain poorly understood,[109,110] and both excitatory and inhibitory effects may occur.[110] Functional mapping from the SEEG point of view is closely intertwined with electro-clinical observations from spontaneous and stimulated seizures, which can bring evidence as to the functional role of individual cortical regions. For example, in a case of language-dominant temporal epilepsy in which lateral temporal cortical stimulation triggers a seizure involving the superior temporal gyrus, and where the patient retains language function over a certain timescale during visible EEG change within key structures, this could help in defining the safe posterior limit of the surgical margins. The occurrence of an after-discharge is considered in
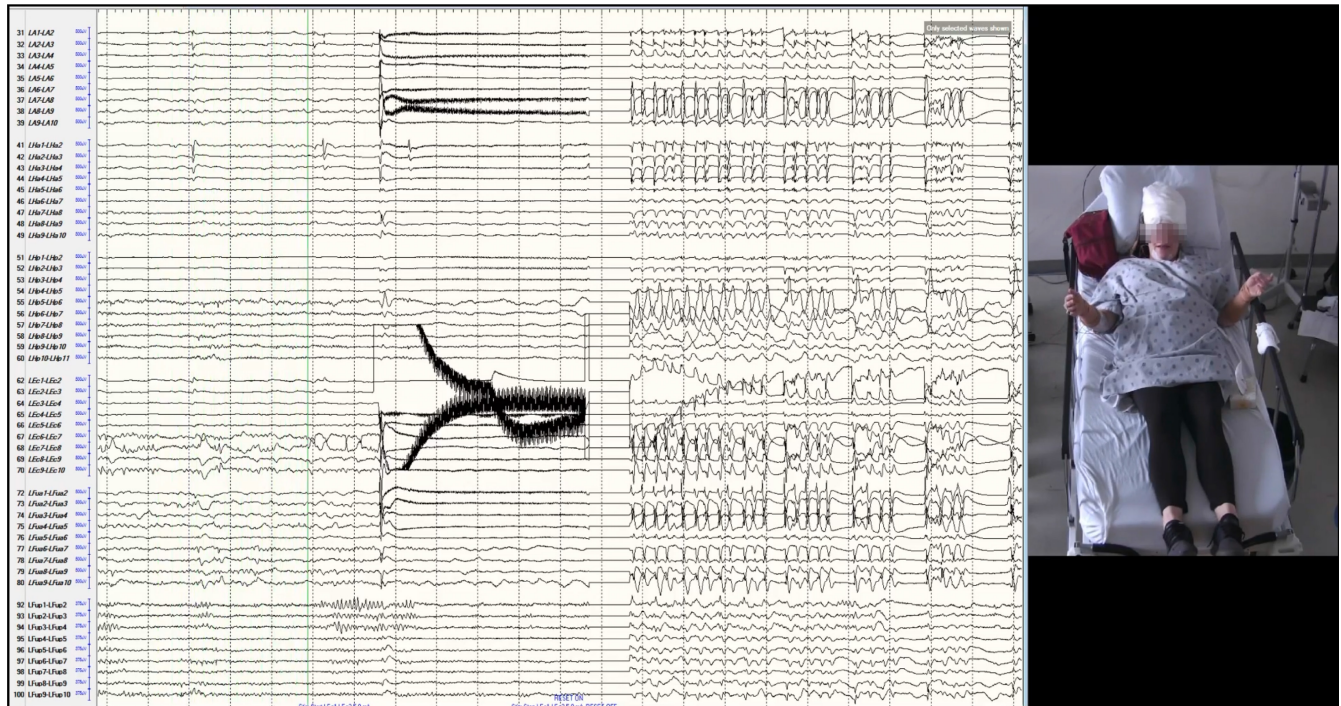
VIDEO 1 Focal seizure with impaired awareness elicited by 50 Hz stimulation at 5.0 mA in a 37-year-old right-handed woman with left mesiotemporal epilepsy. Stimulated contacts LEc 1-2 were located in left entorhinal cortex. Display parameters: Bipolar montage – a selection of electrodes is shown for educational purposes – BP: [1.0–100 Hz]. LA, Left amygdala; LEc, Left entorhinal cortex; LFua, Left anterior fusiform gyrus; LFup, Left posterior fusiform gyrus; LHa, Left anterior hippocampus; LHp, Left posterior hippocampus. Keywords: SYNDROME: focal non-idiopathic mesiotemporal (MTLE with or without HS) ETIOLOGY: hippocampal sclerosis or atrophy PHENOMENOLOGY: consciousness (alteration), automatisms, aphasia (postictal) LOCALIZATION: temporal mesial, temporal lobe (left).
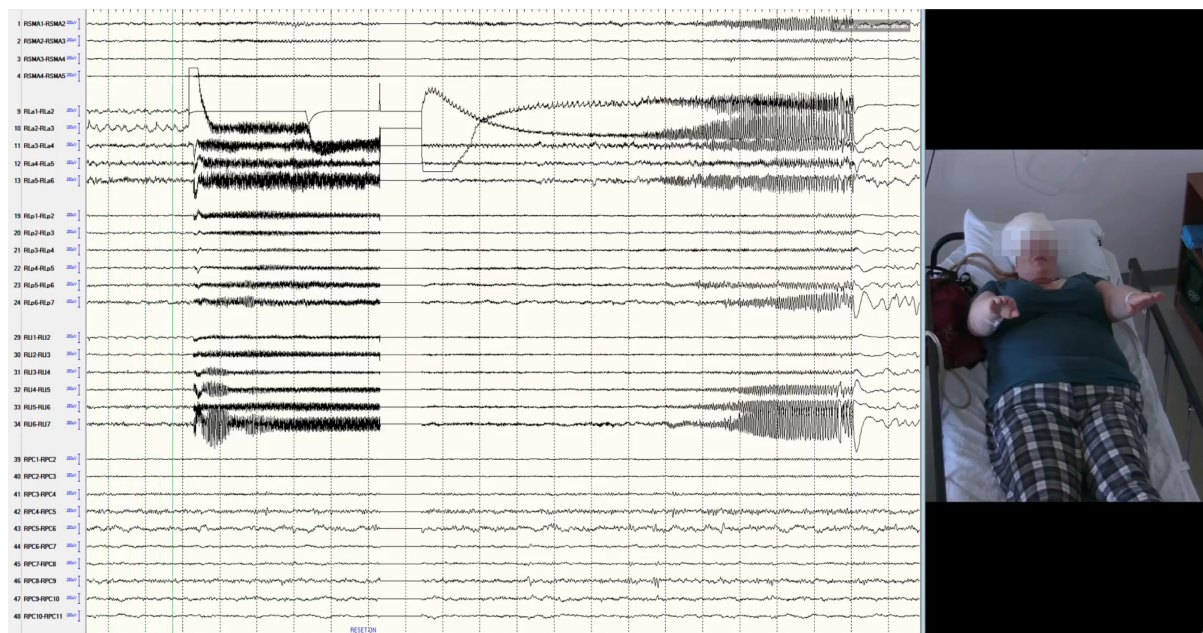
VIDEO 2 Focal aware motor seizure elicited by 50 Hz stimulation at 1.5 mA in a 36-year-old right-handed woman with right postcentral epilepsy. Stimulated contacts RLa 1–2 were located close to motor cortex, and in the anterior margin of the lesion (right paramedian postcentral FCD). Display parameters: Bipolar montage – a selection of electrodes is shown for educational purposes – BP: [1.0–100 Hz]. RLa, Right lesion anterior; RLI, Right lesion inferior; RLp, Right lesion posterior; RPC, Right precuneus; RSMA, Right supplementary motor area. Keywords: SYNDROME: focal non-idiopathic parietal ETIOLOGY: focal cortical dysplasia (type II) PHENOMENOLOGY: left, motor seizure (simple), tonic posture LOCALIZATION: central (left).
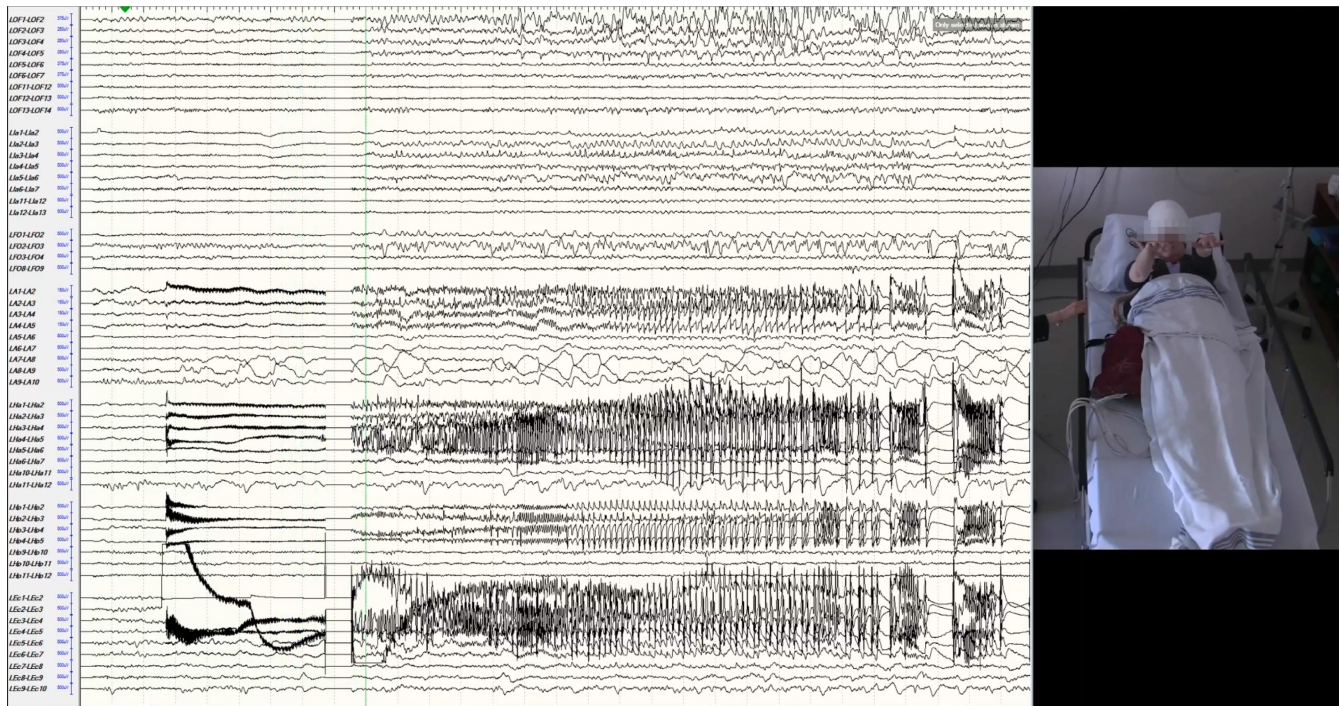
VIDEO 3 Focal seizure with impaired awareness elicited by 50 Hz at 2.0 mA in a 61-year-old right-handed woman with left mesiotemporal epilepsy. Stimulated contacts LEc 1-2 were located in left entorhinal cortex. Display parameters: Bipolar montage – a selection of electrodes is shown for educational purposes – BP: [1.0–100 Hz]. LA, Left amygdala; LEc, Left entorhinal cortex; LFO, Left frontal operculum; LFua, Left anterior fusiform gyrus; LHa, Left anterior hippocampus; LHp, Left posterior hippocampus; Lia, Left anterior insula; LOF, Left orbitofrontal.

Keywords: SYNDROME: focal non-idiopathic mesiotemporal (MTLE with or without HS) ETIOLOGY: lesion (unknown nature) PHENOMENOLOGY: consciousness (alteration), automatisms, fear LOCALIZATION: temporal mesial, temporal lobe (left).

SEEG practice to contribute potentially useful information, in helping to define the effective stimulation threshold and sometimes in revealing a non-local effect of stimulation in connected structures that demonstrates their reduced threshold for excitation.[107] As such, assessing the after-discharge threshold is useful because it would allow inference of a more local and specific effect of stimulation when language disturbance is obtained below this threshold.[111] In general, it is important to keep in mind that the effect of stimulation is far from being focal, and disrupts large networks of cortical areas that are connected; this can be seen when looking at elicited widespread high-frequency responses.[112]

Both high frequency (50 Hz) and low frequency (most often 1 Hz, also 3–6 Hz) can be used in stimulation studies for functional mapping, but 50 Hz stimulation is considered overall most useful for language mapping, as low-frequency stimulation may lack sensitivity for testing this function.[107,111] An effect of stimulation current charge density has been observed, with higher charge densities, essentially reflected in greater stimulation amplitudes, resulting in a higher proportion of positive stimulations[107] and after-discharges.[111] Low-frequency stimulation, in the contrary, can be useful for motor mapping, since it allows also to stimulate fibers and help to localize the motor tract.

Stimulation tasks and mapping strategy are tailored to the exploration of the individual patient. During stimulation, patients are sitting in bed and asked to relax, with team members present (e.g., medical and technical staff) who will perform clinical examination during stimulation. The tasks chosen should be simple enough to avoid errors, which can be checked by testing the patient's ability to perform the tasks before starting stimulation. It is important to avoid over-stimulation of the same electrode pair or structure, by leaving at least a couple of minutes between successive stimulations; too much repetition of stimulation tends to induce a refractory period that may be a source of "false-negative" stimulation results. When language is to be tested, tasks of expressive and receptive language function will be used, including picture naming, automatic speech (e.g., counting or saying the days of the week), word repetition tasks, and reading aloud; stimulation is considered positive if any stimulation-related errors such as tip of the tongue phenomenon, response delay, paraphasia, speech arrest, or pronunciation errors are observed.[107] When motor function is being tested, the patient may be asked to hold their upper limbs outstretched for example, to better enable detection of subtle weakness or clonic jerks; positive stimulation findings may include clonic jerks or transient impairment of motor

function, for example, when stimulating a "negative" motor area. Adding electromyography leads for motor mapping is useful.

Even though functional mapping is possible with SEEG electrodes, grids–strips or performance of an awake electro-corticography after SEEG may still seem preferable by some authors in situations where extensive mapping is required.[4]

3 | CAVEATS IN THE INTERPRETATION OF INTRACRANIAL EEG FINDINGS

Intracranial EEG suffers from a number of significant caveats and limitations, which need to be well understood. The most important issue is that of spatial sampling, the choice of which is determined by the clinical teams' hypotheses as well as surgical issues. Whether using subdural grids or SEEG, only a small volume of the cortex can be explored in a given patient. A detailed comparative analysis of the overall cortical volume sampled by both methods in 20 patients (10 for each method) showed that SEEG provided a 20% greater volume of gray matter sampling than subdural grids.[113] A single SEEG contact (cylinder of 0.5 mm in diameter and 2 mm length, providing a recording surface of $5 \, mm^2$) primarily captures intracranial EEG activities generated within a 5-mm distance, thus sampling a volume of about $30 \, mm^3$. Accordingly, a typical SEEG with 12 electrodes and 150 contacts within the gray matter will sample a total volume of $4.5 \, cm^3$, corresponding to 75 million neurons. This only represents 0.5% of the total human cortical brain volume ($900 \, cm^3$) and number of neurons (16 billions). Of course, intracerebral electrodes are not positioned in a random way, but rather guided by a number of presurgical investigations and the hypothesis regarding the localization of the SOZ and anatomical considerations, which altogether dramatically reduce the cortical regions of interest. Yet, the scale of the sampling issue is such that one always needs to consider the paradigm of the "missing electrode." This is particularly true for MRI-negative FCD type 2, the very small size of which can easily be missed. In such case, the typical interictal and ictal SEEG pattern can be completely undetected if electrodes are located more than 1 cm away from the border of the FCD. In a patient with a very small MRI-negative postero-superior insular FCD, no ictal discharge was even detected during typical somatosensory seizures with preserved awareness, despite several electrodes implanted in his epileptogenic insula, while a second SEEG captured very localized ictal discharges during the same clinical seizures, thanks to an additional electrode located less than 1 cm away from the previous ones.

The above issue invites to distinguish the "true" SOZ from the "apparent" SOZ delineated by intracranial EEG recordings. This distinction is important when considering how the EZ is being defined based on intracranial EEG recordings. It is often considered that the EZ differs from the observed SOZ, due to the fact that operating only the latter fails to control seizures in a significant proportion of patients, an observation that can have different explanations. One possibility would be that part of the epileptogenic tissue is not involved in the initial ictal discharge, but can generate a seizure once the SOZ has been removed. This possibility is consistent with the views that the EZ includes areas of early propagation,[9,114] and/or that it is organized as a distributed network rather than within a single region.[115] However, a credible alternative explanation is that the true SOZ simply differs or is more extensive than the apparent SOZ. There is currently no robust method to solve this dilemma, leaving a large room for personal experience and empirical considerations to guide intracranial EEG interpretation. From there, it is clear that removing areas of early propagation is likely to offer greater chances of seizure freedom, possibly not because these areas are truly epileptogenic, but due to the fact that a larger resection increases the chance of removing the "true" seizure onset. This is actually a generic issue that might apply to many other potential biomarkers of the SOZ (e.g., neuroimaging, neurophysiology) whereby the presence of any findings promoting larger resections necessarily increases the chance of seizure freedom.

One could hope that the intracranial EEG seizure-onset pattern enables to distinguish a true ictal zone from a propagated discharge. This is a complicated issue, however, due to the other factors influencing the type of ictal EEG pattern, namely, the underlying pathology and the affected lobe. Nevertheless, many would consider that LVFA is more likely to reflect the true ictal onset zone than other seizing patterns. This would account for the presence of such patterns to be associated with more favorable postoperative seizure outcome.[20,116] Yet, it is not unusual to observe widely extensive LVFA at ictal onset or later during the seizure that clearly surpasses the extent of the SOZ, suggesting that LVFA can also represent a propagation pattern (see also Figure 13).

Another impact of the intracranial EEG sampling limitation is the risk of misinterpretation of the spatial propagation of the ictal discharge. Looking through the narrow prism of the implanted electrodes (see also solid angle principle by Gloor[29]), one might get the impression that the ictal discharge travels between the sampled brain regions as if the latter were directly connected. In many instances, this is likely not the case, with propagated discharges resulting from multi-synaptic short- and long-term connections and/or cortico-subcortical loops.

Overall, the many unknowns that complicate the interpretation of intracranial EEG data invite to a cautious

approach, whereby all available data need to be considered to reduce the risks of erroneous conclusions. These shall include the known or suspected underlying pathology, results from all other relevant presurgical investigations and all information gathered during intracranial EEG, including interictal abnormalities, ictal semiology, and results from electrical stimulation and radiofrequency thermocoagulation when available.[117–119]

4 | SPECIAL CONSIDERATIONS IN CHILDREN

4.1 | General considerations for intracranial EEG in children

Intracranial EEG recordings are considered a safe and well-tolerated diagnostic method in children. In recent years, a paradigm shift has happened moving from centers using both intracranial depth and subcortical electrodes for chronic implantation toward SEEG being the most common method.[120,121] In young patients, seizure networks are often more widespread and resection sizes are usually larger compared to adults. Patients requiring very early surgery therefore often undergo large resections or disconnections such as multilobectomies and hemispherectomies.[122] In these larger resections, intracranial EEG is of minor importance.[123]

Literature suggests that intracranial stereo-EEG can be safely used in children as young as 18 months of age.[121] Indications are similar to those in adults, and SEEG is usually used to identify a SOZ in patients with inconclusive non-invasive presurgical workups. Most commonly, it is used in non-lesional cases or to define the boundaries of the SOZ in structural epilepsy with larger lesions or multiple lesions. Across Europe, pediatric cases for epilepsy surgeries have become more complex and SEEG usage has increased over the last decade.[124] Overall, 20%–30% of pediatric epilepsy surgery cases undergo intracranial diagnostics prior to surgery.[123,124] Of note, the use of SEEG is rather correlated with lower rates of seizure freedom as epilepsy in children is usually more complex if requiring SEEG.[125] Compared to adults, the percentage of structural cases in pediatric SEEG is higher. Larger developmental lesions are more common.[123] Additionally, cortical maturation might complicate identifying lesions and their boundaries.[126] Due to the differences in etiology and indication for intracranial EEG, children more often have neocortical explorations and less frequently typical mesiotemporal explorations.[127]

4.2 | Interictal patterns

For the most part, interictal epileptic discharges are very similar in children as in adults. Like in scalp EEG,
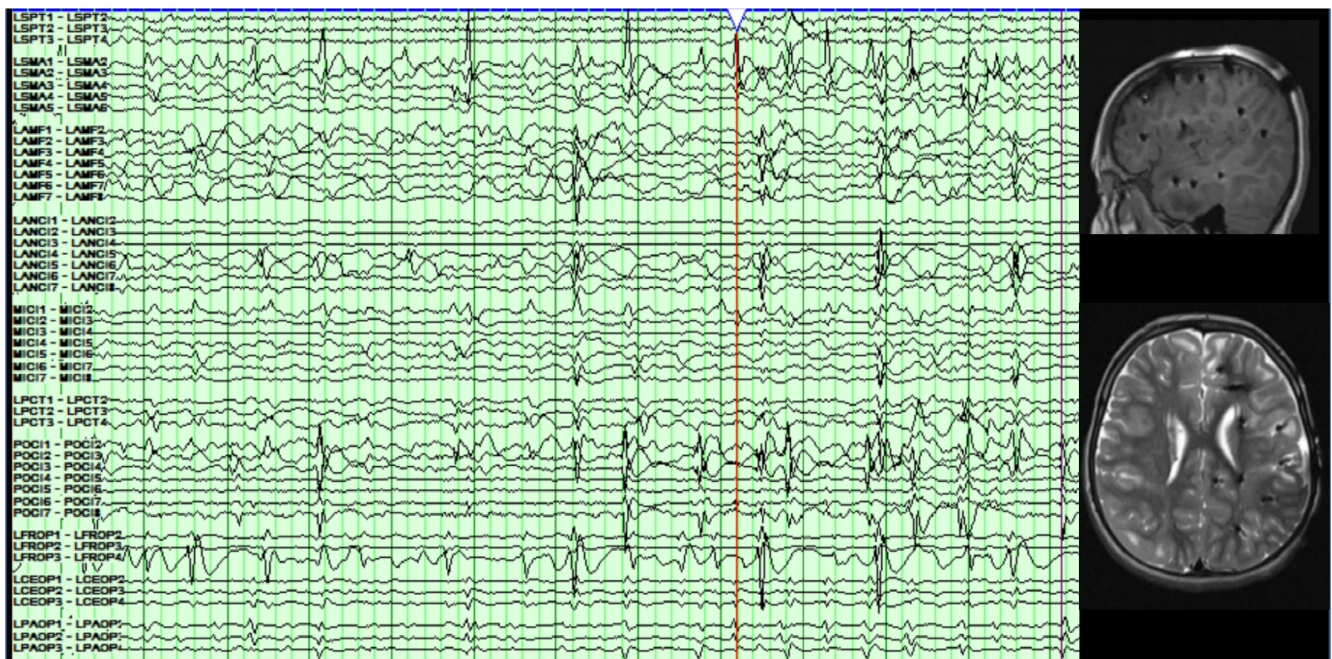
FIGURE 40 Widespread multifocal IEDs in a patient with tuberous sclerosis complex. Seven tubers were covered on the left (SEEG channels displayed above) and two on the right hemisphere. MRI shows distribution of intracranial electrodes aiming to cover the left hemispheric tubers. SEEG shows abundant independent IEDs generated from all covered tubers, matching the epileptic encephalopathy findings seen in the scalp EEG.

epileptic discharges might be more frequent and show a faster propagation than typically noted in adult EEGs. As structural lesions are common, patterns typical for FCDs are often seen. These include continuous or sub-continuous rhythmic spike discharges in a frequency of 1–10 Hz.[103]

Epileptic encephalopathies with frequent and continuous interictal EEG changes are closely linked to the patient's age. These patterns include hypsarrhythmia in West syndrome, spike slow waves, and tonic patterns in Lennox-Gastaut syndrome and sleep activated patterns like epileptic encephalopathy with spike-and-wave activation in sleep (EE-SWAS). They have in common that they are usually poorly localizing and show abundant interictal activity, while normal background rhythms are suppressed.[128] As discussed, earlier most of the children affected by encephalopathic EEG patterns either do not qualify as surgical candidates or undergo large resections without intracranial EEG.

Nevertheless, intracranial EEG can be helpful in those with multiple lesions or to define seizure onset and functional region in the case of large lesion areas.[128,129] Typical examples are patients with infantile spasms in the context of tuberous sclerosis complex or large hemispheric lesions.[130] As can be seen in Figure 40, interictal activity is often widespread and non-localizing. It is important to be aware that epileptic areas cannot be just identified by selecting regions with the highest spiking rates and the risk of falsely localizing is high. Especially in cases with deeper structural regions, propagation of spikes can often be seen over all covered cortical areas.[120] Like for most intracranial investigations, a hypothesis-driven coverage of important areas and recording of seizures is crucial for success.

4.3 | Ictal patterns

There is no systematic difference between seizure-onset patterns in children vs adults. As children might fail to report auras or are unable to describe subjective symptoms, any time lag between start of symptoms and seizure onset on EEG needs to be taken seriously. A combination of scalp and intracranial EEG can help to avoid false localization and lateralization. Depending on etiology, some seizure-onset patterns are more common than others.[131]

A specific seizure semiology for children is infantile spasms. A typical intracranial EEG pattern is shown in Figure 41. The intracranial EEG pattern is very similar to what is seen during spasms in scalp EEG. EEG changes at the time of a spasms can be unilateral or bilateral and are most likely widespread. They consist of LVFA, which can be isolated or in combination with a high-amplitude slow wave. Slow waves can either precede or follow the low-voltage fast activity.[124] The best indicator for localization purposes is focal or focal onset LVFA. In cases with widespread LVFA, electrodes might not be located in the seizure onset and false localization should be considered.[132]
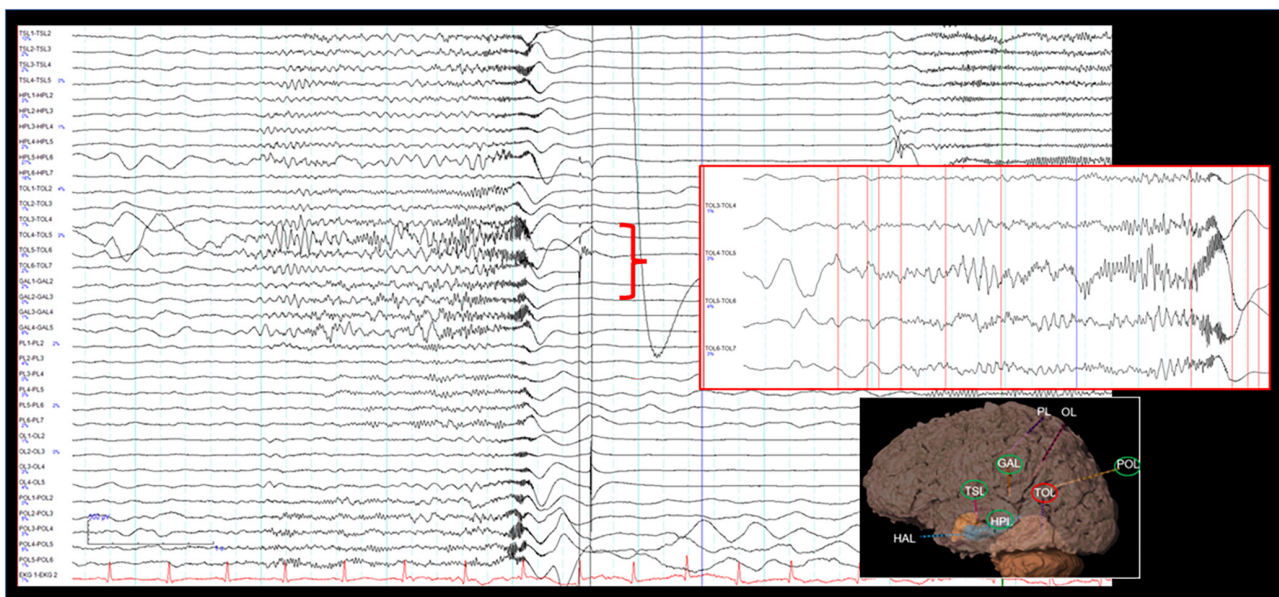
FIGURE 41 Typical ictal SEEG pattern seen in infantile spasms, characterized by widespread LVFA followed by high-amplitude slow wave and generalized suppression. The red box shows a zoomed-in image of the TOL electrode, which showed the earliest LVFA change. This finding can be used as a localization feature in an otherwise widespread seizure-onset pattern. The seizure onset is marked by a vertical blue line.

4.4 | Stimulation

As highlighted earlier in the article, stimulation can be used for functional mapping or SOZ identification during SEEG. Overall, systematic stimulation of all implanted electrodes is less common in children than adults for compliance reasons. However, there is good evidence that functional mapping of motor and language areas can be successfully conducted in children as young as 4–5 years of age.[133] The same is true for the stimulation to elicit typical seizures and auras. Data about stimulation parameters in children traditionally came from use of subdural grids, but has also been validated in SEEG.[134] However, there has been a debate about reproducibility and reliability of stimulation findings in children. Especially, over the motor cortex, higher stimulation parameters than in adults are needed to elicit a functional response.[135] This is likely a result of the not fully myelinated immature brain and more prominent in younger children.[136] In children with epileptic encephalopathies and nearly continuous interictal spiking, both functional responses as well as seizures might be harder to elicit. Failure to adjust the stimulation paradigm and unawareness of these pitfalls might lead false-negative results.

In conclusion, intracranial EEG especially SEEG is safe in children and can help to localize epileptic areas and increase eligibility for epilepsy surgery. Interictal patterns are often more abundant and widespread than in adults and have to be interpreted with caution. Except for infantile spasms, seizure-onset patterns and their interpretation equal to those of adults and depend mostly on etiology and localization.

5 | SPECIAL CONSIDERATIONS IN SUBDURAL GRIDS/STRIPS

Subdural electrodes are typically made of platinum–iridium in forms of strips and grids. Strip electrodes consist of 1–2 rows of electrodes, whereas subdural grids consist of 4–8 rows of electrodes. Each row of electrode has 4–8 contacts. The contacts are disks mounted in a thin, flexible silastic sheet with 2–5 mm diameter exposed to the cortical surface. Inter-contact distance is usually 5–10 mm (Figures 3 and 42). Strip electrodes can be inserted through burr holes. However, both the implantation and removal of subdural grids require craniotomy, which may increase the risks of complications compared with SEEG investigations, including intracranial infection, hemorrhage, and elevated intracranial pressure.[137–139] Furthermore, in case of subdural grids/strips, patients will need to be operated at the end of the procedure.
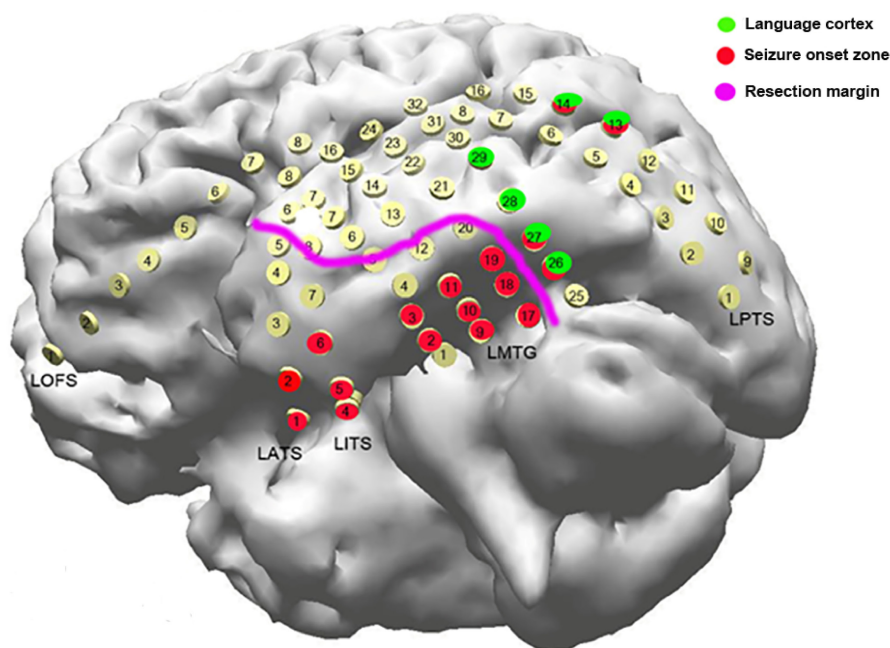
FIGURE 42 A 3-D view of subdural electrodes co-registered onto a patient's cortex using pre-implant brain MRI and post-implant head CT images. A combination of strips and grids was placed on the left temporal and orbitofrontal cortex in the patient with temporal lobe epilepsy. Red contacts mark the seizure-onset zone derived from EEG recording. Green contacts mark the language cortex derived from electrical stimulation mapping. Purple line is the proposed margin for a tailored resection of seizure-onset zone, while sparing the eloquent cortex. LATS, Left anterior temporal 1×8 strip; LITS, Left interior temporal 1×8 strip; LMTG, Left mid-temporal 4×8 grid; LPTS, Left posterior temporal 2×8 strip; LOFS, Left orbitofrontal 1×8 strip.

Intracranial recording
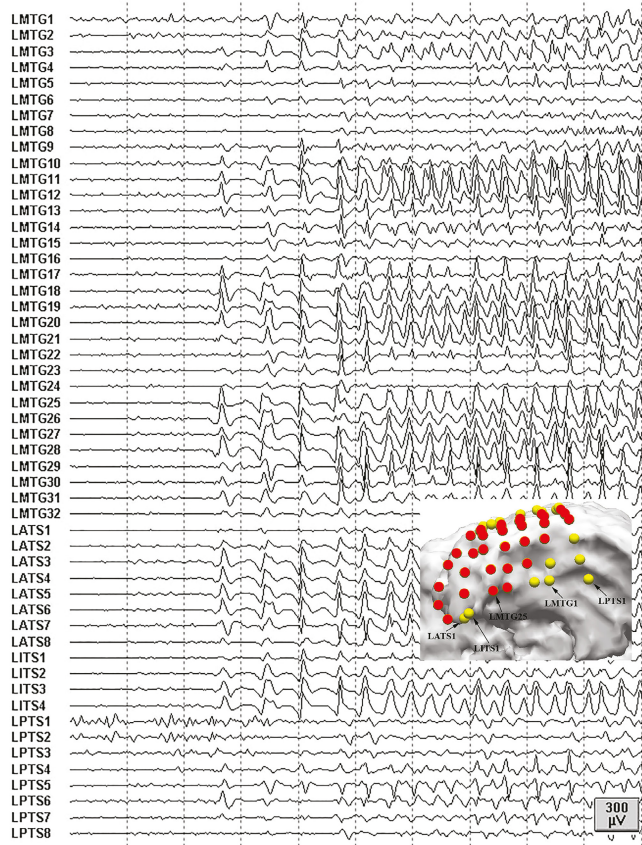
Scalp recording
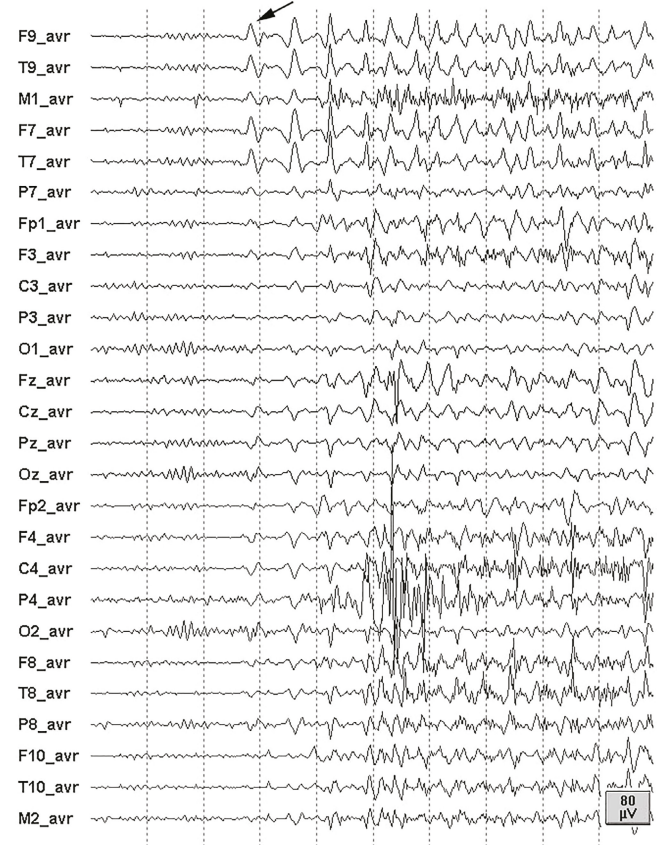
FIGURE 43 Simultaneous intracranial (left panel) and scalp (right panel) EEG recording of a left temporal lobe seizure using subdural electrodes. The seizure-onset zone is neocortical (~20 cm^2 in area, red color), involving most of the inferolateral and lateral temporal electrodes. Given that the cortical ictal discharges are widespread and synchronous at onset, a 2 Hz left anterior–inferior temporal seizure rhythm appears simultaneously on the scalp (marked by arrow). The patient underwent left anterior temporal lobectomy and remained seizure free for 3 years during post-operative follow-up. *Display parameters: common average montage, band pass: (1–50 Hz.* LATS, Left anterior temporal strip; LITS, Left inferior temporal strip; LMTG, Left mid-temporal grid; LPTS, Left posterior temporal strip.

Subdural electrodes are placed directly onto the cortical surface in a free-hand fashion and are commonly used to localize the epileptogenic focus in the cortical convexity, basal cortex, and inter-hemispheric cortex. When implanted in large arrays, they can determine both the extent and location of the SOZ. EEG data from subdural electrodes are easier to interpret because they are predominantly near-field recording from cortical gray matter directly under the electrodes, and localization of neocortical spikes and seizure generators can be accurate (Figure 43).[47] Moreover, subdural electrodes are well adapted for electrical stimulation mapping to localize sensory, motor, and/or language cortex.[140] They are particularly useful for the localization of seizure focus in proximity to eloquent cortex, which allows for the extra-operative mapping of the margins of the SOZ in relation to eloquent cortex, and thus guide a tailored resection of SOZ, while sparing eloquent cortex (Figure 42). Unlike depth electrodes, subdural electrodes are not suited to localize seizure generators in deep brain structures, such as hippocampus and insular cortex.

The relative merits of subdural versus depth electrodes have long been a subject of debate. A wealth of observational studies suggested that both are equally reliable in the localization of SOZ as demonstrated by seizure freedom rates following resective surgery guided by subdural and depth electrodes.[141–143] A systematic review showed that seizure freedom in studies utilizing depth electrodes was observed in 56%–68% patients, as compared with studies utilizing subdural electrodes showing seizure freedom in 30%–70% patients. There was no significant difference in seizure freedom rates between subdural and SEEG electrodes.[144] This was confirmed in a recent comparative multicenter study. Even though the use of SEEG electrodes was associated with a higher seizure freedom rate compared to subdural electrodes (55% vs. 41%), the use of SEEG electrodes went along with less subsequent resections after surgery than subdural grids/strips making surgical results overall comparable.[5] In contrast, side effects and complications were significantly lower in SEEG compared to subdural grids/strips.[5]

In practice, the type of electrodes selected for the intracranial EEG study is dependent upon the strengths and limitations of each type of electrodes as determined by the putative location of the epileptic focus from non-invasive studies.[12] A hybrid approach using both subdural and depth electrodes is often considered to leverage the strengths of both modalities and delineate seizure foci involving both subcortical and cortical networks.[145,146] In recent years, there has been a dramatic surge in the utilization of depth electrodes due to the advances in neuroimaging, stereotactic robot, and minimally invasive surgical techniques.[147,148] Despite this emerging trend, many patients still benefit from intracranial EEG recording using subdural electrodes, particularly in specific circumstances such as seizure focus restricted in the neocortex or in proximity to eloquent cortex. In contrast, situations where subdural grids/strips can be misleading are bottom-of-the sulcus FCDs with a focal onset in the depth and rapid distant propagation or a burned-out ipsilateral hippocampus with rapid seizure propagation to the contralateral site (strips record not from the hippocampus directly, but the para-hippocampal gyrus and this structure may be activated on the contralateral side first in case of a severely atrophic ipsilateral structure).

# 6 | OVERVIEW ON QUANTITATIVE/SIGNAL ANALYSIS APPROACHES

Since the advent of digital EEG recording in the late 1990s, signal analysis of SEEG has been a key methodology in understanding epilepsy as a network disorder.[56]

Computational algorithms and quantitative analysis can complement the traditional evaluation process and (i) help define the initial zone of seizure organization, (ii) provide precise and more objective results, and (iii) improve understanding of EEG patterns and their relation to semiological expression.

Two principal approaches are available to analyze simultaneously recorded multi-channel neuronal activity: *linear* and *non-linear*. Frequency is one of the most used quantitative characteristics of *linear* EEG analysis, because its evolution is a key feature of seizure dynamics. A seizure originates from one or several regions in the brain, characterized by high-frequency (beta and/or gamma) discharges before propagation to a second set of structures generating lower frequency oscillations. The structures involved in seizure onset and initial seizure organization are considered the most epileptogenic and in the traditional SEEG school are collectively called the "EZ" according to Bancaud's original term,[56] and quantitative tools have aimed at detecting the SOZ. Most have aimed at quantifying the change in signal energy (heavily dependent on frequency) at seizure onset (see Table 1). The first of these, the Epileptogenicity Index (EI) was developed by Bartolomei et al.,[149] building on earlier work from the Marseille school.[150] Subsequent methods developed in conjunction with experienced SEEG teams have incorporated additional features when quantifying the SOZ. The Epileptogenicity Map from David et al.[151] used time series of statistical parametric maps to illustrate dynamic ictal changes in 3-D space. Gnatkovsky et al.[152] combined three elements – fast (narrow band) activity, slow depolarizing shift and flattening (i.e., suppression of the background activity) – and validated their method in a prospective sample. In earlier work, these authors had also

TABLE 1 Quantitative tools for detection of the epileptogenic zone.

Year	First author	Journal	Method	Description
2008	Bartolomei[149]	Brain	Epileptogenicity Index (EI)	EI energy ratio compares relative energy of high- versus low-frequency activity at seizure onset and detects earliness of involvement of the energy change in different electrode contacts: structures showing high EI have higher energy ratio and are considered more epileptogenic.
2011	David[151]	Brain	Epileptogenicity Map	Combined SEEG signal quantification with spatial neuroimaging data in the form of time series of statistical parametric maps, to facilitate visualization of dynamic changes
2014	Gnatkovsky[152]	*Epilepsia*	*Computable biomarkers of the EZ*	SOZ/EZ found to be characterized by the combined detection of three biomarkers observed at seizure onset: (1) fast activity at 80–120 Hz associated with (2) very slow transient polarizing shift and (3) voltage depression (flattening).
2018	Grinenko[50]	*Brain*	EZ "fingerprint"	Time-frequency pattern that can differentiate the EZ from areas of propagation, characterized by the association of three elements: pre-ictal spikes, fast activity, and suppression.
2022	Nakatani[84]	*Brain Communications*	Ictal DC shifts ± ictal high-frequency oscillations	Uses EEG datasets recorded with a longer time constant of 10 s using an alternate current amplifier; detection of DC shifts and HFOs in relation to seizure onset
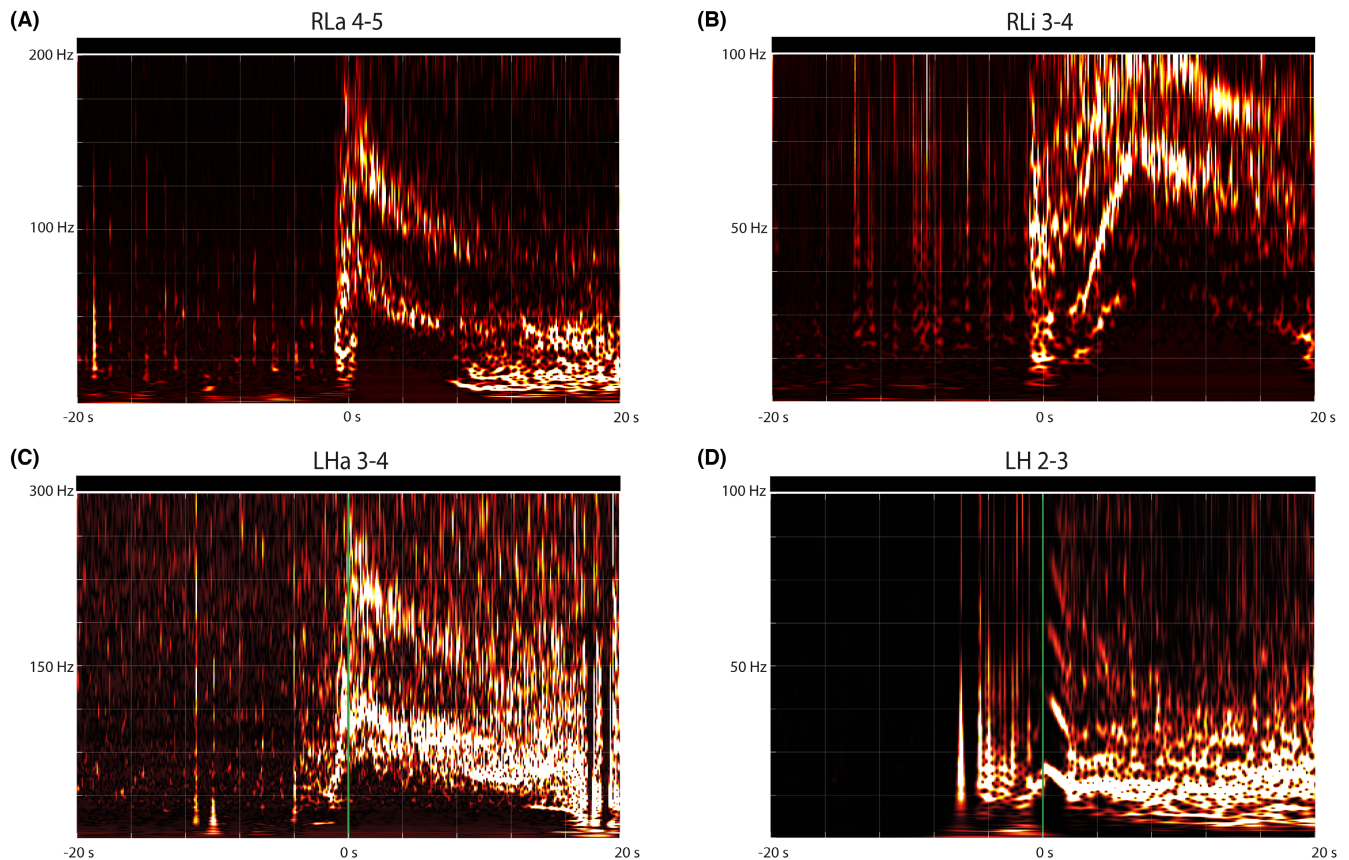
FIGURE 44 Epileptogenic zone fingerprint in different anatomical structures and pathologies. Time-frequency plots obtained from SEEG contacts located inside the SOZ of four patients with focal DRE showcasing pre-ictal spikes, fast activity, and suppression of low frequencies using the method described by Grinenko et al..[50] Spectrograms were obtained from the same patients and channels shown in Figure 20. Spectrograms obtained from the same patients and channels are shown in Figure 11. (A) contacts RLa 4–5 are located in the anterior margin of a lesion (FCD 2B) in the right superior parietal lobule. (B) contacts RLi 3–4 are located in the inferior margin of a lesion (FCD 2A) in the right frontal convexity. (C) contacts LHa 3–4 are located inside a periventricular nodular heterotopia in the vicinity of the left anterior hippocampus. (D) contacts LH 2–3 are located in the left anterior hippocampus in a patient with anterior temporal FCD 3A and hippocampal sclerosis. DRE, Drug-resistant epilepsy; FCD, Focal cortical dysplasia; LH, Left hippocampus; LHa, Left anterior hippocampus; RLa, Right lesion anterior; RLi, Right lingual gyrus.

shown reproducible, patient-specific narrow frequency band patterns at seizure onset[40]; the reproducibility of ictal electrical pattern at the individual patient level is in keeping with earlier observations of temporal lobe seizures.[150] Grinenko and colleagues proposed a novel time-frequency analysis of the epileptogenic "Fingerprint" associating pre-ictal spikes, fast activity, and suppression, allowing the differentiation of the SOZ from the propagation zone (Figure 44).[50] Work from Ikeda and colleagues has highlighted the role of ictal DC shifts (<1 Hz), with or without associated ictal HFOs >80 Hz.[86]

An example of the use of *non-linear* methods of seizure quantification includes work by Schindler and colleagues[153] who analyzed the temporal evolution of the correlation between structures involved in focal seizures, by using a multivariate analysis of the zero-lag correlation matrix with a sliding time window. They found that the zero-lag correlation of multi-channel EEG either remained approximately unchanged or especially in the case of evolution to a bilateral

tonic–clonic seizure decreased during the first half of the seizure. The correlation gradually increases again before the seizures terminate, which might be a mechanism of seizure termination. Since this pattern could occur in different epilepsy localizations, it was proposed to be a generic property of focal onset seizures. Quantitative methods also allow modeling of seizures,[154,155] a rapidly evolving domain that is promising and may in the future contribute to therapeutic decision making.[156] However, trials demonstrating the usefulness of these methods to improve epilepsy surgery outcome are not yet available.

7 | CONCLUSION

This Seminars in Epileptology article aims to provide fundamental principles on intracranial EEG, with a particular focus on SEEG. It serves as a valuable learning resource for trainees in clinical neurophysiology/epileptology offering a

basic understanding of invasive intracranial EEG concepts. Knowledge of invasive intracranial EEG is important for all neurophysiologists/epileptologists. Despite the increasing use of non-invasive technologies, invasive EEG continues to play a significant role in epilepsy presurgical investigation, with new indications and applications extending beyond pure diagnostic purposes. Efforts must be made to better select those patients who really can benefit from SEEG, in view of the high rate of patients who are not operated after it.

AFFILIATIONS

[1]Department of Neurology, Duke University Medical Center and Department of Biomedical Engineering, Duke Pratt School of Engineering, Durham, North Carolina, USA
[2]Analytical Neurophysiology Lab, Montreal Neurological Institute and Hospital, Montreal, Québec, Canada
[3]Neurophysiology Unit, Institute of Neurosurgery Dr. Asenjo, Santiago, Chile
[4]Department of Neurology, Medical University of Innsbruck, Innsbruck, Austria
[5]Danish Epilepsy Centre, Dianalund, Denmark
[6]Aarhus University, Aarhus, Denmark
[7]Brno Epilepsy Center, Department of Neurology, St. Anne's University Hospital and Medical Faculty of Masaryk University, Member of the ERN-EpiCARE, Brno, Czechia
[8]Behavioral and Social Neuroscience Research Group, Central European Institute of Technology, Masaryk University, Brno, Czechia
[9]Department of Epileptology, University Hospital Bonn, Bonn, Germany
[10]Department of Paediatrics and Department of Neuroscience, Cumming School of Medicine, University of Calgary, Calgary, Alberta, Canada
[11]Hotchkiss Brain Institute and Alberta Children's Hospital Research Institute, University of Calgary, Calgary, Alberta, Canada
[12]Department of Neurology, University of Florida, Gainesville, Florida, USA
[13]Wilder Center for Epilepsy Research, University of Florida, Gainesville, Florida, USA
[14]Epilepsy Research Centre, Department of Medicine (Austin Health), University of Melbourne, Melbourne, Victoria, Australia
[15]Bladin-Berkovic Comprehensive Epilepsy Program, Department of Neurology, Austin Health, Melbourne, Victoria, Australia
[16]Department of Neuroscience, Central Clinical School, Monash University, Melbourne, Victoria, Australia
[17]Department of Neurology, Alfred Health, Melbourne, Victoria, Australia
[18]Department of Neurology, Royal Melbourne Hospital, Melbourne, Victoria, Australia
[19]Department of Clinical Neurosciences, CHUV, Lausanne University Hospital, Lausanne, Switzerland
[20]Department of Neurology, Feinberg School of Medicine, Northwestern Memorial Hospital, Chicago, Illinois, USA
[21]Department of Neurology, The University of Chicago, Chicago, Illinois, USA
[22]Department of Neurology and Neurosurgery, UMC Utrecht Brain Center, University Medical Center Utrecht, Utrecht, the Netherlands
[23]Stichting Epilepsie Instellingen Nederland (SEIN), Heemstede, The Netherlands
[24]Department of Neurosciences, Mater Misericordiae Hospital, Brisbane, Queensland, Australia
[25]Mater Research Institute, Faculty of Medicine, University of Queensland, St Lucia, Queensland, Australia

CONFLICT OF INTEREST STATEMENT

BF has received speaker honoraria from UCB, Eisai, and Paladin labs, outside the submitted work. She is an Associate Editor for Epileptic Disorders, the Journal of Clinical Neurophysiology, and the Journal of Sleep Research. PP has received speaker honoraria or consultancy fees to his institution from Chiesi, Eisai, LivaNova, Novartis, Sun Pharma, Supernus, and UCB Pharma, outside the submitted work. He is an Associate Editor for Epilepsia Open.

ORCID

B. Frauscher https://orcid.org/0000-0001-6064-1529
D. Mansilla https://orcid.org/0000-0002-5445-2526
C. Abdallah https://orcid.org/0000-0001-7232-6673
A. Astner-Rohracher https://orcid.org/0000-0002-1132-302X
S. Beniczky https://orcid.org/0000-0002-6035-6581
M. Brazdil https://orcid.org/0000-0001-7979-2343
G. Kalamangalam https://orcid.org/0000-0002-0178-4332
P. Perucca https://orcid.org/0000-0002-7855-7066
P. Ryvlin https://orcid.org/0000-0001-7775-6576
S. Schuele https://orcid.org/0000-0003-3261-7120
J. Tao https://orcid.org/0000-0002-7448-2183
M. Zijlmans https://orcid.org/0000-0003-1258-5678
A. McGonigal https://orcid.org/0000-0001-6775-5318

REFERENCES

1. Engel J. What can we do for people with drug-resistant epilepsy? The 2016 Wartenberg lecture. Neurology. 2016;87:2483–9. https://doi.org/10.1212/WNL.0000000000003407
2. Vakharia VN, Duncan JS, Witt JA, Elger CE, Staba R, Engel J. Getting the best outcomes from epilepsy surgery. Ann Neurol. 2018;83:676–90. https://doi.org/10.1002/ANA.25205
3. Jayakar P, Gotman J, Harvey AS, Palmini A, Tassi L, Schomer D, et al. Diagnostic utility of invasive EEG for epilepsy surgery: indications, modalities, and techniques. Epilepsia. 2016;57:1735–47. https://doi.org/10.1111/EPI.13515

4. Gavvala J, Zafar M, Sinha SR, Kalamangalam G, Schuele S. Stereotactic EEG practices: a survey of United States tertiary referral epilepsy centers. J Clin Neurophysiol. 2022;39:474–80. https://doi.org/10.1097/WNP.0000000000000794

5. Jehi L, Morita-Sherman M, Love TE, Bartolomei F, Bingaman W, Braun K, et al. Comparative effectiveness of stereotactic electroencephalography versus subdural grids in epilepsy surgery. Ann Neurol. 2021;90:927–39. https://doi.org/10.1002/ANA.26238

6. McGonigal A, Bartolomei F, Chauvel P. On seizure semiology. Epilepsia. 2021;62:2019–35. https://doi.org/10.1111/EPI.16994

7. Bancaud J, Talairach J, Bonis A. La stéréo-électroencéphalographie dans l'épilepsie: informations neurophysiopathologiques apportées par l'investigation fonctionnelle stéréotaxique. Paris: Masson; 1965.

8. Rosenow F, Lüders H. Presurgical evaluation of epilepsy. Brain. 2001;124:1683–700. https://doi.org/10.1093/BRAIN/124.9.1683

9. Kahane P, Landré E, Minotti L, Francione S, Ryvlin P. The Bancaud and Talairach view on the epileptogenic zone: a working hypothesis. Epileptic Disord. 2006;8(Suppl 2):S16–26.

10. Chauvel P, Gonzalez-Martinez J, Bulacio J. Presurgical intracranial investigations in epilepsy surgery. Handb Clin Neurol. 2019;161:45–71. https://doi.org/10.1016/B978-0-444-64142-7.00040-0

11. Isnard J, Taussig D, Bartolomei F, Bourdillon P, Catenoix H, Chassoux F, et al. French guidelines on stereoelectroencephalography (SEEG). Neurophysiol Clin. 2018;48:5–13. https://doi.org/10.1016/J.NEUCLI.2017.11.005

12. Englot DJ. A modern epilepsy surgery treatment algorithm: incorporating traditional and emerging technologies. Epilepsy Behav. 2018;80:68–74. https://doi.org/10.1016/J.YEBEH.2017.12.041

13. Mirandola L, Mai RF, Francione S, Pelliccia V, Gozzo F, Sartori I, et al. Stereo-EEG: diagnostic and therapeutic tool for periventricular nodular heterotopia epilepsies. Epilepsia. 2017;58:1962–71. https://doi.org/10.1111/EPI.13895

14. Bourdillon P, Cucherat M, Isnard J, Ostrowsky-Coste K, Catenoix H, Guénot M, et al. Stereo-electroencephalography-guided radiofrequency thermocoagulation in patients with focal epilepsy: a systematic review and meta-analysis. Epilepsia. 2018;59:2296–304. https://doi.org/10.1111/EPI.14584

15. Gonzalez-Martinez J, Bulacio J, Alexopoulos A, Jehi L, Bingaman W, Najm I. Stereoelectroencephalography in the "difficult to localize" refractory focal epilepsy: early experience from a north American epilepsy center. Epilepsia. 2013;54:323–30. https://doi.org/10.1111/J.1528-1167.2012.03672.X

16. Hall JA, Khoo HM. Robotic-assisted and image-guided MRI-compatible Stereoelectroencephalography. Can J Neurol Sci. 2018;45:35–43. https://doi.org/10.1017/CJN.2017.240

17. Cardinale F, Rizzi M, Vignati E, Cossu M, Castana L, d'Orio P, et al. Stereoelectroencephalography: retrospective analysis of 742 procedures in a single centre. Brain. 2019;142:2688–704. https://doi.org/10.1093/BRAIN/AWZ196

18. Astner-Rohracher A, Zimmermann G, Avigdor T, Abdallah C, Barot N, Brázdil M, et al. Development and validation of the 5-SENSE score to predict focality of the seizure-onset zone as assessed by Stereoelectroencephalography. JAMA Neurol. 2022;79:70–9. https://doi.org/10.1001/JAMANEUROL.2021.4405

19. Bartolomei F, Trébuchon A, Bonini F, Lambert I, Gavaret M, Woodman M, et al. What is the concordance between the seizure onset zone and the irritative zone? A SEEG quantified study. Clin Neurophysiol. 2016;127:1157–62. https://doi.org/10.1016/J.CLINPH.2015.10.029

20. Lagarde S, Buzori S, Trebuchon A, Carron R, Scavarda D, Milh M, et al. The repertoire of seizure onset patterns in human focal epilepsies: determinants and prognostic values. Epilepsia. 2019;60:85–95. https://doi.org/10.1111/EPI.14604

21. Henkel A, Noachtar S, Pfänder M, Lüders HO. The localizing value of the abdominal aura and its evolution: a study in focal epilepsies. Neurology. 2002;58:271–6. https://doi.org/10.1212/WNL.58.2.271

22. Epstein CM. Digital EEG: trouble in paradise? J Clin Neurophysiol. 2006;23:190–3. https://doi.org/10.1097/01.WNP.0000220083.90279.22

23. Zelmann R, Frauscher B, Phellan Aro R, Gueziri H-E, Collins DL. SEEGAtlas: a framework for the identification and classification of depth electrodes using clinical images. J Neural Eng. 2023;20:20. https://doi.org/10.1088/1741-2552/ACD6BD

24. Kahane P, Minotti L, Hoffmann D, Lachaux JP, Ryvlin P. Invasive EEG in the definition of the seizure onset zone: depth electrodes. In: Rosenow F, Lüders HO, editors. Handbook of Clinical Neurophysiology, Vol. 3. Presurgical assessment of the epilepsies with clinical neurophysiology and functional imaging. Elsevier BV: Amsterdam; 2003. p. 109–33.

25. Sperling MR. Intracranial electroencephalography. In: Ebersole JS, Pedley TA, editors. Current Practice of Clinical Electroencephalography. 3rd ed. Philadelphia: Lippincott Williams & Wilkins; 2003.

26. Frauscher B, Von Ellenrieder N, Zelmann R, Doležalová I, Minotti L, Olivier A, et al. Atlas of the normal intracranial electroencephalogram: neurophysiological awake activity in different cortical areas. Brain. 2018;141:1130–44. https://doi.org/10.1093/BRAIN/AWY035

27. Jasper H, Penfield W. Electrocorticograms in man: effect of voluntary movement upon the electrical activity of the precentral gyrus. Arch Psychiatr Nervenkr. 1949;183:163–74. https://doi.org/10.1007/BF01062488

28. Kural MA, Duez L, Sejer Hansen V, Larsson PG, Rampp S, Schulz R, et al. Criteria for defining interictal epileptiform discharges in EEG: a clinical validation study. Neurology. 2020;94:E2139–47. https://doi.org/10.1212/WNL.0000000000009439

29. Gloor P. Neuronal generators and the problem of localization in electroencephalography: application of volume conductor theory to electroencephalography. J Clin Neurophysiol. 1985;2:327–54. https://doi.org/10.1097/00004691-198510000-00002

30. Paredes-Aragon E, AlKhaldi NA, Ballesteros-Herrera D, Mirsattari SM. Stereo-encephalographic Presurgical evaluation of temporal lobe epilepsy: an evolving science. Front Neurol. 2022;13:867458. https://doi.org/10.3389/FNEUR.2022.867458

31. Palmini A, Gambardella A, Andermann F, Dubeau F, da Costa JC, Olivier A, et al. Intrinsic epileptogenicity of human dysplastic cortex as suggested by corticography and surgical results. Ann Neurol. 1995;37:476–87. https://doi.org/10.1002/ANA.410370410

32. Ferrier CH, Alarcon G, Engelsman J, Binnie CD, Koutroumanidis M, Polkey CE, et al. Relevance of residual histologic and electrocorticographic abnormalities for surgical outcome in frontal lobe epilepsy. Epilepsia. 2001;42:363–71. https://doi.org/10.1046/J.1528-1157.2001.06900.X

33. Shakhatreh L, Janmohamed M, Baker AA, Willard A, Laing J, Rychkova M, et al. Interictal and seizure-onset EEG patterns in malformations of cortical development: a systematic review. Neurobiol Dis. 2022;174:105863. https://doi.org/10.1016/J.NBD.2022.105863

34. Cuello-Oderiz C, von Ellenrieder N, Sankhe R, Olivier A, Hall J, Dubeau F, et al. Value of ictal and interictal epileptiform discharges and high frequency oscillations for delineating the epileptogenic zone in patients with focal cortical dysplasia. Clin Neurophysiol. 2018;129:1311–9. https://doi.org/10.1016/J.CLINPH.2018.02.003

35. Francione S, Nobili L, Cardinale F, Citterio A, Galli C, Tassi L. Intra-lesional stereo-EEG activity in Taylor's focal cortical dysplasia. Epileptic Disord. 2003;5(Suppl 2):S105–14.

36. Di Giacomo R, Uribe-San-Martin R, Mai R, Francione S, Nobili L, Sartori I, et al. Stereo-EEG ictal/interictal patterns and underlying pathologies. Seizure. 2019;72:54–60. https://doi.org/10.1016/J.SEIZURE.2019.10.001

37. Mohamed AR, Bailey CA, Freeman JL, Maixner W, Jackson GD, Harvey AS. Intrinsic epileptogenicity of cortical tubers revealed by intracranial EEG monitoring. Neurology. 2012;79:2249–57. https://doi.org/10.1212/WNL.0B013E3182768923

38. Kannan L, Vogrin S, Bailey C, Maixner W, Harvey AS. Centre of epileptogenic tubers generate and propagate seizures in tuberous sclerosis. Brain. 2016;139:2653–67. https://doi.org/10.1093/BRAIN/AWW192

39. Sklenarova B, Zatloukalova E, Cimbalnik J, Klimes P, Dolezalova I, Pail M, et al. Interictal High-Frequency Oscillations, Spikes, and Connectivity profiles: a Fingerprint of Epileptogenic Brain Pathologies. 2023.

40. Gnatkovsky V, Pelliccia V, de Curtis M, Tassi L. Two main focal seizure patterns revealed by intracerebral electroencephalographic biomarker analysis. Epilepsia. 2019;60:96–106. https://doi.org/10.1111/EPI.14610

41. Lee SA, Spencer DD, Spencer SS. Intracranial EEG seizure-onset patterns in neocortical epilepsy. Epilepsia. 2000;41:297–307. https://doi.org/10.1111/J.1528-1157.2000.TB00159.X

42. Kane N, Acharya J, Benickzy S, Caboclo L, Finnigan S, Kaplan PW, et al. A revised glossary of terms most commonly used by clinical electroencephalographers and updated proposal for the report format of the EEG findings. Revision 2017. Clin Neurophysiol Pract. 2017;2:170–85. https://doi.org/10.1016/J.CNP.2017.07.002

43. Perucca P, Dubeau F, Gotman J. Intracranial electroencephalographic seizure-onset patterns: effect of underlying pathology. Brain. 2014;137:183–96. https://doi.org/10.1093/BRAIN/AWT299

44. Faught E, Kuzniecky RI, Hurst DC. Ictal EEG wave forms from epidural electrodes predictive of seizure control after temporal lobectomy. Electroencephalogr Clin Neurophysiol. 1992;83:229–35. https://doi.org/10.1016/0013-4694(92)90116-Y

45. Spanedda F, Cendes F, Gotman J. Relations between EEG seizure morphology, interhemispheric spread, and mesial temporal atrophy in bitemporal epilepsy. Epilepsia. 1997;38:1300–14. https://doi.org/10.1111/J.1528-1157.1997.TB00068.X

46. Wennberg R, Arruda F, Quesney LF, Olivier A. Preeminence of extrahippocampal structures in the generation of mesial temporal seizures: evidence from human depth electrode recordings. Epilepsia. 2002;43:716–26. https://doi.org/10.1046/J.1528-1157.2002.31101.X

47. Spencer SS, Guimaraes P, Katz A, Kim J, Spencer D. Morphological patterns of seizures recorded intracranially. Epilepsia. 1992;33:537–45. https://doi.org/10.1111/J.1528-1157.1992.TB01706.X

48. Velasco AL, Wilson CL, Babb TL, Engel J. Functional and anatomic correlates of two frequently observed temporal lobe seizure-onset patterns. Neural Plast. 2000;7:49–63. https://doi.org/10.1155/NP.2000.49

49. Schiller Y, Cascino GD, Busacker NE, Sharbrough FW. Characterization and comparison of local onset and remote propagated electrographic seizures recorded with intracranial electrodes. Epilepsia. 1998;39:380–8. https://doi.org/10.1111/J.1528-1157.1998.TB01390.X

50. Grinenko O, Li J, Mosher JC, Wang IZ, Bulacio JC, Gonzalez-Martinez J, et al. A fingerprint of the epileptogenic zone in human epilepsies. Brain. 2018;141:117–31. https://doi.org/10.1093/BRAIN/AWX306

51. Salami P, Peled N, Nadalin JK, Martinet LE, Kramer MA, Lee JW, et al. Seizure onset location shapes dynamics of initiation. Clin Neurophysiol. 2020;131:1782–97. https://doi.org/10.1016/J.CLINPH.2020.04.168

52. Singh S, Sandy S, Wiebe S. Ictal onset on intracranial EEG: do we know it when we see it? State of the evidence. Epilepsia. 2015;56:1629–38. https://doi.org/10.1111/EPI.13120

53. Alter AS, Dhamija R, McDonough TL, Shen S, McBrian DK, Mandel AM, et al. Ictal onset patterns of subdural intracranial electroencephalogram in children: how helpful for predicting epilepsy surgery outcome? Epilepsy Res. 2019;149:44–52. https://doi.org/10.1016/J.EPLEPSYRES.2018.10.008

54. Frauscher B, von Ellenrieder N, Dubeau F, Gotman J. Different seizure-onset patterns in mesiotemporal lobe epilepsy have a distinct interictal signature. Clin Neurophysiol. 2017;128:1282–9. https://doi.org/10.1016/J.CLINPH.2017.04.020

55. Gastaut H, Broughton RJ. Epileptic Seizures: Clinical and Electrographic Features, Diagnosis and Treatment. Springfield, Illinois, USA: Charles C. Thomas Publisher; 1972.

56. Bartolomei F, Lagarde S, Wendling F, McGonigal A, Jirsa V, Guye M, et al. Defining epileptogenic networks: contribution of SEEG and signal analysis. Epilepsia. 2017;58:1131–47. https://doi.org/10.1111/EPI.13791

57. Chauvel P, McGonigal A. Emergence of semiology in epileptic seizures. Epilepsy Behav. 2014;38:94–103. https://doi.org/10.1016/J.YEBEH.2013.12.003

58. Bartolomei F, Trébuchon A, Gavaret M, Régis J, Wendling F, Chauvel P. Acute alteration of emotional behaviour in epileptic seizures is related to transient desynchrony in emotion-regulation networks. Clin Neurophysiol. 2005;116:2473–9. https://doi.org/10.1016/J.CLINPH.2005.05.013

59. Aupy J, Noviawaty I, Krishnan B, Suwankpakdee P, Bulacio J, Gonzalez-Martinez J, et al. Insulo-opercular cortex generates oroalimentary automatisms in temporal seizures. Epilepsia. 2018;59:583–94. https://doi.org/10.1111/EPI.14011

60. Zalta A, Hou JC, Thonnat M, Bartolomei F, Morillon B, McGonigal A. Neural correlates of rhythmic rocking in prefrontal seizures. Neurophysiol Clin. 2020;50:331–8. https://doi.org/10.1016/J.NEUCLI.2020.07.003

61. Bragin A, Engel J, Wilson CL, Fried I, Buzsáki G. High-frequency oscillations in human brain. Hippocampus. 1999;9:137–42. https://doi.org/10.1002/(sici)1098-1063(1999)9:2<137::aid-hipo5>3.0.co;2-0

62. van't Klooster MA, Van Klink NEC, Leijten FSS, Zelmann R, Gebbink TA, Gosselaar PH, et al. Residual fast ripples in the

intraoperative corticogram predict epilepsy surgery outcome. Neurology. 2015;85:120–8. https://doi.org/10.1212/WNL.0000000000001727

63. Akiyama T, Otsubo H, Ochi A, Galicia EZ, Weiss SK, Donner EJ, et al. Topographic movie of ictal high-frequency oscillations on the brain surface using subdural EEG in neocortical epilepsy. Epilepsia. 2006;47:1953–7. https://doi.org/10.1111/j.1528-1167.2006.00823.x

64. Zelmann R, Lina JM, Schulze-Bonhage A, Gotman J, Jacobs J. Scalp EEG is not a blur: it can see high frequency oscillations although their generators are small. Brain Topogr. 2014;27:683–704. https://doi.org/10.1007/S10548-013-0321-Y

65. RamachandranNair R, Ochi A, Imai K, Benifla M, Akiyama T, Holowka S, et al. Epileptic spasms in older pediatric patients: MEG and ictal high-frequency oscillations suggest focal-onset seizures in a subset of epileptic spasms. Epilepsy Res. 2008;78:216–24. https://doi.org/10.1016/J.EPLEPSYRES.2007.12.007

66. Foffani G, Uzcategui YG, Gal B, Menendez de la Prida L. Reduced spike-timing reliability correlates with the emergence of fast ripples in the rat epileptic hippocampus. Neuron. 2007;55:930–41. https://doi.org/10.1016/J.NEURON.2007.07.040

67. Jacobs J, LeVan P, Chander R, Hall J, Dubeau F, Gotman J. Interictal high-frequency oscillations (80–500 Hz) are an indicator of seizure onset areas independent of spikes in the human epileptic brain. Epilepsia. 2008;49:1893–907. https://doi.org/10.1111/J.1528-1167.2008.01656.X

68. Brázdil M, Pail M, Halámek J, Plešinger F, Cimbálník J, Roman R, et al. Very high-frequency oscillations: novel biomarkers of the epileptogenic zone. Ann Neurol. 2017;82:299–310. https://doi.org/10.1002/ANA.25006

69. Fedele T, Burnos S, Boran E, Krayenbühl N, Hilfiker P, Grunwald T, et al. Resection of high frequency oscillations predicts seizure outcome in the individual patient. Sci Rep. 2017;7:13836. https://doi.org/10.1038/S41598-017-13064-1

70. Zhang Y, Chung H, Ngo JP, Monsoor T, Hussain SA, Matsumoto JH, et al. Characterizing physiological high-frequency oscillations using deep learning. J Neural Eng. 2022;19(6). https://doi.org/10.1088/1741-2552/aca4fa

71. Frauscher B, von Ellenrieder N, Zelmann R, Rogers C, Nguyen DK, Kahane P, et al. High-frequency oscillations in the Normal human brain. Ann Neurol. 2018;84:374–85. https://doi.org/10.1002/ANA.25304

72. Van Klink NEC, Van't Klooster MA, Zelmann R, Leijten FSS, Ferrier CH, Braun KPJ, et al. High frequency oscillations in intra-operative electrocorticography before and after epilepsy surgery. Clin Neurophysiol. 2014;125:2212–9. https://doi.org/10.1016/J.CLINPH.2014.03.004

73. Alkawadri R, Gaspard N, Goncharova II, Spencer DD, Gerrard JL, Zaveri H, et al. The spatial and signal characteristics of physiologic high frequency oscillations. Epilepsia. 2014;55:1986–95. https://doi.org/10.1111/EPI.12851

74. Pail M, Cimbálník J, Roman R, Daniel P, Shaw DJ, Chrastina J, et al. High frequency oscillations in epileptic and non-epileptic human hippocampus during a cognitive task. Sci Rep. 2020;10:18147. https://doi.org/10.1038/S41598-020-74306-3

75. Melani F, Zelmann R, Mari F, Gotman J. Continuous high frequency activity: a peculiar SEEG pattern related to specific brain regions. Clin Neurophysiol. 2013;124:1507–16. https://doi.org/10.1016/J.CLINPH.2012.11.016

76. Mooij AH, Huiskamp GJM, Aarts E, Ferrier CH, Braun KPJ, Zijlmans M. Accurate differentiation between physiological and pathological ripples recorded with scalp-EEG. Clin Neurophysiol. 2022;143:172–81. https://doi.org/10.1016/J.CLINPH.2022.08.014

77. Zweiphenning W, van't Klooster MA, van Klink NEC, Leijten FSS, Ferrier CH, Gebbink T, et al. Intraoperative electrocorticography using high-frequency oscillations or spikes to tailor epilepsy surgery in The Netherlands (the HFO trial): a randomised, single-blind, adaptive non-inferiority trial. Lancet Neurol. 2022;21:982–93. https://doi.org/10.1016/S1474-4422(22)00311-8

78. Boran E, Ramantani G, Krayenbühl N, Schreiber M, König K, Fedele T, et al. High-density ECoG improves the detection of high frequency oscillations that predict seizure outcome. Clin Neurophysiol. 2019;130:1882–8. https://doi.org/10.1016/J.CLINPH.2019.07.008

79. Zweiphenning WJEM, van Diessen E, Aarnoutse EJ, Leijten FSS, van Rijen PC, Braun KPJ, et al. The resolution revolution: comparing spikes and high frequency oscillations in high-density and standard intra-operative electrocorticography of the same patient. Clin Neurophysiol. 2020;131:1040–3. https://doi.org/10.1016/J.CLINPH.2020.02.006

80. Thomas J, Kahane P, Abdallah C, Avigdor T, Zweiphenning WJEM, Chabardes S, et al. A subpopulation of spikes predicts successful epilepsy surgery outcome. Ann Neurol. 2023;93:522–35. https://doi.org/10.1002/ANA.26548

81. Ren L, Kucewicz MT, Cimbalnik J, Matsumoto JY, Brinkmann BH, Hu W, et al. Gamma oscillations precede interictal epileptiform spikes in the seizure onset zone. Neurology. 2015;84:602–8. https://doi.org/10.1212/WNL.0000000000001234

82. Gumnit RJ, Takahashi T. Changes in direct current activity during experimental focal seizures. Electroencephalogr Clin Neurophysiol. 1965;19:63–74. https://doi.org/10.1016/0013-4694(65)90007-6

83. Ikeda A, Taki W, Kunieda T, Terada K, Mikuni N, Nagamine T, et al. Focal ictal direct current shifts in human epilepsy as studied by subdural and scalp recording. Brain. 1999;122(Pt 5):827–38. https://doi.org/10.1093/BRAIN/122.5.827

84. Nakatani M, Inouchi M, Daifu-Kobayashi M, Murai T, Togawa J, Kajikawa S, et al. Ictal direct current shifts contribute to defining the core ictal focus in epilepsy surgery. Brain Commun. 2022;4:fcac222. https://doi.org/10.1093/BRAINCOMMS/FCAC222

85. Amzica F, Steriade M. Neuronal and glial membrane potentials during sleep and paroxysmal oscillations in the neocortex. J Neurosci. 2000;20:6648–65. https://doi.org/10.1523/JNEUROSCI.20-17-06648.2000

86. Ikeda A, Takeyama H, Bernard C, Nakatani M, Shimotake A, Daifu M, et al. Active direct current (DC) shifts and "red slow": two new concepts for seizure mechanisms and identification of the epileptogenic zone. Neurosci Res. 2020;156:95–101. https://doi.org/10.1016/J.NEURES.2020.01.014

87. Imamura H, Matsumoto R, Inouchi M, Matsuhashi M, Mikuni N, Takahashi R, et al. Ictal wideband ECoG: direct comparison between ictal slow shifts and high frequency oscillations. Clin Neurophysiol. 2011;122:1500–4. https://doi.org/10.1016/J.CLINPH.2010.12.060

88. Hannan S, Ho A, Frauscher B. Clinical utility of sleep recordings during presurgical epilepsy evaluation with stereo-electroencephalography: a systematic review. J Clin Neurophysiol. 2023.

89. Ho A, Hannan S, Thomas J, Avigdor T, Abdallah C, Dubeau F, et al. Rapid eye movement sleep affects interictal epileptic activity differently in mesiotemporal and neocortical areas. Epilepsia. 2023;64:3036–48. https://doi.org/10.1111/EPI.17763

90. Lambert I, Roehri N, Giusiano B, Carron R, Wendling F, Benar C, et al. Brain regions and epileptogenicity influence epileptic interictal spike production and propagation during NREM sleep in comparison with wakefulness. Epilepsia. 2018;59:235–43. https://doi.org/10.1111/EPI.13958

91. Fouad A, Azizollahi H, Le Douget JE, Lejeune FX, Valderrama M, Mayor L, et al. Interictal epileptiform discharges show distinct spatiotemporal and morphological patterns across wake and sleep. Brain Commun. 2022;4:fcac183. https://doi.org/10.1093/BRAINCOMMS/FCAC183

92. Frauscher B, Von Ellenrieder N, Dubeau F, Gotman J. EEG desynchronization during phasic REM sleep suppresses interictal epileptic activity in humans. Epilepsia. 2016;57:879–88. https://doi.org/10.1111/EPI.13389

93. Frauscher B, Von Ellenrieder N, Ferrari-Marinho T, Avoli M, Dubeau F, Gotman J. Facilitation of epileptic activity during sleep is mediated by high amplitude slow waves. Brain. 2015;138:1629–41. https://doi.org/10.1093/BRAIN/AWV073

94. von Ellenrieder N, Dubeau F, Gotman J, Frauscher B. Physiological and pathological high-frequency oscillations have distinct sleep-homeostatic properties. Neuroimage Clin. 2017;14:566–73. https://doi.org/10.1016/J.NICL.2017.02.018

95. Ng M, Pavlova M. Why are seizures rare in rapid eye movement sleep? Review of the frequency of seizures in different sleep stages. Epilepsy Res Treat. 2013;2013:1–10. https://doi.org/10.1155/2013/932790

96. Hannan S, Thomas J, Jaber K, El Kosseifi C, Ho A, Abdallah C, et al. The Differing Effects of Sleep on Ictal and Interictal Network Dynamics in Drug-Resistant Epilepsy. Ann Neurol. 2023. https://doi.org/10.1002/ana.26796

97. Peter-Derex L, Klimes P, Latreille V, Bouhadoun S, Dubeau F, Frauscher B. Sleep disruption in epilepsy: ictal and Interictal epileptic activity matter. Ann Neurol. 2020;88:907–20. https://doi.org/10.1002/ANA.25884

98. Penfield W, Jasper HH Sequel to: Penfield W. Epilepsy and the functional anatomy of the human brain. 1954:896.

99. Gordon B, Lesser RP, Rance NE, Hart J, Webber R, Uematsu S, et al. Parameters for direct cortical electrical stimulation in the human: histopathologic confirmation. Electroencephalogr Clin Neurophysiol. 1990;75:371–7. https://doi.org/10.1016/0013-4694(90)90082-U

100. Prime D, Rowlands D, O'Keefe S, Dionisio S. Considerations in performing and analyzing the responses of cortico-cortical evoked potentials in stereo-EEG. Epilepsia. 2018;59:16–26. https://doi.org/10.1111/EPI.13939

101. Blume WT, Jones DC, Pathak P. Properties of after-discharges from cortical electrical stimulation in focal epilepsies. Clin Neurophysiol. 2004;115:982–9. https://doi.org/10.1016/j.clinph.2003.11.023

102. Munari C, Kahane P, Tassi L, Francione S, Hoffmann D, Lo Russo G, et al. Intracerebral low frequency electrical stimulation: a new tool for the definition of the "epileptogenic area"? Acta Neurochir Suppl (Wien). 1993;58:181–5. https://doi.org/10.1007/978-3-7091-9297-9_42

103. Chassoux F, Devaux B, Landré E, Turak B, Nataf F, Varlet P, et al. Stereoelectroencephalography in focal cortical dysplasia: a 3D approach to delineating the dysplastic cortex. Brain. 2000;123(Pt 8):1733–51. https://doi.org/10.1093/BRAIN/123.8.1733

104. Sperling MR, O'Connor MJ. Auras and subclinical seizures: characteristics and prognostic significance. Ann Neurol. 1990;28:320–8. https://doi.org/10.1002/ANA.410280304

105. Gollwitzer S, Hopfengärtner R, Rössler K, Müller T, Olmes DG, Lang J, et al. Afterdischarges elicited by cortical electric stimulation in humans: when do they occur and what do they mean? Epilepsy Behav. 2018;87:173–9. https://doi.org/10.1016/J.YEBEH.2018.09.007

106. Cuello Oderiz C, Von Ellenrieder N, Dubeau F, Eisenberg A, Gotman J, Hall J, et al. Association of Cortical Stimulation-Induced Seizure with Surgical Outcome in patients with focal drug-resistant epilepsy. JAMA Neurol. 2019;76:1070–8. https://doi.org/10.1001/JAMANEUROL.2019.1464

107. Trébuchon A, Chauvel P. Electrical stimulation for seizure induction and functional mapping in Stereoelectroencephalography. J Clin Neurophysiol. 2016;33:511–21. https://doi.org/10.1097/WNP.0000000000000313

108. McGonigal A, Lagarde S, Trébuchon-Dafonseca A, Roehri N, Bartolomei F. Early onset motor semiology in seizures triggered by cortical stimulation during SEEG. Epilepsy Behav. 2018;88:262–7. https://doi.org/10.1016/J.YEBEH.2018.09.017

109. Kovac S, Kahane P, Diehl B. Seizures induced by direct electrical cortical stimulation–Mechanisms and clinical considerations. Clin Neurophysiol. 2016;127:31–9. https://doi.org/10.1016/J.CLINPH.2014.12.009

110. Borchers S, Himmelbach M, Logothetis N, Karnath HO. Direct electrical stimulation of human cortex – the gold standard for mapping brain functions? Nat Rev Neurosci. 2011;13:63–70. https://doi.org/10.1038/NRN3140

111. Aron O, Jonas J, Colnat-Coulbois S, Maillard L. Language mapping using stereo electroencephalography: a review and expert opinion. Front Hum Neurosci. 2021;15:619521. https://doi.org/10.3389/FNHUM.2021.619521

112. Perrone-Bertolotti M, Alexandre S, Jobb AS, De Palma L, Baciu M, Mairesse MP, et al. Probabilistic mapping of language networks from high frequency activity induced by direct electrical stimulation. Hum Brain Mapp. 2020;41:4113–26. https://doi.org/10.1002/HBM.25112

113. Tantawi M, Miao J, Matias C, Skidmore CT, Sperling MR, Sharan AD, et al. Gray matter sampling differences between subdural electrodes and Stereoelectroencephalography electrodes. Front Neurol. 2021;12:669406. https://doi.org/10.3389/FNEUR.2021.669406

114. Cossu M, Cardinale F, Colombo N, Mai R, Nobili L, Sartori I, et al. Stereoelectroencephalography in the presurgical evaluation of children with drug-resistant focal epilepsy. J Neurosurg. 2005;103:333–43. https://doi.org/10.3171/ped.2005.103.4.0333

115. Gupta K, Grover P, Abel TJ. Current conceptual understanding of the epileptogenic network from Stereoelectroencephalography-based connectivity inferences. Front Neurol. 2020;11:569699. https://doi.org/10.3389/FNEUR.2020.569699

116. Michalak AJ, Greenblatt A, Wu S, Tobochnik S, Dave H, Raghupathi R, et al. Seizure onset patterns predict outcome after stereo-electroencephalography-guided laser amygdalohippocampotomy. Epilepsia. 2023;64:1568–81. https://doi.org/10.1111/EPI.17602

117. Shields JA, Greven ACM, Shivamurthy VKN, Dickey AS, Matthews RE, Laxpati NG, et al. Stereoelectroencephalography-guided radiofrequency ablation of the epileptogenic zone as a treatment and predictor of future success of further surgical intervention. Epilepsia. 2023;64:2081–93. https://doi.org/10.1111/EPI.17673

118. Contento M, Pizzo F, López-Madrona VJ, Lagarde S, Makhalova J, Trébuchon A, et al. Changes in epileptogenicity biomarkers after stereotactic thermocoagulation. Epilepsia. 2021;62:2048–59. https://doi.org/10.1111/EPI.16989

119. Simula S, Garnier E, Contento M, Pizzo F, Makhalova J, Lagarde S, et al. Changes in local and network brain activity after stereotactic thermocoagulation in patients with drug-resistant epilepsy. Epilepsia. 2023;64:1582–93. https://doi.org/10.1111/EPI.17613

120. Tomlinson SB, Buch VP, Armstrong D, Kennedy BC. Stereoelectroencephalography in pediatric epilepsy surgery. J Korean Neurosurg Soc. 2019;62:302–12. https://doi.org/10.3340/JKNS.2019.0015

121. Taussig D, Chipaux M, Fohlen M, Dorison N, Bekaert O, Ferrand-Sorbets S, et al. Invasive evaluation in children (SEEG vs subdural grids). Seizure. 2020;77:43–51. https://doi.org/10.1016/J.SEIZURE.2018.11.008

122. Peltola ME, Liukkonen E, Granström ML, Paetau R, Kantola-Sorsa E, Valanne L, et al. The effect of surgery in encephalopathy with electrical status epilepticus during sleep. Epilepsia. 2011;52:602–9. https://doi.org/10.1111/J.1528-1167.2010.02783.X

123. Perry MS, Shandley S, Perelman M, Singh RK, Wong-Kisiel L, Sullivan J, et al. Surgical evaluation in children <3 years of age with drug-resistant epilepsy: patient characteristics, diagnostic utilization, and potential for treatment delays. Epilepsia. 2022;63:96–107. https://doi.org/10.1111/EPI.17124

124. Barba C, Mai R, Grisotto L, Gozzo F, Pellacani S, Tassi L, et al. Unilobar surgery for symptomatic epileptic spasms. Ann Clin Transl Neurol. 2016;4:36–45. https://doi.org/10.1002/ACN3.373

125. Liava A, Mai R, Tassi L, Cossu M, Sartori I, Nobili L, et al. Paediatric epilepsy surgery in the posterior cortex: a study of 62 cases. Epileptic Disord. 2014;16:141–73. https://doi.org/10.1684/EPD.2014.0648

126. Barkovich AJ. Concepts of myelin and myelination in neuroradiology. AJNR Am J Neuroradiol. 2000;21:1099–109.

127. Kim W, Shen MY, Provenzano FA, Lowenstein DB, McBrian DK, Mandel AM, et al. The role of stereo-electroencephalography to localize the epileptogenic zone in children with nonlesional brain magnetic resonance imaging. Epilepsy Res. 2021;179:106828. https://doi.org/10.1016/J.EPLEPSYRES.2021.106828

128. Chipaux M, Dorfmüller G, Fohlen M, Dorison N, Metten MA, Delalande O, et al. Refractory spasms of focal onset-a potentially curable disease that should lead to rapid surgical evaluation. Seizure. 2017;51:163–70. https://doi.org/10.1016/J.SEIZURE.2017.08.010

129. de la Vaissière S, Milh M, Scavarda D, Carron R, Lépine A, Trébuchon A, et al. Cortical involvement in focal epilepsies with epileptic spasms. Epilepsy Res. 2014;108:1572–80. https://doi.org/10.1016/J.EPLEPSYRES.2014.08.008

130. Neal A, Bouet R, Lagarde S, Ostrowsky-Coste K, Maillard L, Kahane P, et al. Epileptic spasms are associated with increased stereo-electroencephalography derived functional connectivity in tuberous sclerosis complex. Epilepsia. 2022;63:2359–70. https://doi.org/10.1111/EPI.17353

131. Lagarde S, Bonini F, McGonigal A, Chauvel P, Gavaret M, Scavarda D, et al. Seizure-onset patterns in focal cortical dysplasia and neurodevelopmental tumors: relationship with surgical prognosis and neuropathologic subtypes. Epilepsia. 2016;57:1426–35. https://doi.org/10.1111/EPI.13464

132. Zakaria T, Noe K, So E, Cascino GD, Wetjen N, Van Gompel JJ, et al. Scalp and intracranial EEG in medically intractable extratemporal epilepsy with normal MRI. ISRN Neurol. 2012;2012:1–9. https://doi.org/10.5402/2012/942849

133. Hyslop A, Duchowny M. Electrical stimulation mapping in children. Seizure. 2020;77:59–63. https://doi.org/10.1016/J.SEIZURE.2019.07.023

134. Taussig D, Chipaux M, Lebas A, Fohlen M, Bulteau C, Ternier J, et al. Stereo-electroencephalography (SEEG) in 65 children: an effective and safe diagnostic method for pre-surgical diagnosis, independent of age. Epileptic Disord. 2014;16:280–95. https://doi.org/10.1684/EPD.2014.0679

135. Chitoku S, Otsubo H, Harada Y, Jay V, Rutka JT, Weiss SK, et al. Extraoperative cortical stimulation of motor function in children. Pediatr Neurol. 2001;24:344–50. https://doi.org/10.1016/S0887-8994(01)00264-8

136. Jayakar P, Alvarez LA, Duchowny MS, Resnick TJ. A safe and effective paradigm to functionally map the cortex in childhood. J Clin Neurophysiol. 1992;9:288–93. https://doi.org/10.1097/00004691-199204010-00009

137. Van Gompel JJ, Worrell GA, Bell ML, Patrick TA, Cascino GD, Raffel C, et al. Intracranial electroencephalography with subdural grid electrodes: techniques, complications, and outcomes. Neurosurgery. 2008;63:498–505. https://doi.org/10.1227/01.NEU.0000324996.37228.F8

138. Sacino MF, Huang SS, Schreiber J, Gaillard WD, Oluigbo CO. Is the use of stereotactic electroencephalography safe and effective in children? A meta-analysis of the use of stereotactic electroencephalography in comparison to subdural grids for invasive epilepsy monitoring in pediatric subjects. Neurosurgery. 2019;84:1190–200. https://doi.org/10.1093/NEUROS/NYY466

139. Arya R, Mangano FT, Horn PS, Holland KD, Rose DF, Glauser TA. Adverse events related to extraoperative invasive EEG monitoring with subdural grid electrodes: a systematic review and meta-analysis. Epilepsia. 2013;54:828–39. https://doi.org/10.1111/EPI.12073

140. Ojemann G, Ojemann J, Lettich E, Berger M. Cortical language localization in left, dominant hemisphere. An electrical stimulation mapping investigation in 117 patients. J Neurosurg. 1989;71:316–26. https://doi.org/10.3171/JNS.1989.71.3.0316

141. Remick M, Akwayena E, Harford E, Chilukuri A, White GE, Abel TJ. Subdural electrodes versus stereoelectroencephalography for pediatric epileptogenic zone localization: a retrospective cohort study. Neurosurg Focus. 2022;53:E4. https://doi.org/10.3171/2022.7.FOCUS2269

142. Larrew T, Skoch J, Ihnen SKZ, Arya R, Holland KD, Tenney JR, et al. Comparison of outcomes after stereoelectroencephalography and subdural grid monitoring in pediatric tuberous sclerosis complex. Neurosurg Focus. 2022;53:E5. https://doi.org/10.3171/2022.7.FOCUS22335

143. Joswig H, Lau JC, Abdallat M, Parrent AG, MacDougall KW, McLachlan RS, et al. Stereoelectroencephalography versus subdural strip electrode implantations: feasibility, complications, and outcomes in 500 intracranial monitoring cases for drug-resistant epilepsy. Neurosurgery. 2020;87:E23–30. https://doi.org/10.1093/NEUROS/NYAA112

144. Katz JS, Abel TJ. Stereoelectroencephalography versus subdural electrodes for localization of the epileptogenic zone: what is the evidence? Neurotherapeutics. 2019;16:59–66. https://doi.org/10.1007/S13311-018-00703-2

145. Lee AT, Nichols NM, Speidel BA, Fan JM, Cajigas I, Knowlton RC, et al. Modern intracranial electroencephalography for epilepsy localization with combined subdural grid and depth electrodes with low and improved hemorrhagic complication rates. J Neurosurg. 2022;138:1–7. https://doi.org/10.3171/2022.5.JNS221118

146. Takayama Y, Ikegaya N, Iijima K, Kimura Y, Yokosako S, Muraoka N, et al. Single-institutional experience of chronic intracranial electroencephalography based on the combined usage of subdural and depth electrodes. Brain Sci. 2021;11:1–17. https://doi.org/10.3390/BRAINSCI11030307

147. Oluigbo CO, Gaillard WD, Koubeissi MZ. The end justifies the means-a call for nuance in the increasing Nationwide adoption of Stereoelectroencephalography over subdural electrode monitoring in the surgical evaluation of intractable epilepsy. JAMA Neurol. 2022;79:221–2. https://doi.org/10.1001/JAMANEUROL.2021.4994

148. Tao JX, Wu S, Lacy M, Rose S, Issa NP, Yang CW, et al. Stereotactic EEG-guided laser interstitial thermal therapy for mesial temporal lobe epilepsy. J Neurol Neurosurg Psychiatry. 2018;89:542–8. https://doi.org/10.1136/JNNP-2017-316833

149. Bartolomei F, Chauvel P, Wendling F. Epileptogenicity of brain structures in human temporal lobe epilepsy: a quantified study from intracerebral EEG. Brain. 2008;131:1818–30. https://doi.org/10.1093/BRAIN/AWN111

150. Wendling F, Badier JM, Chauvel P, Coatrieux JL. A method to quantify invariant information in depth-recorded epileptic seizures. Electroencephalogr Clin Neurophysiol. 1997;102:472–85. https://doi.org/10.1016/S0013-4694(96)96633-3

151. David O, Blauwblomme T, Job AS, Chabards S, Hoffmann D, Minotti L, et al. Imaging the seizure onset zone with stereoelectroencephalography. Brain. 2011;134:2898–911. https://doi.org/10.1093/BRAIN/AWR238

152. Gnatkovsky V, Francione S, Cardinale F, Mai R, Tassi L, Lo Russo G, et al. Identification of reproducible ictal patterns based on quantified frequency analysis of intracranial EEG signals. Epilepsia. 2011;52:477–88. https://doi.org/10.1111/J.1528-1167.2010.02931.X

153. Schindler K, Leung H, Elger CE, Lehnertz K. Assessing seizure dynamics by analysing the correlation structure of multichannel intracranial EEG. Brain. 2007;130:65–77. https://doi.org/10.1093/BRAIN/AWL304

154. Jirsa VK, Proix T, Perdikis D, Woodman MM, Wang H, Bernard C, et al. The virtual epileptic patient: individualized whole-brain models of epilepsy spread. Neuroimage. 2017;145:377–88. https://doi.org/10.1016/J.NEUROIMAGE.2016.04.049

155. Cao M, Galvis D, Vogrin SJ, Woods WP, Vogrin S, Wang F, et al. Virtual intracranial EEG signals reconstructed from MEG with potential for epilepsy surgery. Nat Commun. 2022;13:994. https://doi.org/10.1038/S41467-022-28640-X

156. Bernabei JM, Li A, Revell AY, Smith RJ, Gunnarsdottir KM, Ong IZ, et al. Quantitative approaches to guide epilepsy surgery from intracranial EEG. Brain. 2023;146:2248–58. https://doi.org/10.1093/BRAIN/AWAD007

SUPPORTING INFORMATION

Additional supporting information can be found online in the Supporting Information section at the end of this article.

Test yourself

1. Which answers are true regarding the indication and purpose of SEEG:
    I   Given its low complication profile, SEEG has become the method of choice for invasive intracranial EEG investigation around the world.
    II The purpose of SEEG is to identify the SOZ, delineate the wider epileptic network and resection margins, and localize relevant eloquent cortex in relation to the epileptic network.
    III 95% of patients undergoing SEEG will benefit from a subsequent surgical intervention.
        A. I, II, and III are true.
        B. I, II, and III are false.
        C. I and II are true, III is false.
        D. I is true, II and III are false.
        E. II and III are true, I is false.

2. Which of the following statements regarding intracranial EEG seizure-onset patterns is correct?
    A. Low-voltage fast activity is not seen with subdural grids or strips.
    B. Sharp activity at ≤13 Hz is seen in 60%–70% of patients undergoing intracranial EEG investigations.
    C. Burst of high-amplitude polyspikes is typically followed by low-voltage fast activity.
    D. Delta brush is the second most common intracranial EEG seizure-onset pattern.
    E. Burst suppression typically evolves to low-frequency high-amplitude periodic spikes.

3. Regarding seizure semiology, which of the following statements is FALSE?
    A. Seizure semiology usually reflects the propagation of seizures.
    B. Both spatial and temporal aspects of EEG change are related to clinical seizure expression.
    C. Hyperkinetic seizures are highly specific for frontal lobe origin.
    D. Auditory aura is highly suggestive for lateral temporal lobe localization.
    E. Signal analysis of SEEG ictal data can show changes in coupling between specific brain structures, correlated with semiological expression.

4. What interictal SEEG pattern is typical for focal cortical dysplasia?
    A. Continuous or subcontinuous epileptiform discharges.
    B. High-voltage gamma activity.
    C. Repetitive bursting spikes.
    D. Low-voltage fast activity.
    E. Physiological background activity inside the dysplastic cortex.

5. Which of the following statements are true regarding infraslow activity and high-frequency oscillations (HFOs):
    I   DC shifts and HFOs both occur more inside than outside the seizure-onset zone.
    II DC shifts and HFOs both occur more often at seizure onset than after the seizure onset.
    III DC shifts and HFOs are two mutually exclusive phenomena.
        A. I + II are true, III is false.
        B. I + II are false, III is true.
        C. I is true, II and III are false.
        D. II is true, I and III are false.
        E. All are true.

6. Subdural grids/strips is the best indicated method for intracranial EEG in which of the following situations?
    A. Mesial temporal epilepsy.
    B. Periventricular nodular heterotopia.
    C. Insulo-opercular epilepsy.
    D. Neocortical focal epilepsy in the proximity to eloquent cortex.
   E. Orbitofrontal focal epilepsy.

7. Which of the following statements is true for cortical stimulation?
    A. Cortical stimulation is performed exclusively for seizure stimulation.
    B. Cortical stimulation evoked habitual electro-clinical seizures are a positive predicting factor to achieve a seizure-free surgical outcome.
    C. The only purpose of cortical stimulation is mapping of physiological functions.
    D. Electrode contacts evoking auras with no EEG correlate are localized to the epileptogenic zone.
    E. After-discharges are specific for the epileptogenic zone.

8. Which of the following statements is true:
    A. Whether using subdural grids or SEEG, only a tiny portion of the cortex can be explored in a given patient.
    B. Exploring the insula with three orthogonal electrodes inserted via the frontal, centro-parietal, and temporal operculum is sufficient to exclude an insular seizure generator.
    C. Subdural grids/strips are a good alternative to avoid the spatial sampling bias of SEEG.
    D. Subdural grids/strips and SEEG are equally well poised to explore bottom-of-the sulcus dysplasias.
    E. Only low-voltage fast activity is going along with seizure freedom post-resection.

9. Which of the following statements are true regarding computerized signal analysis approaches in SEEG?
    A. The Epileptogenicity Index is applicable for all seizure-onset patterns independent of the fast activity content.
    B. Time-frequency analysis is needed to visualize high-frequency oscillations.
    C. Computerized signal analysis approaches are widely implemented in clinical practice.
    D. The epileptogenic "fingerprint" is based on pre-ictal spikes, fast activity, and suppression of slow frequencies in the epileptogenic zone.
    E. Computerized signal analysis is needed to assess presence of a DC shift.

10. Which of the following statements are true regarding the following SEEG markers for prognostication:
    I   A seizure-onset pattern without low-voltage fast activity does result in seizure-free outcome in 70% of cases.
    II Habitual electro-clinical seizures evoked by low-frequency stimulation are predictive of a good post-surgical outcome.
    III Most interictal patterns allow for correct prediction of the underlying pathology.
       A. I+II are true, III is false.
       B. I+II are false, III is true.
       C. I is true, II and III are false.
       D. II is true, I and III are false.
       E. All are true.

Answers may be found in the supporting information S1

APPENDIX A

Case 1. A 25-year-old right-handed woman had drug-resistant, sleep-related hyper-motor epilepsy with seizure onset at age 12 years. Seizures were characterized by an ill-defined sensation going along with tactile hypersensitivity involving the entire body, which would be like a "wave starting in the middle of her stomach and going up and down" followed by restlessness, anxiety, and at times left leg clonic movements and smiling. Prolonged video-EEG recording demonstrated seizures occurring mostly out of sleep, with sudden onset of tonic posture of the left arm, lasting approximately 30 s. Sometimes, a left leg clonic movement followed by an impaired awareness was observed after the tonic left arm movement. Ictal onset was difficult to evaluate due to muscular artifact. Later, a low-amplitude alpha rhythmic activity over the central midline and right parasagittal head region was seen. The interictal EEG remained inconclusive. The 3-Tesla MRI showed an unusual sulco-gyral morphology of the right posterior cingulate with subtle transmantle sign that could correspond to a FCD type II. The FDG-positron emission tomography (PET) showed no area of hypometabolism. Source imaging was non-contributory, as no spikes were recorded. The neuropsychological evaluation showed deficits consistent with frontal lobe interference with a right predominance. The SEEG implantation was planned to confirm the generator in the suspected FCD
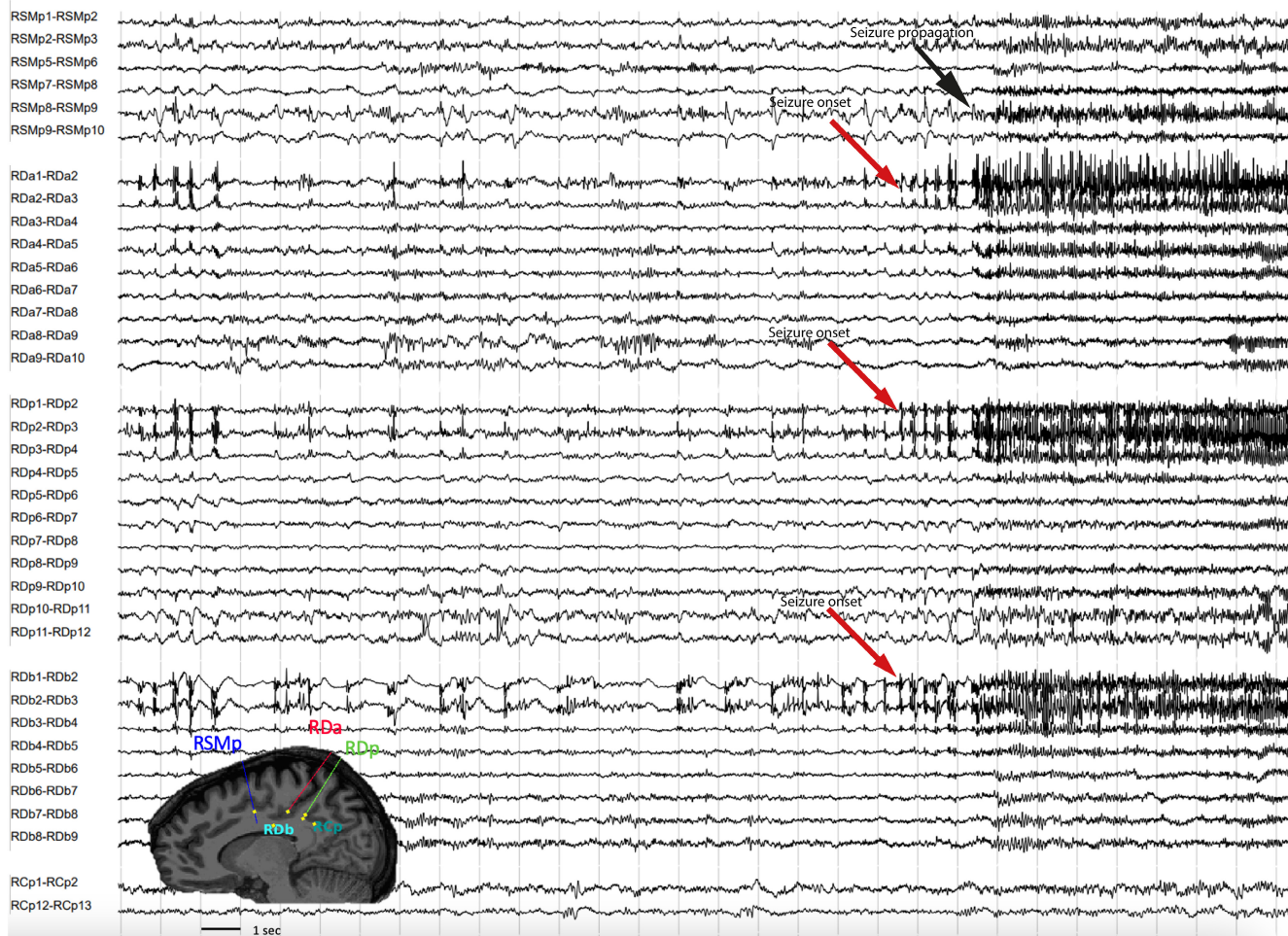
FIGURE A1   Typical pattern of FCD II. Ictal SEEG recording from a 25-year-old woman with a right precuneal–cingulate DRE. The SOP is characterized by repetitive polyspike and waves seen in the contacts RDb1-3, RDa1-6, and RDp1-4, followed by a LVFA seen in the same contacts (red arrows). The seizure propagated to RSMp8-9 (black arrow) before reaching other contacts. Three electrodes (RDa, RDp, and RDb) were targeting the suspected FCD visible in the structural MRI to allow a better delineation of the surgical borders and thermo-coagulate the most active channels. RDa was targeting the anterior part of the FCD; RDp was targeting the posterior part of the FCD; RDb was targeting the base of the FCD; RSMp was targeting the mid-cingulate gyrus; and RCp was targeting the posterior cingulate gyrus. This patient underwent a tailored precuneal–cingulate resection. The pathology confirmed FCD IIa. She is Engel Ia with a follow-up of 4 years. *Display parameters*: *Bipolar montage – a selection of electrodes is shown for educational purposes – BP: [0.5–100 Hz].* FCD, Focal cortical dysplasia; DRE, Drug-resistant epilepsy; LVFA, Low-voltage fast activity; SOP, Seizure-onset pattern; SEEG, Stereo-electroencephalography.

area over the right posterior cingulate gyrus, to delineate the resection borders, and to rule out the alternative hypotheses of an anterior insula generator with fast mesio-frontal propagation or a mesio-frontal generator. A right hemispheric SEEG implantation with 16 depth electrodes was performed. Ictal (Figure A1) and interictal (Figure A2) EEG demonstrated a typical FCD type II pattern over the right precuneal–cingulate cortex. The patient underwent a tailored precuneal–cingulate resection. Pathology confirmed FCD IIa, and the patient has been seizure-free (Engel Ia) for 4 years of follow-up.

APPENDIX B

Case 2. A 22-year-old right-handed woman had drug-resistant temporal epilepsy with seizure onset at age 11 years. Seizures were characterized by rising epigastric sensation and anxiety, followed by impaired awareness, flushing, staring, oromandibular and bimanual automatisms, and hypersalivation before the clinical end. These auras were often times followed by speech arrest, and post-ictal aphasia. Prolonged video-EEG recording captured focal seizures with a left temporal onset, which very rapidly spread to left precentral and anterior
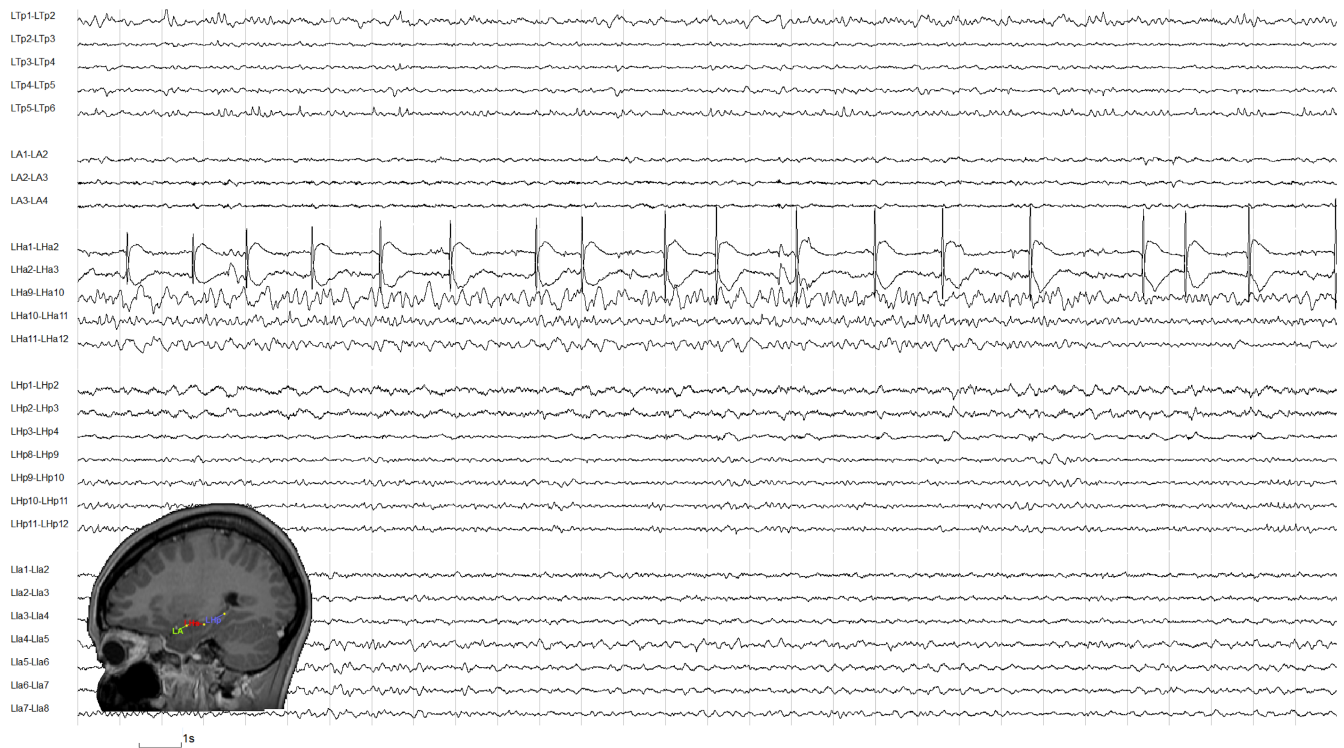
FIGURE A2 Typical interictal pattern of FCD II recording from a 25-year-old woman with a right precuneal–cingulate DRE. The interictal activity from NREM 3 sleep is characterized by a pseudo-continuous polyspike and polyspike-waves seen mostly in the contacts RDb1-5, RDa1-6, RDp1-4, and RSMp7-10. RDa, RDp, and RDb were targeting the FCD visible in the structural MRI. RDa was targeting the anterior part of the FCD; RDp was targeting the posterior part of the FCD; RDb was targeting the base of the FCD; RSMp was targeting the mid-cingulate gyrus; and RCp was targeting the posterior cingulate gyrus. * shows one of the spindles. This patient underwent a tailored precuneal–cingulate resection. The pathology confirmed FCD IIa. She is Engel Ia with a follow-up of 4 years. *Display parameters: Bipolar montage – a selection of electrodes is shown for educational purposes – BP: [0.5–100 Hz].* Abbreviations: FCD, Focal cortical dysplasia; DRE, Drug-resistant epilepsy; SOP, Seizure-onset pattern; SEEG, Stereo-electroencephalography; NREM, Non-rapid eye movement.

frontal regions. Interictally, there were left anterior-mid-temporal spikes with a voltage field extending to ipsilateral precentral, frontal pole, or vertex regions. These findings raised the question of a temporal-plus epilepsy with involvement of the anterior insula. MRI showed a T2/FLAIR hyperintensity, decreased volume and internal architecture loss on left hippocampus, and accompanied by poor gray-white matter differentiation and atrophy of left temporal pole. Functional MRI showed bilateral frontal and temporal activations for language. FDG-PET showed left temporal hypometabolism with mesial predominance, and extension to temporo-occipital, lower parietal, and anterior frontal regions. The SEEG implantation was planned to confirm a left mesiotemporal generator, to delineate the resection borders, and to rule out the alternative hypothesis of a perisylvian/anterior insula generator. A left-hemisphere SEEG implantation with 14 electrodes was performed. Ictal (Figure B1) and interictal (Figure B2) SEEG recording demonstrated a typical hippocampal sclerosis pattern on mesiotemporal contacts. The patient underwent a standard left anterior temporal lobectomy, and pathology confirmed a hippocampal sclerosis. The patient has been seizure free (Engel Ia) for 4 years of follow-up.
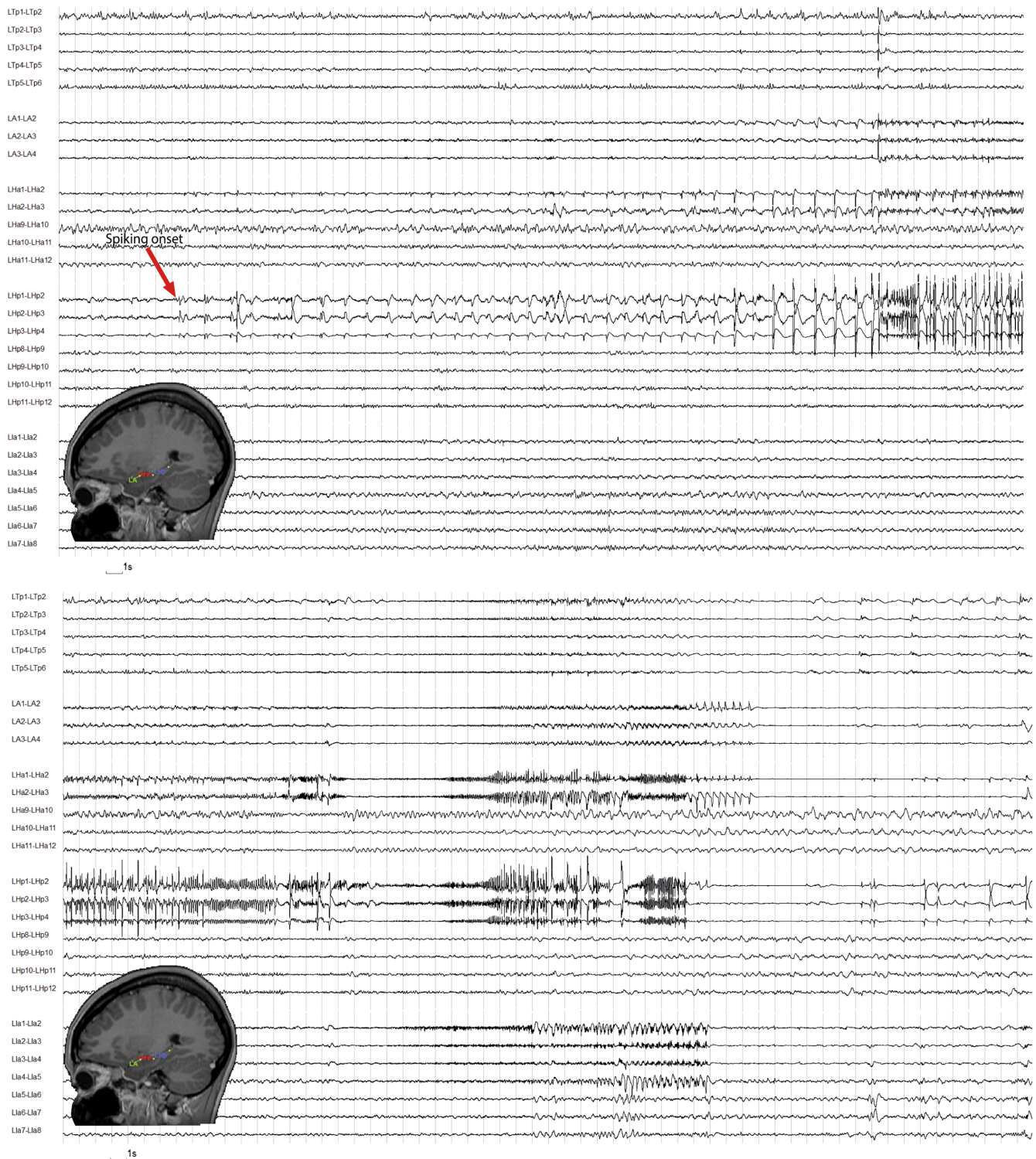
FIGURE B1 Typical pattern of HS. Ictal SEEG recording from a 22-year-old woman with a left mesial temporal lobe DRE. The pattern displayed is characterized by the appearance of low-frequency high-amplitude spikes seen involving contacts LHp 1–3 and LHa 1–2 (red arrow) that seconds later evolved into a rhythmic sharply contoured alpha–theta activity involving other mesiotemporal adjacent contacts (LA 1–3), and later also anterior insula and temporal pole contacts. SEEG was planned to rule out a perisylvian generator (see Case 2). LHa was targeting the left anterior hippocampus; LHp was targeting the left posterior hippocampus; LA was targeting the left amygdala; LIa was targeting the left anterior insula; LTp was targeting the left temporal pole. This patient underwent a left anterior temporal lobectomy. Pathology confirmed a HS, patient is Engel Ia with a follow-up of 4 years. *Display parameters: Bipolar montage – a selection of electrodes is showed for educational purposes – BP: [1.0–100 Hz].* Case and figure showed with the courtesy of Dr Philippe Kahane from the University Hospital of Grenoble (France). HS, Hippocampal sclerosis; DRE, Drug-resistant epilepsy; SOP, Seizure-onset pattern; SEEG, Stereo-electroencephalography.

FIGURE B2 Typical interictal pattern of HS. Recording from a 22-year-old woman with a left mesial temporal lobe DRE. The interictal activity is characterized by abundant high-amplitude spikes involving contacts LHa 1–2. SEEG was planned to rule out a perisylvian generator (see Appendix B). LHa was targeting the left anterior hippocampus; LHp was targeting the left posterior hippocampus; LA was targeting the left amygdala; LIa was targeting the left anterior insula; LTp was targeting the left temporal pole. This patient underwent a left anterior temporal lobectomy. Pathology confirmed a HS, patient is Engel Ia with a follow-up of 4 years. *Display parameters: Bipolar montage – a selection of electrodes is shown for educational purposes – BP: [1.0–100 Hz].* Case and figures showed with the courtesy of Dr Philippe Kahane from the University Hospital of Grenoble (France). HS, Hippocampal sclerosis; DRE, Drug-resistant epilepsy; SOP, Seizure-onset pattern; SEEG, Stereo-electroencephalography.